Cape Peninsula
University of Technology

PHYSICAL OCEANOGRAPHY OF SODWANA BAY AND ITS EFFECT ON LARVAL TRANSPORT AND CORAL BLEACHING

BY

TAMARYN MORRIS

Thesis submitted in fulfilment of the requirements for the

Master of Technology: Oceanography

in the Faculty of Applied Sciences at the

CAPE PENINSULA UNIVERSITY OF TECHNOLOGY

Supervisors:

Mr Conrad Sparks

Mr Michael Roberts

Prof. Michael Schleyer

Cape Town

August 2009

Declaration

I, Tamaryn Morris, declare that the contents of this thesis represent my own unaided work, and that the thesis has not previously been submitted for academic examination towards any qualification. Furthermore, it represents my own opinions and not necessarily those of the Cape Peninsula University of Technology.

Signed T Morris Date August 2009

Abstract

A collaborative study between Marine and Coastal Management (MCM) and the Oceanographic Research Institute (ORI) was initiated in March 2001 to investigate the physical oceanography of Sodwana Bay, South Africa, and the affects on coral communities resident to the area. A bottom-mounted Acoustic Doppler Current Profiler (ADCP) and three Underwater Temperature Recorders (UTR) were deployed to complement the long-term monitoring UTR deployed on Nine-Mile Reef (NMR) in 1994. The study was terminated after 30 months, whereby all instruments were removed except for the long-term monitoring UTR.

Results from the ADCP deployed on NMR (26 m) showed southerly currents 73% and northerly currents 27% of the study period. The average surface velocity was 27 cm s^{-1}, with maximum velocities of 108 cm s^{-1} to the south and 106 cm s^{-1} to the north. Northerly reversals occurred 206 times over the study period with an average duration of 23 hours. The primary driving force of the northerly reversals was southerly winds, with cyclonic mesoscale eddies shown to have an influence on occasion.

Coral larvae spawned into the water column are subject tothe current dynamics surrounding them, until they are developed enough to settle onto suitable substratum. Due to the narrow shelf region, consistant southerly flow could cause biological material to be lost from the shelf. The presence of northerly reversals would help retain larvae to Sodwana Bay, a mechanism called self-seeding of natal reefs. Mesoscale features interacting with the shelf have the ability of entraining larvae into large-scale circulations. The competency period of most coral species may be sufficient to take advantage of these transport mechanism, but planulae may not be viable for settlement due to the their usage of stored energy over time.

The anomalous long-term temperature monitoring data from Nine-mile Reef showed a natural cyclical trend of warming and cooling for the 14 year data set. The warming phase coincided with bleaching events in 1998 and 2000, thereafter the area experienced a cooling phase and no bleaching has been recorded since. Upwelling along the shelf edge was considered the dominant type for the region, with the canyons incising the shelf providing only occasional avenues for cold water onto the shelf. Dynamic uplift of the thermocline onto the shelf during cyclonic eddy interaction with the shelf was considered a possible third mechanism for upwelling. Cold water was not always transported inshore to the shallower reefs from the shelf edge, which may have a negative affect during times of elevated surface temperatures. However good connectivity existed between the northern and southern reaches of Sodwana Bay.

Two important factors which aid a coral community to resist coral bleaching are strong currents and upwelling. Both of these are found on the northern KwaZulu-Natal shelf and possibly spared the region from detrimental bleaching in the past.

Acknowledgements

- I would like to thank the following scientists and technicians for their help with the deployment, servicing and retrieval of oceanographic equipment used for this study:
    - From the Oceanographic Research Institute (ORI): Professor Michael Schleyer, Dr. Louis Celliers, Sean Bailey.
    - From Marine and Coastal Management (MCM) and Bayworld Centre for Research and Education (BCRE): Michael Roberts, Marcel van den Berg, Rick Harding and Daniel Engelbrecht.

- Acknowledgements with regards to Figure 2.2:
    - This image was derived from interpreted seafloor GIS data provided by the Marine Geoscience Unit, Council for Geoscience on behalf of the NRF Consortium. Copyright Council for Geoscience and the NRF Consortium.
    - GIS data (as above) and instrument positions were kindly plotted by Dr. Louis Celliers, ORI, Durban.

- Funders of the project:
    - Bayworld Centre for Research and Education (BCRE) and the Cape Peninsula University of Technology (CPUT) for student support and participation at conferences (see below).
    - Marine Living Resources Fund (MLRF), National Research Foundation (NRF) and the South African Association for Marine Biological Research (SAAMBR) for financial assistance with the field work.
    - Marine and Coastal Management (MCM) and the Oceanographic Research Institute (ORI) for field support.
    - Ezemvelo KwaZulu-Natal Wildlife for accommodation and the iSimangaliso Wetland Park Authority (formerly the Greater St. Lucia Wetland Park) for permission to conduct research within the reserve.
    - Mazda Wildlife Fund for the 4 x 4 vehicle used to tow the research craft.
    - BP (SA) for funding the research craft.

- Instruments were serviced as part of the following African Coelacanth Ecosystems Programme (ACEP) Cruises:
    - Alg 119: April / May 2003
    - Alg 122: July / August 2003
    - Alg 134: April / May 2005
    - Alg 147: April / May 2006
    - Alg 150: August / September 2006

- An extremely huge thank you to Mr. Marcel van den Berg for his endless hours of patience with the data processing and training, especially CMS! This project would just not have been the same without you.

- Miss Tarron Lamont for her help and extremely valuable advice with regards to the sea surface height anomalies (SSHA) data processing and plotting.

- Mr. Bjorn Backeberg with his help with regards LyX, BibTex and Latex. An amazing writing programme, once you get the hang of it!

- The data contained within this project was presented at three conferences:

    - 5th Western Indian Ocean Marine Science Association (WIOMSA) Conference, 22 - 26 October 2007

      Poster: The Currents on the Sodwana Bay shelf (South Africa).
      Authors: Morris, T., Roberts, M. J. and Schleyer, M. H.

    - Southern African Marine Science Symposium (SAMSS), 29 June - 3 July 2008

      Oral: Comparative temperature studies on coral reef communities in Sodwana Bay, South Africa.
      Authors: Morris, T., Roberts, M. J., Schleyer, M. H. and van den Berg, M. A.

    - Deep Ocean Exchange with the Shelf (DOES), 6-8 October 2008

      Poster: Physical oceanography of Sodwana Bay: Characteristics, driving forces and implications.
      Authors: Morris, T., Roberts, M. J., Schleyer, M. H. and van den Berg, M. A.

- I would like to thank my supervisors on this project: Mr. Conrad Sparks of the Cape Peninsula University of Technology, Mr. Michael Roberts of Marine and Coastal Management and Bayworld Centre for Research and Education and Professor Michael Schleyer of the Oceanographic Research Institute in Durban, for all their help and guidance and giving me the opportunity to take part in this phenomenal project.

- And lastly, but by no means least, my extended and extremely supportive family, especially Momzanite, Daddy Bear and Rox. And to my friends, who after much patience, eventually became my personal cheer-leading squad. Your faith in me has made me the person I am today!

If we knew what it was we were doing, it would not be called research, would it?

-Albert Einstein-

Contents

Glossary

Sverdrup (Sv): Measurement of volume transport – i.e. 35 x 106 / m3 = 35 Sv

NMR: Nine-mile Reef

NMD: Nine-mile Deep

TMR: Two-mile Reef

FMD: Five-mile Reef

ADCP: Acoustic Doppler Current Profiler – for measuring current speed and direction (moored)

UTR: Underwater Temperature Recorder – for measuring temperature (moored)

SSHA: Sea Surface Height Anomalies

SeaWiFS: Sea-viewing Wide Field-of-view Sensor, used to capture derived chlorophyll *a* imagery.

SST: Sea Surface Temperatures

ORI: Oceanographic Research Institute

MCM: Marine and Coastal Management

KZN: KwaZulu-Natal

List of Figures

List of Tables

Chapter 1

Introduction

1.1 Introduction

Coral reefs are extremely diverse ecosystems yet account for a very small percentage of the world's oceans (Conand et al., 1999). These bountiful and colourful communities occur throughout the world's tropical and temperate oceans and have became synonymous with research on global climate change after the 1998 and 2000 global bleaching events (Goreau et al., 2000; Sheppard, 2003). Coral reefs occur all along the east African coastline, interrupted in their distribution only by riverine systems such as the Zambezi River (Obura et al., 2000). The northern KwaZulu-Natal shelf represents the southernmost distribution of coral reefs along the east African coast and the only coral reefs within South Africa (Schleyer, 2000). Studies on these coral complexes have focused primarily on species diversity, distribution and community structure (Schleyer, 1999; Schleyer and Celliers, 2003b,a; Celliers and Schleyer, 2008), coral bleaching (Celliers and Schleyer, 2002; Floros et al., 2004) and, more recently, coral recruitment strategies (Glassom et al., 2006).

In comparison, little to no physical oceanographic studies have been undertaken to understand this narrow, species-rich shelf region located between Richards Bay and the Mozambican border (Harris, 1978; Gründlingh, 1984; Gründlingh and Pearce, 1984; Lutjeharms, 2006). Numerous studies undertaken on the Great Barrier Reef have shown the advantage of understanding the physical dynamics impacting on a coral reef community in terms of larval transport (Black et al., 1991; Miller and Mundy, 2003; Byers and Pringle, 2006). Understanding the long-term trends and changes associated with climatic phenomena and the subsequent response of the ocean to these, greatly enhances the understanding of physiological changes to coral reefs during times of stress (Riegl and Pillar, 2003; Le Treut et al., 2007; Sheppard, 2003).

The objective of this study was to determine the physical oceanographic characteristics of Sodwana Bay on the northern KwaZulu-Natal coast, and determine how these parameters affect the coral reef communities inhabiting the area. The study was initiated with a long-term temperature recorder deployed at the northern end of the embayment in 1994. The study was complemented in 2001 with three additional temperature sensors to the south and further offshore of the original recorder, and a single continuously moored Acoustic Doppler Current Profiler (ADCP) to measure flow entering the embayment from the north. These instruments were removed in 2003 apart from the original long-term temperature recorder.

Key questions for this dissertation will include, what physical forces are responsible for the predominant current regime and potential anomalous characteristics? Does upwelling occur at Sodwana Bay, and if so, what types? How does the physical oceanography relate to and potential influence the coral community resident to Sodwana Bay?

1.2 Literature Review

1.2.1 Meteorology

The east African coastline is affected by the shifting of the Inter-Tropical Convergence Zone (ITCZ), a low-pressure belt surrounding the earth at the equator and formed by the ascent of warm moist air from higher latitudes (Preston-Whyte and Tyson, 1988). The ITCZ migrates from the southern to the northern hemisphere between January and July and vise verse between August and December (Preston-Whyte and Tyson, 1988). The ITCZ affects the sub-tropical region north of 20° S in two near-surface airsteams during the summer: 1) The north-east monsoon wind travelling southward from the equator and 2) deep tropical easterlies from the Indian Ocean (Preston-Whyte and Tyson, 1988).

The wind field over southern African is further affected by two major cells in the southern hemisphere: the Hadley Cell and the Ferrel Cell. The Hadley Cell is thermally direct (warm air rising, cold air sinking) and the Ferrel Cell is thermally indirect (cold air rising, warm air sinking), (Preston-Whyte and Tyson, 1988). The interaction of these two cells causes jet flows resulting in high-pressure and low-pressure systems. The South Indian Anti-cyclone on the east coast of South Africa produces a northerly component of wind near the ground (Preston-Whyte and Tyson, 1988), particularly from June to August (Newell et al., 1972).

KwaZulu-Natal has a warm, humid, sub-tropical climate. The climate is centred at 30° S with the southern sub-tropical high-pressure belt playing a dominant role in this climatic zone (Hunter, 1988). Air temperatures along the coastline have a low seasonal range due to the diminishing effect of the Indian Ocean, yet diurnal variations may be large (Hunter, 1988). A 30-year record shows a mean annual range of between 16° C and 25° C (Hunter, 1988). The mean annual relative humidity is 79% (Hunter, 1988).

The KwaZulu-Natal coastline runs in a roughly northeasterly–southwesterly direction, with the exception of the Natal Bight, and wind directions tend to follow this coastal orientation (Hunter, 1988). During the summer months, the southwesterly and northeasterly winds are balanced in their frequency in the south with northeasterly winds dominating in the north, whereas winter months experience an increase in off-shore flow (Hunter, 1988). Shillington (1992), after Hunter (1984), determined that there is a periodicity of 4-6 days in synoptic weather cycles from five years of barometric air pressure data. By far the most studied of the weather systems is the "coastal low". This is a shallow coastal depression, formed when a large-scale atmospheric flow interacts with the southern African escarpment, and propagates in an anti-clockwise direction along the coast from Port Elizabeth towards Durban (Hunter, 1988). These "coastal lows" cause dramatic wind changes from the northeast to the southwest in a matter of minutes (Schumann, 1981; Shillington, 1992) and are usually accompanied by a cold front travelling in a southeasterly direction (Hunter, 1988).

The mean annual temperature for a single-year study at Lake Sibaya Research Station, along the coast adjacent to Sodwana Bay, was 21.6° C (Maud, 1980), with a mean winter sea surface temperature of 22° C and 26° C in summer (Schleyer, 1999, from SADCO data, 1960-1995). The majority of the coastline

has a mean annual rainfall ranging between 1000 mm and 1100 mm (Hunter, 1988; Maud, 1980). The KwaZulu-Natal coastline experiences summer rainfall, with winter months yielding a 30% decrease in rainfall records (Maud, 1980). Two noticeable exceptions to rainfall patterns occur at Kosi Bay which receives 980 mm and Cape St. Lucia 1200 mm of rain per annum (Hunter, 1988). Sodwana Bay is located between these two anomalous areas and it is thus assumed that the rainfall here is within the average range (between 1000 mm and 1100 mm). The northern KwaZulu-Natal coastline also lies in a northeasterly–southwesterly orientation and winds blow parallel to this, giving rise to dominant southerly swells (Schleyer, 1999). The region has an average tidal range of 2 m, which classes it as high micro-tidal or low meso-tidal (Ramsay et al., 1996).

1.2.2 Geology

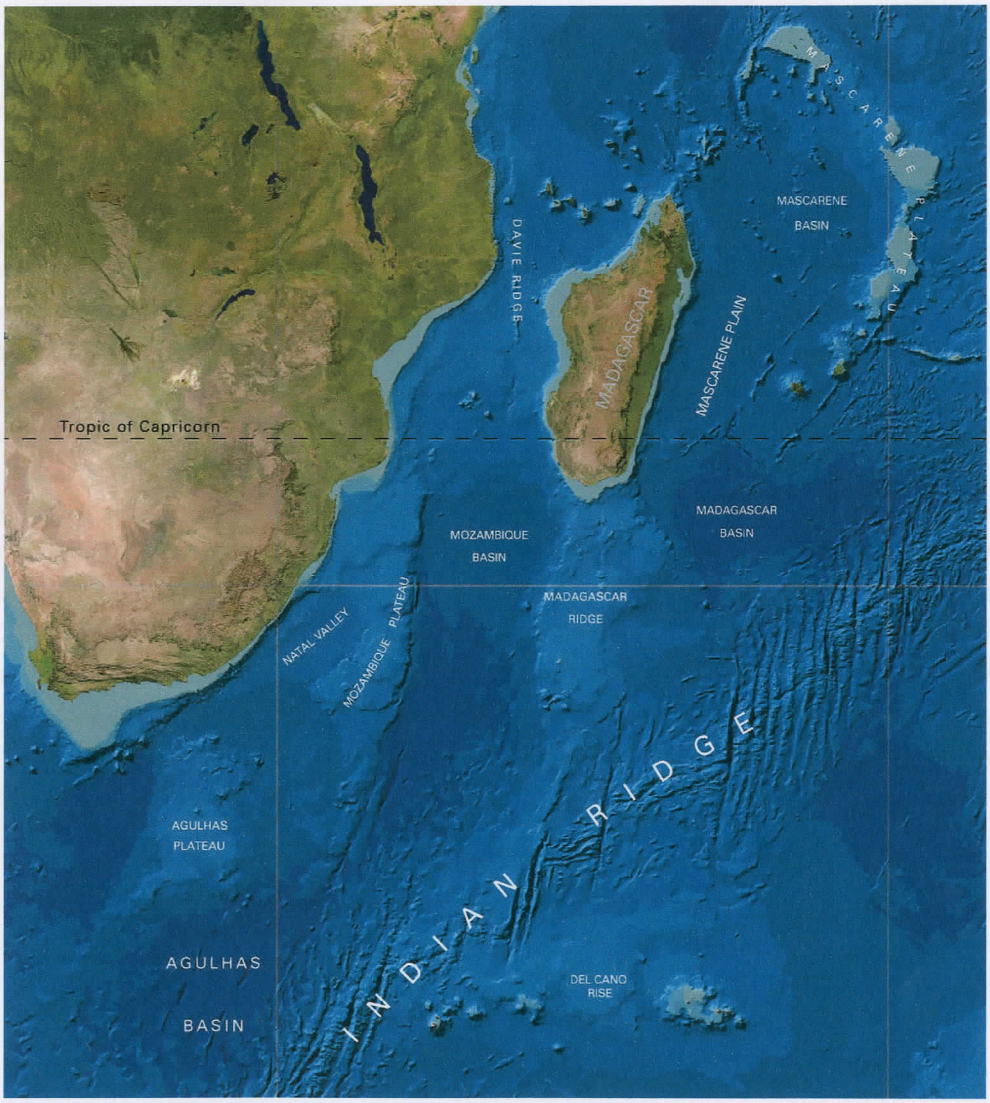

Figure 1.1: The sea-floor of the South West Indian Ocean. Image reproduced from the GEBCO world map, http://www.GEBCO.net

The east coast of South Africa has a very narrow shelf with the continental break being on average two to seven kilometers offshore (Ramsay, 1994). The only exception is the Natal Bight with a shelf

width of approximately 45 km (Shillington, 1992). The shelf gradient along the KwaZulu-Natal coast is also steep in comparison to the global average of 0.116°, varying between 1.0 and 2.5° (Ramsay, 1997). The Natal Valley is located offshore of northern KwaZulu-Natal, with depths exceeding 2000 m, and the Mozambique Basin further east has water depths of 5000 m (Martin, 1978). North of the Mozambique and South African border is the Delagoa Bight, which exhibits an unusual topographic layout (Martin, 1978; Lutjeharms, 2006) whereby a tongue at the 200 m isobath extends into the bight from the north. Flemming and Hay (1988) described the sediment load along the KwaZulu-Natal shelf as being in permanent suspension and eventually transported off the shelf by means of long-shore and wind-induced currents and ocean swells. The majority of this sediment originated from river systems along the coastline, for example the Thukela River which flows into the Natal Bight (Flemming and Hay, 1988).

Northern KwaZulu-Natal has a linear, clastic, sandy shoreline with little sediment input from non-marine sources such as riverine run-off (Ramsay, 1994) as the major river systems occur further south. The shoreline is made up of long barrier beaches with zeta bays of Holocene age, a log-spiral curve bay caused by littoral erosion (Ramsay, 1994; Cooper, 1991): Sodwana Bay is one of the largest of these. During the late Pleistocene, sea levels were 100-130 m lower than present, which exposed the shallow northern KwaZulu-Natal shelf sub-aerially for a considerable amount of time (Ramsay, 1994). The present day shelf is on average 3 km wide, with the shelf break between 45 and 70 m, and is characterised by submarine canyons (Ramsay, 1994). Bang (1968) first described three submarine canyons found in the Sodwana Bay region; White Sands Canyon, Wright Canyon and Jesser Canyon. The first two canyons are mature-phase canyons as their heads have breached the shelf and are deeply incised. These canyon heads extend onto the shelf edge as shallow as 38 m. Jesser canyon is a youthful canyon as it is less deeply-incised and it does not traverse the shelf (Farre et al., 1983). The canyons exhibit a classic v-shaped morphology with gradients varying between 10 and 41°. The northern canyon walls are also steeper than the southern, and this is believed to be caused by the flow of the Agulhas Current (Ramsay, 1994). The origin of these canyons is probably attributable to a process called "mass-wasting", whereby increased sediment loading on the continental shelf along Cretaceous-fault lines resulted in large-scale slumping of the sediment load, causing canyons to form (Miller and Ramsay, 2002). The "mass-wasting" would have taken place in Mio-Pliocene times when high sedimentation rates and seismic activity were at an optimum (Miller and Ramsay, 2002).

1.2.3 Oceanography

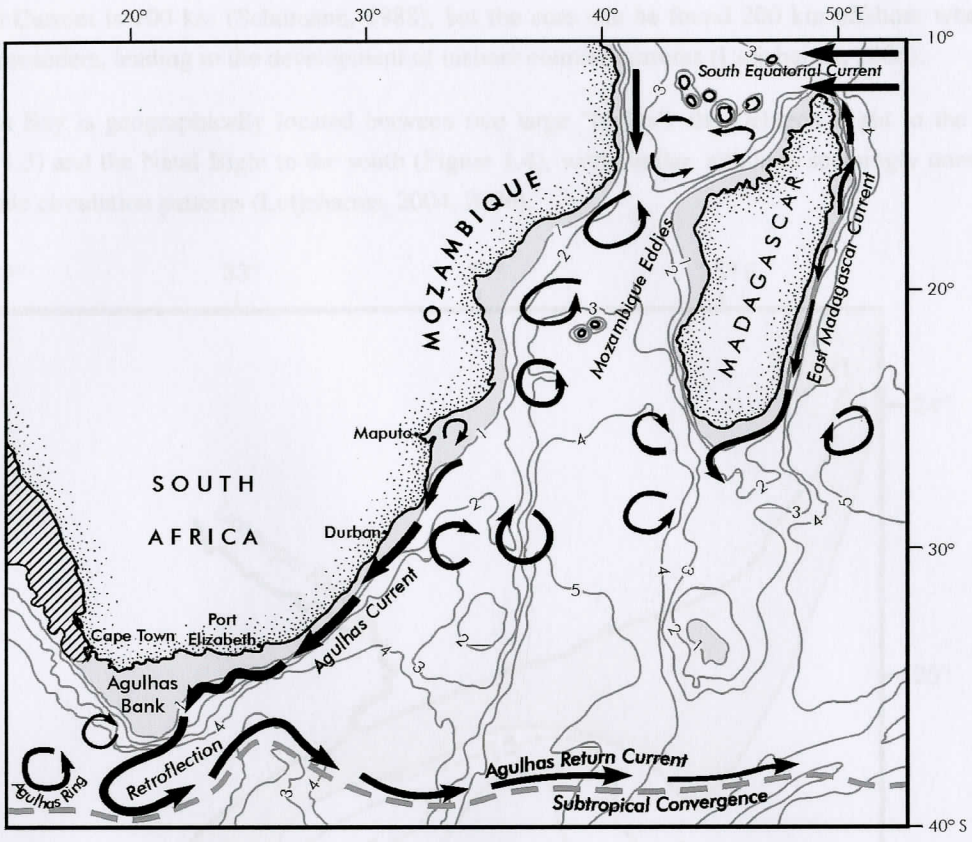

Figure 1.2: The south western Indian Ocean circulation (after Lutjeharms, 2004).

The Agulhas Current is a warm, western boundary current of the South West Indian Ocean subgyre (Lutjeharms et al., 2001), an anti-cyclonic wind-driven circulation system present throughout the year (Lutjeharms, 2006). Figure 1.2 portrays general circulation patterns in the South West Indian Ocean. It compares well in terms of current width and average speeds to the Gulf Stream and Kuroshio Currents, two of the most powerful western boundary currents of the Northern Hemisphere (Lutjeharms, 2006). The Agulhas Current plays a vital role in the global thermohaline circulation system, as the inter-ocean salt and heat exchange between the Indian and Atlantic oceans at the Agulhas Retroflection zone is critical in ensuring that the global "conveyor belt" operates successfully (Lutjeharms, 2006). Large-scale ocean models have shown that, should this exchange or inter-ocean leakage fail in any way, abnormalities will occur throughout the remaining thermohaline circulation system (Lutjeharms, 2006). According to Shouten (2002) the volume transport of the Agulhas Current at 65 Sv, based on the following estimated source water volume fluxes: 30 Sv from the South West Indian Ocean re-circulation, 25 Sv from eddies retroflected from the east coast of Madagascar and 5 Sv from eddies travelling south through the Mozambique Channel (after Stramma and Lutjeharms, 1997). Schumann (1983) suggested that the Agulhas Current originates between 25° and 30° S, while Lutjeharms (2006) suggested that the Agulhas Current was fully constituted south of Ponto do Ouro (26° 50.32 S, 32° 53.10 E). This indicates that the source waters and constitution of the Agulhas Current is not yet fully understood. Gründlingh (1980) calculated a 75 Sv volume flux off Port Edward (31° 3.0 S, 30° 13.0 E) if extrapolated throughout the water column, although 83% of the volume transport occurred in the top 1000 m. No seasonality has been recorded in

the volume transport of the Agulhas Current, despite the seasonal monsoons and wind field variations over the equatorial regions of the Indian Ocean (Pearce and Gründlingh, 1982). The mean width of the Agulhas Current is 100 km (Schumann, 1988), but the core can be found 200 km offshore when the current meanders, leading to the development of inshore counter-currents (Lutjeharms, 2006).

Sodwana Bay is geographically located between two large "bights", the Delagoa Bight to the north (Figure 1.3) and the Natal Bight to the south (Figure 1.4), with similar, although seemingly unrelated, large-scale circulation patterns (Lutjeharms, 2004, 2006).

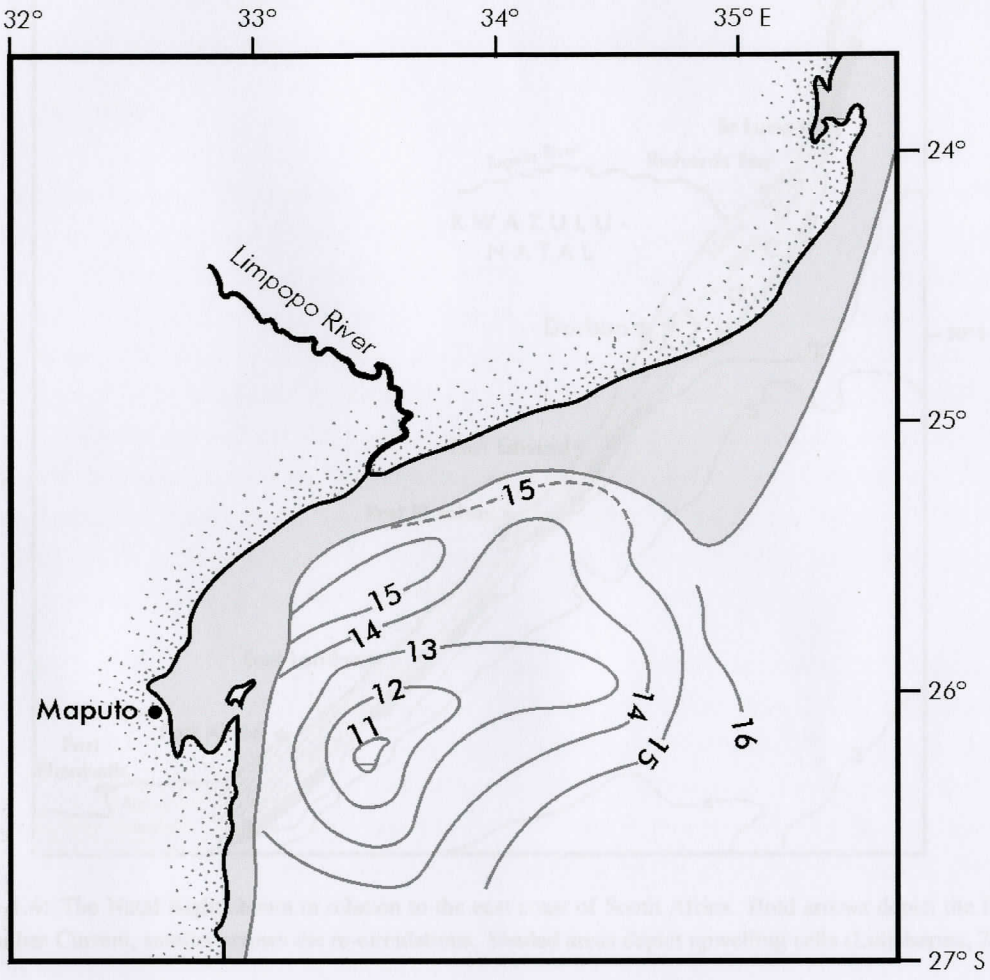

Figure 1.3: The Delagoa Bight and conceptual trapped lee eddy depicted using the isotherms at 200 m (Lutjeharms, 2004)

Lutjeharms and Da Silva (1988) described a cyclonic eddy, the core of which is upwelled from 900 m, in the Delagoa Bight (Figure 1.3). The cyclonic eddy described had the characteristics of a trapped lee eddy forced by water flow past the bight. The origins of this eddy are as yet unknown, but it had been documented 11 times in 23 years and sediment records show the eddy has occurred in the bight for the last 1.8 million years (Lutjeharms, 2006). Lamont et al. (prep) suggested that the Delagoa Bight eddy is a transient feature, which becomes entrapped within the bight due to topographic influences, most probably the 200 m isobath extending southwards. Martin (1978) presented circumstantial evidence of a semi-permanent counter-current flowing north past Ponto do Ouro and may be connected with the cyclonic

eddy in the Delagoa Bight and may potentially cause dynamic shelf upwelling. Further historical data of ship drifts collected from Voluntary Observation Ships (VOS) demonstrated northerly currents between Sodwana Bay (27° 32 S, 32° 41 E) and Kosi Bay on the Mozambique - South African border (Harris, 1978). The frequency of these northerly currents was greater in the north, suggesting a counter-current connected to an eddy in the Delagoa Bight. Harris (1978) calculated from the ship drift data that the southerly flows were stronger (0.5 m s^{-1}) than the northerly flows (0.25 m s^{-1}).

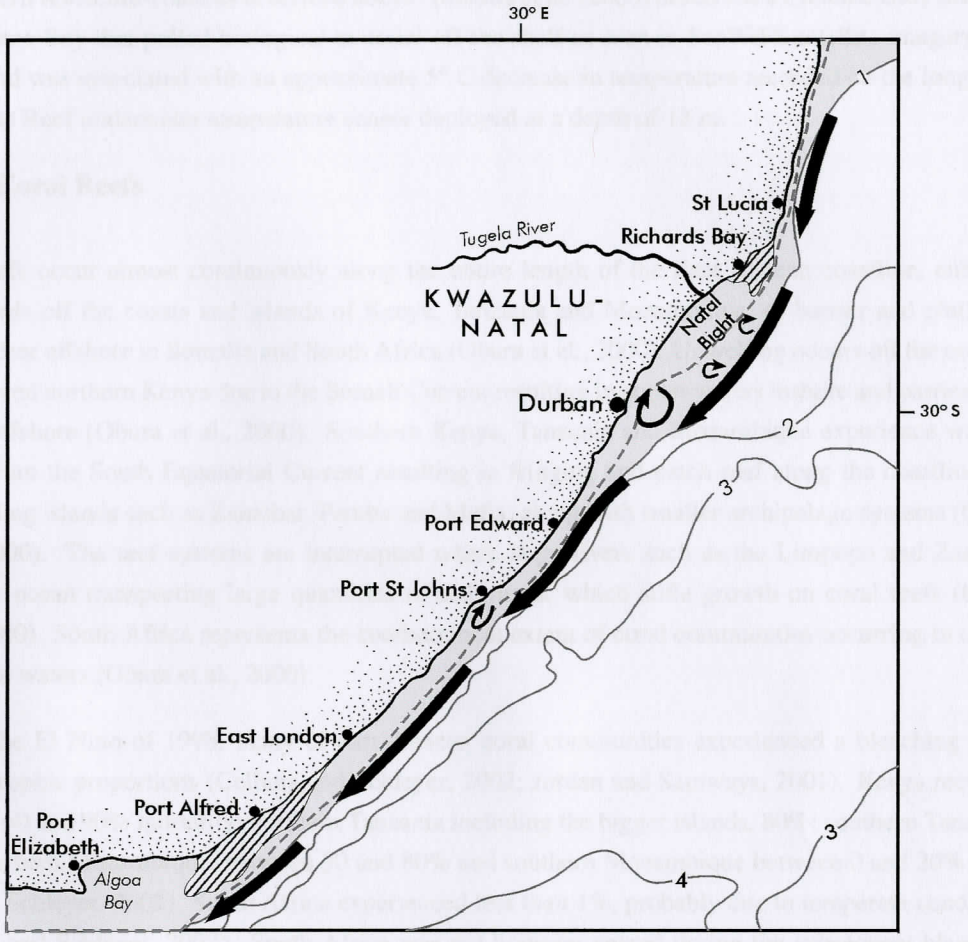

Figure 1.4: The Natal Bight shown in relation to the east coast of South Africa. Bold arrows depict the flow of the Agulhas Current, smaller arrows the re-circulations. Shaded areas depict upwelling cells (Lutjeharms, 2004).

Lutjeharms (2006) describes a second persistent feature of cold, less saline water that is upwelled to 250 m southwest of Durban, resulting in a cyclonic eddy and forcing a semi-permanent inshore counter-current along the Natal Bight (Figure 1.4). The "Natal Pulse" is caused by barotrophic instabilities in the Natal Bight (Shouten, 2002) due to vortex-shedding from the above-mentioned cyclonic circulation. The pulse is a cold core cyclonic eddy with a diameter of approximately 130 km, and allows substantial counter-currents to develop inshore as it propagates southwards at approximately 20 cm s^{-1} (Shillington, 1992). It is an irregular solitary meander occurring 4 – 6 times per year (Lutjeharms et al., 2001). Altimetric data has suggested that large-scale eddies, travelling south through the Mozambique Channel, may be responsible for strengthening these "pulses" and potentially even assist in the formation thereof (Shouten, 2002).

Mesoscale eddies have been observed using thermal infrared images off northern KwaZulu-Natal from

the late 1970's and are thought to originate north of 28° S, due to topographic influences (Gründlingh and Pearce, 1984). One particular eddy off St. Lucia had a diameter of 100 km and circular transport varying between 6 and 18 Sv (Gründlingh, 1984). Some of these large eddies have been seen to encompass the entire Agulhas Current diameter, causing a lapse in current flow downstream of the eddy (Lutjeharms, 2006). Furthermore, Lutjeharms (2006) suggests that the Delagoa Bight eddy could potentially create "pulses" similar to those off the Natal Bight and propagate southwards, given the occurrences of eddies off northern KwaZulu-Natal as described above. Roberts et al. (2006) described a cyclonic eddy offshore of Sodwana Bay that pulled biological material off the shelf as seen in SeaWiFS satellite imagery presented and was associated with an approximate 5° C decrease in temperature recorded on the long-term Nine-mile Reef underwater temperature sensor deployed at a depth of 18 m.

1.2.4 Coral Reefs

Coral reefs occur almost continuously along the entire length of the East African coastline, either as fringe reefs off the coasts and islands of Kenya, Tanzania and Mozambique, or barrier and platforms reefs further offshore in Somalia and South Africa (Obura et al., 2000). Upwelling occurs off the coast of Somalia and northern Kenya due to the Somali Current resulting in cooler waters inshore and barrier reefs further offshore (Obura et al., 2000). Southern Kenya, Tanzania and Mozambique experience warmer waters from the South Equatorial Current resulting in fringing and patch reef along the coastline and surrounding islands such as Zanzibar, Pemba and Mafia, along with smaller archipelago systems (Obura et al., 2000). The reef systems are interrupted where large rivers such as the Limpopo and Zambezi enter the ocean transporting large quantities of sediments, which stifle growth on coral reefs (Obura et al., 2000). South Africa represents the southernmost extent of coral communities occurring in cooler temperate waters (Obura et al., 2000).

Due to the El Nino of 1998, many of east African coral communities experienced a bleaching event of catastrophic proportions (Celliers and Schleyer, 2002; Jordan and Samways, 2001). Kenya recorded between 60 and 90% mortality; northern Tanzania including the bigger islands, 80%; southern Tanzania, 50%; northern Mozambique, between 30 and 80% and southern Mozambique between 0 and 20% (Celliers and Schleyer, 2002). South Africa experienced less than 1%, probably due to temperate conditions (Celliers and Schleyer, 2002). South Africa was not however spared during the subsequent bleaching event in 2000 (Celliers and Schleyer, 2002).

Communities in Kenya, Tanzania and Mozambique who reside along the coast rely on the coral reefs as a source of income as artisanal and commercial fishermen and tourism operators (Obura et al., 2000). South African coral reefs are remote from large populations and occur within two marine reserves, St Lucia established in 1979 and Maputaland established in 1986, and thus only play host to tourism and recreational activities (Schleyer, 1999).

The major coral reef systems along the northern KwaZulu-Natal coast were categorised according to geographical locality: the northern complex, opposite the Kosi Lake system, the central complex at Sodwana Bay and the southern complex at Leven Point as shown in Figure 2.1 (Schleyer, 1999). Initial research concentrated on biological surveys, species composition and reef descriptions and ninety species of hard corals, forty species of soft corals and 30 species of ascidians and sponges have been described (Muthiga et al., 2008). Furthermore the corals were found to be of temperate and tropical Indo-Pacific origin (Riegl et al., 1995). Northern KwaZulu-Natal corals are not true coral reefs which grow by means of biogenic

accretion and thus may be considered marginal (Schleyer, 2000). These coral communities colonised the beachrock and aeolianite outcrops resultant from the glacial maximum sea-level rise (Ramsay, 1994), and range from depths of 8 to 35 m. Northern KwaZulu-Natal reef systems also lack traditional geomorphological traits such as lagoons, reef crests and steep reef slopes (Schleyer, 1999). They are considered topographically homogeneous with ridges and gullies lying perpendicular to swell direction (Schleyer, 1999). Two reef types were identified due to biological considerations; reef-top sub-communities dominated by soft corals, and gully sub-communities dominated by hard corals due to higher levels of sedimentation in the gullies (Schleyer, 1999). Hard corals are thought to be active sand-shedders that withstand increased levels of sedimentation, whilst soft corals are passive (Schleyer, 1999). Schleyer and Celliers (2003b) showed that high levels of turbulence on reef-tops and soft corals found at reef-sediment interfaces proved that the accepted division of coral colonies due to sediment tolerance was incorrect. Some species of soft corals have either high profiles, flexible stalks or soft and pliable anatomy, enabling them to rid themselves of destructive sediment (Schleyer and Celliers, 2003b). A ten-year photographic study initiated to analyse changes in coral communities illustrated an increase in hard corals while soft corals are decreasing, except at the reef-sediment interface where sediment-tolerant soft corals dominate (Schleyer and Celliers, 2003a). The coral reefs and sponge communities contribute surficial bioclastic sediment to the surrounding area, which is transported southwards with the Agulhas Current (Ramsay, 1994).

More recently, investigations have concentrated on climate change and the impacts on South Africa's high-latitude marginal reefs. Coral bleaching occurs when symbiotic zooxanthella, which produces oxygen and food for the corals by means of photosynthesis, are expelled from the coral polyps (Celliers and Schleyer, 2002). The loss of these symbiotic algae can be due to certain environmental conditions: elevated sea temperatures, solar radiation, reduced salinity, bacterial infections, sedimentation and exposure at low tides (Celliers and Schleyer, 2002). Sodwana Bay experienced a 0.27° C $year^{-1}$ increase in temperature recorded over a six-year period (1994-2000) by an Underwater Temperature Recorder (UTR) at Nine-mile Reef, Sodwana Bay (Celliers and Schleyer, 2002). This compared well to a gradual 0.01° C $year^{-1}$ increase over a 50-year period (1950-2000) extrapolated from regional sea surface temperature satellite data (Celliers and Schleyer, 2002). The 2000 coral bleaching event was more substantial than 1998 and was caused by the increase in sea surface temperatures and solar radiation penetrating onto horizontal reef faces (Celliers and Schleyer, 2002). Floros et al. (2004) showed an increase in coral bleaching from <1% in 1998 to between 5 and 10% in 2002. Sebastian and Sink (2005) showed reefs in Southern Mozambique and Northern KwaZulu-Natal to exhibit vulnerability to bleaching even in low thermal stress conditions. Furthermore, they showed that due to patchy distribution of surveyed reefs and thus limited connectivity, post-bleaching coral recovery may be limited.

Riegl (2003) suggested that Ekman veering of the Agulhas Current along the shelf edge allowed cooler water to upwell onto the shelf which prevented bleaching in 1998 and 2002 from reaching catastrophic proportions as experienced in other regions of the Mozambique Channel (Celliers and Schleyer, 2002). This hypothesis was proposed based on the NMR six-year UTR record showing an annual cold water event occurred in the marine summer, attributed to upwelling, in every year except 1998 (Riegl and Pillar, 2003). Further evidence of cool events in Sodwana Bay is given in extrapolated sea surface temperature data derived from remote sensing datasets (Riegl and Pillar, 2003). Canyon-induced upwelling is explored in Riegl and Pillar (2003) where they suggest the canyon-heads dissecting the shelf slope are perfect avenues for upwelled water to reach the shelf. Riegl and Pillar (2003) concluded that high-latitude reefs

may be well positioned to survive global climate change with regards to physical warming of the ocean, however damaging chemical processes were not explored.

1.2.5 Larval Transport

The majority of coral species use broad-cast spawning (external fertilisation) as their preferred method of sexual reproduction, as opposed to brooders which use internal fertilisation and release larvae into the water (Miller and Mundy, 2003; Black et al., 1991). Assuming an instantaneous release of larvae, advection by shelf currents and diffusion by turbulence and re-circulation, Williams et al. (1984) concluded, using current meters and drogue data within the constraints of a model, that larvae were lost from their natal reefs within a few days (and even hours) of being spawned. It was also assumed that larvae remain within the water column for between two and eight weeks before they settle onto suitable substratum (Black et al., 1991). Largier (2003) describes seven indirect methods of estimating larval dispersal, owing to the size of spawned larvae in the water column: a) Population genetics, b) observations of the rate of invasion of exotic species, c) microchemistry of crab exoskeletons, fish otoliths and mollusc shells, d) inferences from correlations between settlement and oceanography, e) observations of meroplankton distribution, f) larval biology studies and g) numerical methods. All seven methods rely on a large degree of interpretation and aggregation. A number of numerical models have been developed to understand the larval dispersion over the Great Barrier Reef (GBR) in Australia (Black et al., 1991; Williams et al., 1984; Byers and Pringle, 2006). Black et al. (1991) showed, using a 3-dimensional model comprised of a number of 2-dimensional models, that larval positioning within the water column had a major impact on their retention possibilities. Larvae at the surface were dispersed mainly by wind-driven currents and mid-water larvae by shelf currents. Larvae which remain close to the sea-floor had a 95% chance of retention on the natal reefs. Black et al. (1991) also showed that only 3% of larvae originated on a reef from upstream sources as opposed to 45% from with-in reef spawning.

The majority of recruitment to coral reefs was thought to come from neighbouring reefs upstream and spawned material exported to reefs downstream (Williams et al., 1984). However, should this theory be true, coral reefs would be seen to "move" downstream as older generations die off, eventually disappearing altogether in cooler waters. Instead a 'drift paradox' exists whereby adult populations persist, regardless of mean current direction (Byers and Pringle, 2006). Retention and upstream dispersal are reliant on a number of factors: a) spawning in multiple sessions or seasons to make use of current fluctuations – an energetically efficient dispersal mechanism, b) smaller planktonic phases and c) high reproductive rate over their entire life span. Laboratory experiments have yielded differing results with regards to planktonic phases. Williams et al. (1984) showed that planulae from acroporid and faviid species developed 2-3 days after spawning, began actively searching for suitable substrata after 5-7 days and only settled between 14 and 36 days after spawning. In a second experiment, larvae of two faviid species settled on substrata within 2.5 and 2.75 days after spawning and metamorphosis began after 3.75 days (Miller and Mundy, 2003). Thus Miller and Mundy (2003) concluded that the dispersal potential would be less and that reefs could be largely self-seeding.

Coral planulae do have the capacity, based on their energetics, to forgo settlement once they become ciliated, which allows them to settle, (18 - 72 hours in broadcast spawners and almost immediately in brooders) and survive in their planktonic state for a period of time known as a competency period (Richmond, 1997). Richmond (1987) found that *Pocillopora domicornis* could survive 100 days before

settling successfully based on calculations of stored energy reserve and metabolic expenditure. The dry weight of planulae was made up of 17% protein, 70% lipid and 13% carbohydrates (Richmond, 1987). The soft coral *Heteroxenia fuscescens*, widely distributed along the east coast of Africa, has a competency period of 49 days, possibly aiding their distribution (Zaslow and Benayahu, 1996). These competency periods for planktonic planulae provide an opportunity for larvae to be retained, or even returned, to regions of suitable habitat for settlement. The question of viability of these planulae are brought into question by Nishikawa and Sakai (2005) who show only 18% and 25% viable planulae for *Acropora digitifera* and *Acropora tenuis* respectively. Furthermore Nishikawa and Sakai (2005) stated that competency periods and survival rates are unlikely to be robust indications of gene flow and the implications for long distance dispersal thus remains unclear.

A study of coral recruitment in Sodwana Bay showed that recruitment peaked between March and May (Glassom et al., 2006). The broadcast spawners on the reefs had a peak spawning period during January and February and dominated the ceramic tiles used in this study as settling plates in March (Glassom et al., 2006). Brooders peak spawning occurs during April and May, with most recruitment on settling plates in May (Glassom et al., 2006). High recruitment was also recorded on NMR and Glassom et al. (2006) suggested oceanographic influences (eddies and counter-currents) may be responsible for the self-seeding evident on this reef. This high recruitment would be due either to seeding from reefs from the north, or as Byers and Pringle (2006) suggested from studies undertaken on the Great Barrier Reef, retention to the natal reef of spawned material.

What emerged from the literature reviewed was a lack of information with regards physical oceanography on the northern KwaZulu-Natal coastline and what affect the physical oceanographic processes would have on the unique fauna inhabiting the region with regards coral bleaching events and coral larval transport.

1.3 Project Description

The Oceanographic Research Institute (ORI) began their biological research on the coral reef communities in the 1980's by compiling inventories of the corals inhabiting the reefs and the structures thereof (Schleyer, 1999). Research on the reefs gained momentum in the 1990's and a temperature sensor was established on NMR as a long-term monitoring site in March 1994. The objective was to correlate sea temperature changes with biological anomalies on the corals reefs (Schleyer, 1999). These data revealed that elevated temperatures occurred during the coral bleaching events of 1998 (Obura et al., 2000) and 2000 (Celliers and Schleyer, 2002). One temperature recorder was not sufficient in determining the impacts of physical oceanographic parameters on the coral communities and their subsequent response to these influences. A collaborative study was thus initiated between Marine and Coastal Management (MCM) and ORI in March 2001 to address this issue.

Historically very little is known oceanographically about northern KwaZulu-Natal and in particular Sodwana Bay (Harris, 1978; Gründlingh and Pearce, 1984; Lutjeharms, 2004, 2006). In addition to this lack of data, the location of the source of the Agulhas Current is unknown and is assumed to be fully constituted between 25° and 30° S (Schumann, 1983) or somewhere south of Ponto do Ouro (Lutjeharms, 2006). Sodwana Bay falls within the definition of the Agulhas Current "source area", and thus working on the assumption that the Agulhas Current is fully constituted north of Sodwana Bay, an Acoustic Doppler Current Profiler (ADCP) was deployed to the north of the embayment instead of to the south to monitor the Agulhas Current and its affect on the shelf region at Sodwana Bay. Anecdotal evidence, reported by SCUBA diving operators and research staff involved with the study, reported northerly currents at Sodwana Bay. The resolution of these changes to assumed current flow, and the driving forces thereof, will form part of the objectives of this study.

Riegl and Pillar (2003) speculated that the submarine canyons described by Ramsay (1994) at Sodwana Bay would create avenues of cold water onto the shelf, cooling the coral communities significantly and preventing coral bleaching. This mechanism of upwelling, along with suspected shelf edge upwelling caused by the southward propagation of the Agulhas Current, will be investigated by analysing the temperature sensors deployed for the study period. The long-term Underwater Temperature Recorder (UTR), deployed in 1994, was complemented by a recorder offshore and one to the south to provide cross-shelf and along-shelf dynamics respectively. One recorder on the Wright Canyon head (Figure 2.2) will provide the data required to study canyon-induced upwelling in the region.

The physical oceanographic characteristics, driving forces and dynamics will be applied to biological processes affecting the the coral communities resident to Sodwana Bay in order to determine any relationships and interactions. These relationships will be determined in an applied manner as insufficient biological information is available to determine, for instance, the larvae dispersal of corals spawning at Sodwana Bay. Recommendations will be made on the results of this study and any future research which would be beneficial in the continued oceanographic understanding of the northern KwaZulu-Natal shelf with relevance to the coral communities unique to the region.

1.4 Key Questions

1. What are the current characteristics of Nine-mile Reef, and by assumption, Sodwana Bay?
2. Do northerly reversals in current flow occur at Sodwana Bay?
3. What are the driving forces of the current characteristics described above?
4. Does upwelling occur at Sodwana Bay? If so, what types of upwelling occur?
5. What are the implications of the physical oceanographic parameters described by the above objectives on:
   (a) Coral larval transport?
   (b) Coral bleaching in the context of global climate change?

Chapter 2

Materials and Methods

2.1 Study Area

The northern KwaZulu-Natal coast, referred to locally as Maputaland, extends from Cape St. Lucia (28° 0.0 S, 32° 30.0 E) to Ponto do Ouro on the border between South Africa and Mozambique (Figure 2.1). The coastline is divided into two marine reserves, the Maputaland Marine Reserve in the north and the St. Lucia Marine Reserve in the south, which form the iSimangaliso Wetland Park (IWP), formerly the Greater St. Lucia Wetland Park (GSLWP), administered by Ezemvelo KZN Wildlife (Figure 2.1). The St. Lucia Marine Reserve was established in 1979 and the Maputaland Marine Reserve in 1986 after only initial inventory studies were carried out in the early 1980s (Schleyer, 1999), effectively protecting ecologically sensitive and valuable marine fauna and flora from human impact. In December 1999, the GSLWP was proclaimed the only Marine World Heritage Site in South Africa. Two areas were set aside as sanctuaries (dark shading on Fig. 2.1) resulting in further protection from human interference. Some areas in the reserves are open to SCUBA diving and pelagic game fishing activities, and Sodwana Bay in particular is subjected to considerable tourism activity each year.

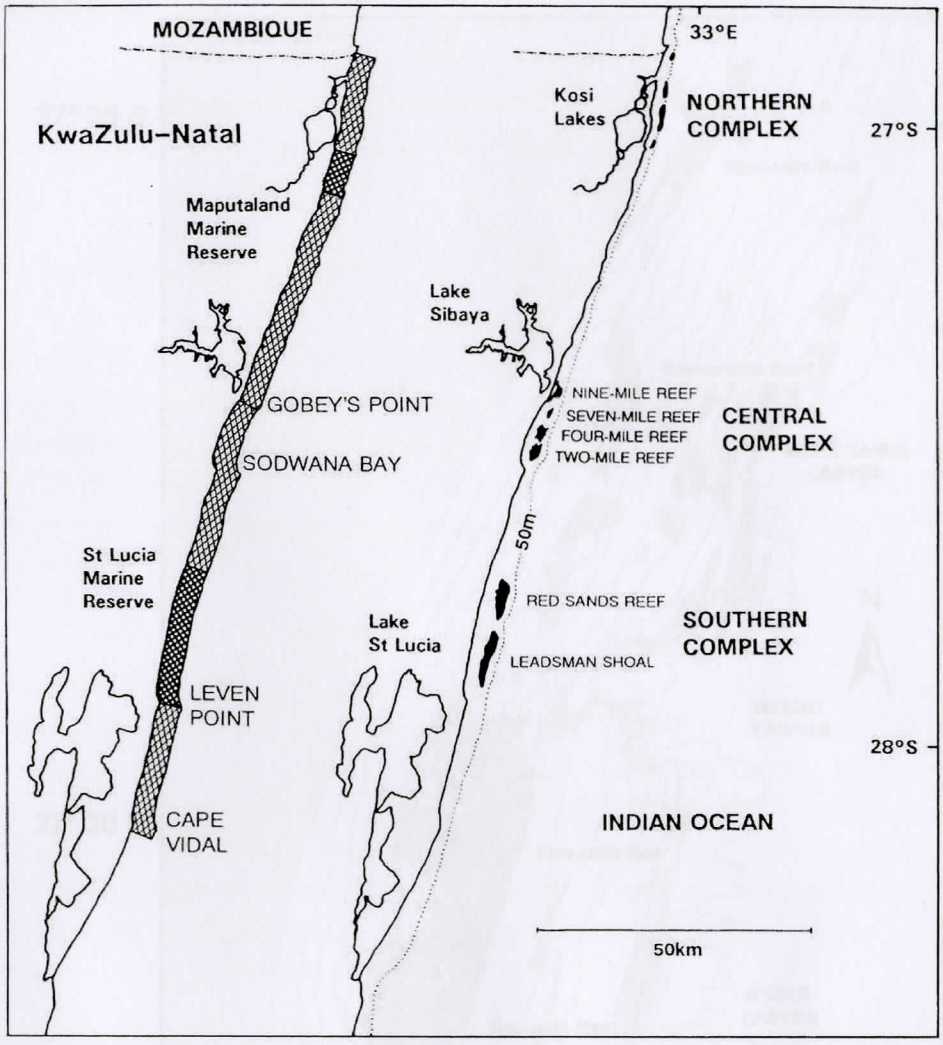

Figure 2.1: The northern KwaZulu-Natal coastline with the Maputaland Marine Reserve extending north of Gobey's Point and the St. Lucia Marine Reserve to the south. The darker shaded areas are sanctuary areas, and the lighter shading reserves. The coral reef complexes are depicted on the right. (Schleyer, 1999; Riegl et al., 1995)

The iSimangaliso Wetland Park is divided topographically into three large coral reef complexes; the northern, central and southern complexes as illustrated in Figure 2.1 (right). The northern and southern complexes are not as easily accessible and research in these areas has been limited, until recently when road systems were upgraded. The northern complex is made up of smaller reefs clustered close to the Kosi Mouth, and the southern complex has two large reefs at Red Sands and Leadsman Shoal.

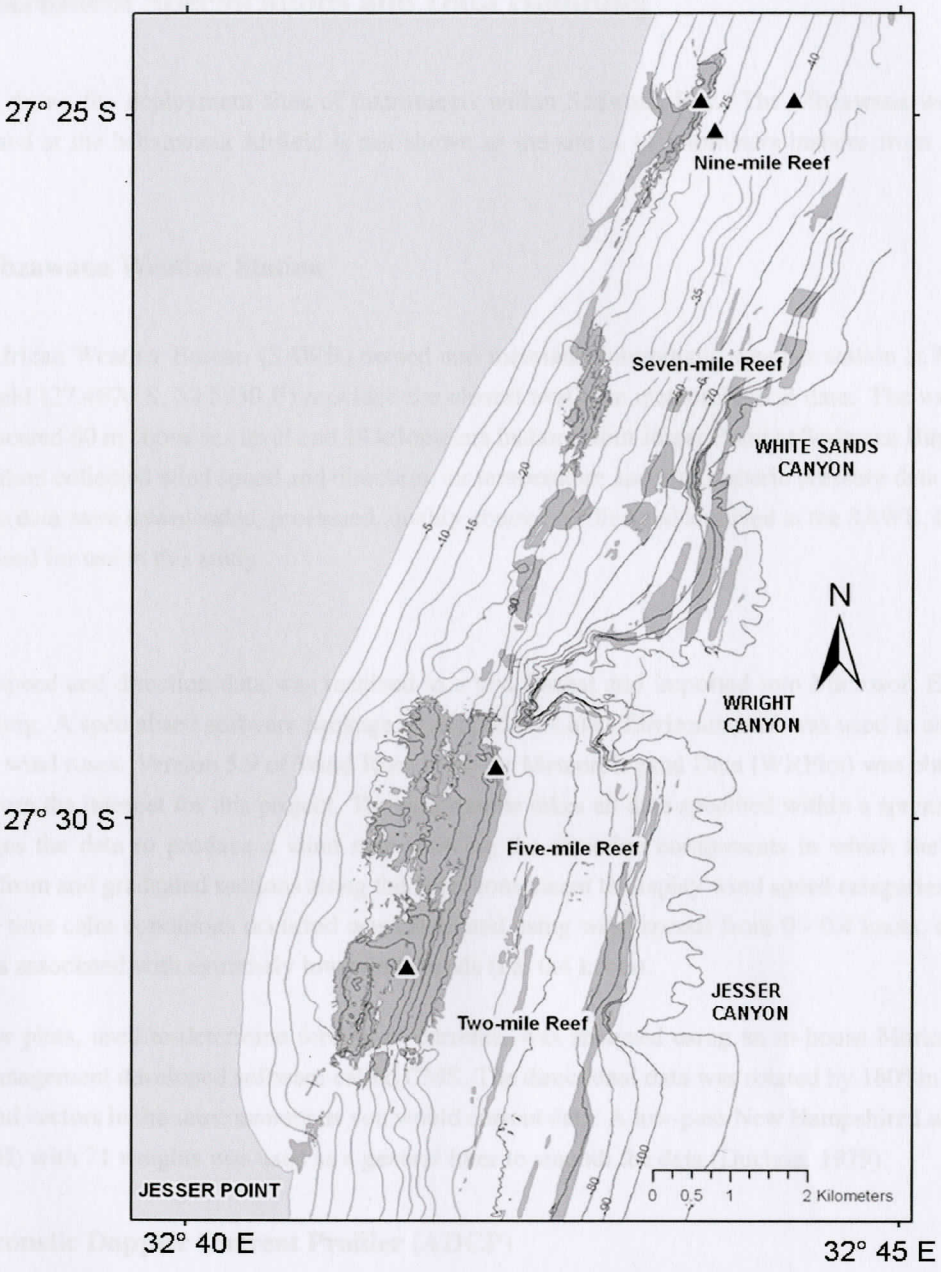

Figure 2.2: Instrument positions within Sodwana Bay. Figure produced by Dr. Celliers, with data from the Marine Geoscience Unit in Durban.

Sodwana Bay consists of the reefs encompassed within the central complex. The reefs are named according to their approximate distance from the beach launch site at Jesser Point. The major reef systems are Two-mile Reef (TMR), Four-mile Reef and Nine-mile Reef (NMR), with smaller reefs at Quarter-mile, Five-mile (FMR) and Seven-mile (Figure 2.2). Sodwana Bay is incised by three canyons: two mature-phase canyons, Wright and White Sands Canyons, and a youthful-phase canyon named Jesser Canyon. The mature-phase canyons make headlands on the shelf edge. The most prominent of which is Wright Canyon.

2.2 Instrument Specifications and Data Handling

Figure 2.2 shows the deployment sites of instruments within Sodwana Bay. The Mbzawana weather station, based at the Mbzawana Airfield is not shown as the site is 14 kilometers inshore from Jesser Point.

2.2.1 Mbzawana Weather Station

A South African Weather Bureau (SAWB) owned and maintained automatic weather station at Mbzawana Airfield (27.4670 S, 32.5830 E) provided the closest available meteorological data. The weather station is located 60 m above sea level and 14 kilometers inshore from Jesser Point at Sodwana Bay. The weather station collected wind speed and direction, air temperature and atmospheric pressure data every hour. These data were downloaded, processed, quality control verified and archived at the SAWB, before being released for use in this study.

The wind speed and direction data was received in a text format and imported into Microsoft Excel® for processing. A specialised software package developed by Lakes Environmental was used to analyse the data as wind roses. Version 5.9 of Wind Rose Plots for Meteorological Data (WRPlot) was obtained freeware from the internet for this project. The programme takes all data specified within a spreadsheet and averages the data to produce a wind rose showing the direction components in which the wind originated from and graduated sections along the wind component to display wind speed categories. The percentage time calm conditions occurred was calculated using wind speeds from 0 - 0.4 knots, due to the stillness associated with extremely low wind speeds (i.e. 0.4 knots).

Stick vector plots, used to determine forcing of currents, was analysed using an in-house Marine and Coastal Management developed software called CMS. The directional data was rotated by 180° in order to view wind vectors in the same manner as you would current data. A low-pass New Hampshire Lanczos Filter (UNH) with 71 weights was used as a general filter to smooth the data (Duchon, 1979).

2.2.2 Acoustic Doppler Current Profiler (ADCP)

An RD Instruments 300 kHz Workhorse Sentinel Acoustic Doppler Current Profiler (ADCP) was deployed offshore of NMR in 26 m of water in March 2001 (27° 25.111 S, 32° 43.700 E). A stainless steel box frame weighted down with two concrete filled PVC tubes was used as a superstructure on which the ADCP could be bolted onto for deployments. Four anchored sub-surface buoys were deployed on the corners of the frame to assist SCUBA divers in locating the instrument. Due to the size of the frame and the potential damage it could cause coral reefs, the structure was deployed on sand, slightly offshore of the NMR reef community. The region is famed for sand dunes travelling along the coast. To counteract this problem, the centre box frame can be raised with additional stainless steel rods to lift the ADCP above the sand. Figure 2.3 was taken from video footage of the deployment of the superstructure in March 2001, with the ADCP bolted to the top.

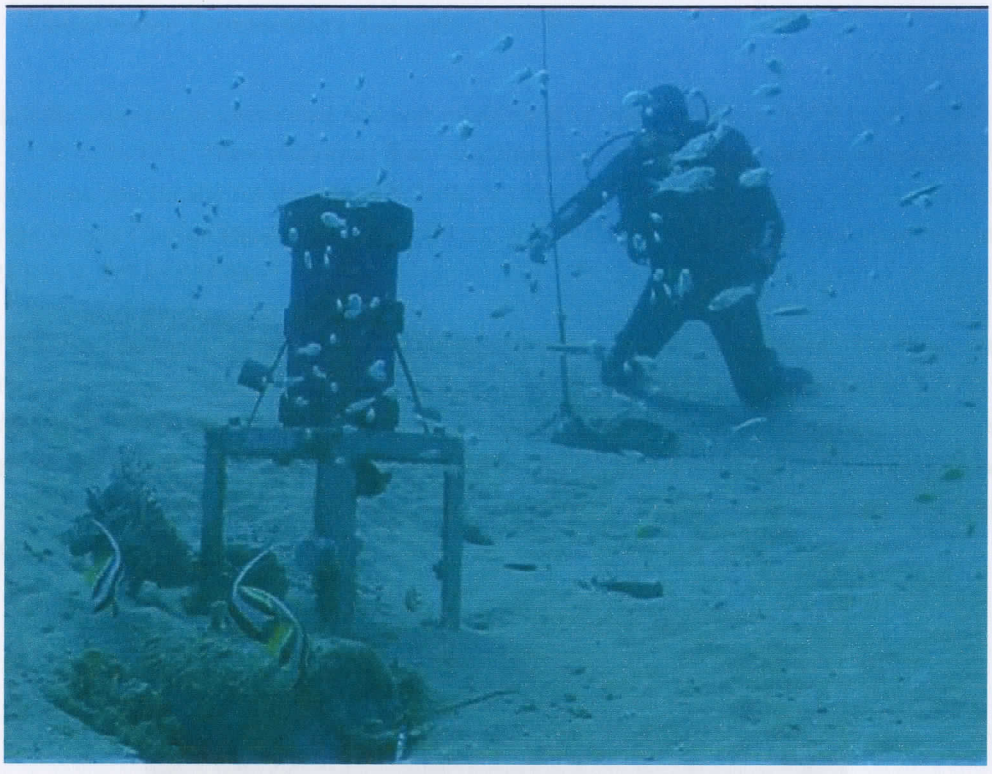

Figure 2.3: ADCP frame with instrument deployed above. The square metal box in the middle was built up, when needed, to counteract the influence of sand dunes (Photo: Prof. Schleyer).

Retrieval of the ADCP would take place early on the day of servicing. The downloading of data and servicing of the instrument would take an afternoon to complete and the ADCP would be re-deployed the following morning. Servicing of the battery pack powering the ADCP took place every three to four months to avoid battery failure. The loss of 24 hours of data to service the ADCP was justified to prevent significant data loss due to equipment failure, which was avoided during this study. Unfortunately, current conditions were not monitored during this break in data collection.

The instrument was configured to collect data every 30 minutes in 2 m bins. A blanking distance of 2 m from the transducer head at 26 m to 24 m does not record usable data and was discarded. Depth bins, where the percentage of good data was less than 75%, were discarded as bad data. The 2 m bin was considered bad 100% of the time, the 4 m bin 63.3% of the time. Thus the 6 m bin was used during data analysis as the surface measurement and 22 m as the bottom measurement.

ADCP data was downloaded from the instrument using software supplied with the ADCP by RD Instruments. The data was converted to ASCII format and imported into Microsoft Excel®. The data was prepared into monthly and six monthly data sets and converted for analysis into the specialised software package, CMS, developed in-house at Marine and Coastal Management. The data was corrected to true north by applying the magnetic variation for the area; -20° (20° W). This variation was obtained from the compass rose on SAN chart 134. Progressive, component and stick vector plots were produced from this corrected data.

2.2.3 Underwater Temperature Recorders (UTR)

A long-term temperature monitoring site was established in March 1994 on NMR at 18 m (27° 24.89 S, 32° 43.60 E) by ORI. Three additional Star-Oddi Starmon Underwater Temperature Recorders (UTR) were deployed specifically for this project: TMR in 12 m of water (27° 31.058 S, 32° 41.550 E), FMR above the Wright Canyon Head at 37 m (27° 29.635 S, 32° 42.168 E) and Nine-Mile Deep also at 37 m (27° 24.894 S, 32° 44.253 E).

The UTRs were deployed on concrete blocks designed specifically for this purpose. The block was cast and allowed to set with four bolts positioned thread-side up, to allow the bolting down of PVC straps across the UTR PVC canister, which holds the instrument. A special hollow was molded onto the drying concrete to fit the UTR canister and this prevented the UTR being washed away by surge (Figure 2.4). The concrete blocks were wedged between rocks or underneath ledges on well-mapped coral reefs and sponge beds.

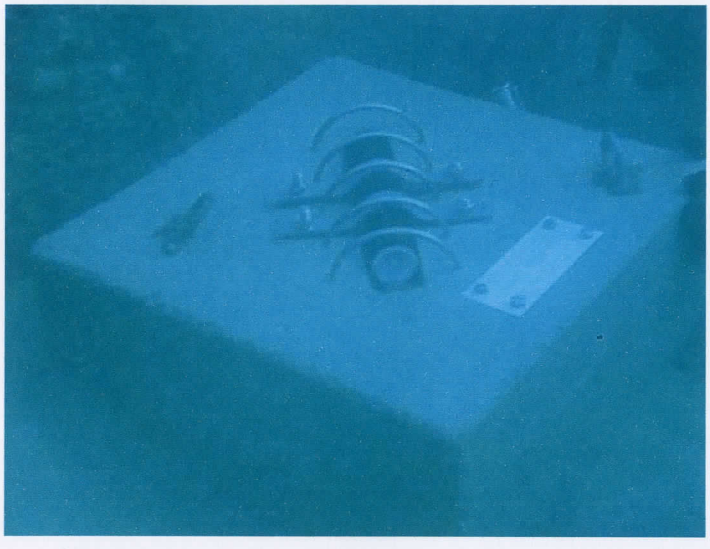

Figure 2.4: UTR block with instrument deployed underneath PVC straps and stainless steel rings (Photo: Prof. Schleyer).

The UTR instruments were set-up to collect a temperature reading every hour. The UTR instruments arrived from the manufacturer calibrated with an accuracy of 0.01 ° C. From time to time the instruments are set-up alongside a "master" probe, which is maintained in a temperature controlled environment at factory calibration standards. Temperature recorders tend to drift from the calibration values fairly slowly, making the instruments simple to maintain.

UTR data was downloaded from the instruments using Sea Star, software supplied by the manufacturer with the instrument, and imported into Microsoft Excel®. The hourly data records were averaged into daily values, which were in turn averaged into monthly values. Hourly data was used for the interpretation of the data, however refined it may be. In certain cases courser daily and monthly data plots were used.

2.2.4 Satellite Applications / Remotely Sensed Data

Sea Surface Height Anomaly (SSHA) images were compiled using data from Topex/Poseidon, ERS and ENVISAT missions. The images were produced by SSALTO/DUACS and distributed by AVISO, with support from CNES. Details of the processing of altimeter images have been outlined in the SSALTO/DUACS User Handbook (M)SLA and (M)ADT Near-Real Time and Delayed Time Products. All data quality control and assurance for the SSHA images took place at the source (SSALTO/DUACS User Handbook, 2004). Delayed time images were used for this work. Delayed time images were produced at weekly intervals.

SSHA images were imported into Ocean Data View for visualisation (Schlitzer, 2007). A configuration file was compiled by Miss Tarron Lamont of MCM to delineate the geographical area of interest and the range and colour bar settings.

Chapter 3

Results

3.1 Meteorological Data

The wind data were analysed and plotted into wind rose diagrams to illustrate prominent wind components and seasonal characteristics. Wind components are shown from the direction they originated. Figure 3.1 was plotted to represent the entire period of study (01 March 2001 to 31 August 2003). This constituted 21488 hourly data records (895.3 days), with only 448 hours (18.7 days) of data gaps for the period of analysis. Calm periods were recorded for 17.46% of the study period (0 - 0.4 knots, as per Lakes Environmental Wind Rose Plotting Software). The average wind speed measured for the study period was 2.80 m s^{-1} (SD: 2.06 m s^{-1}, variance: 4.27 m s^{-1}).

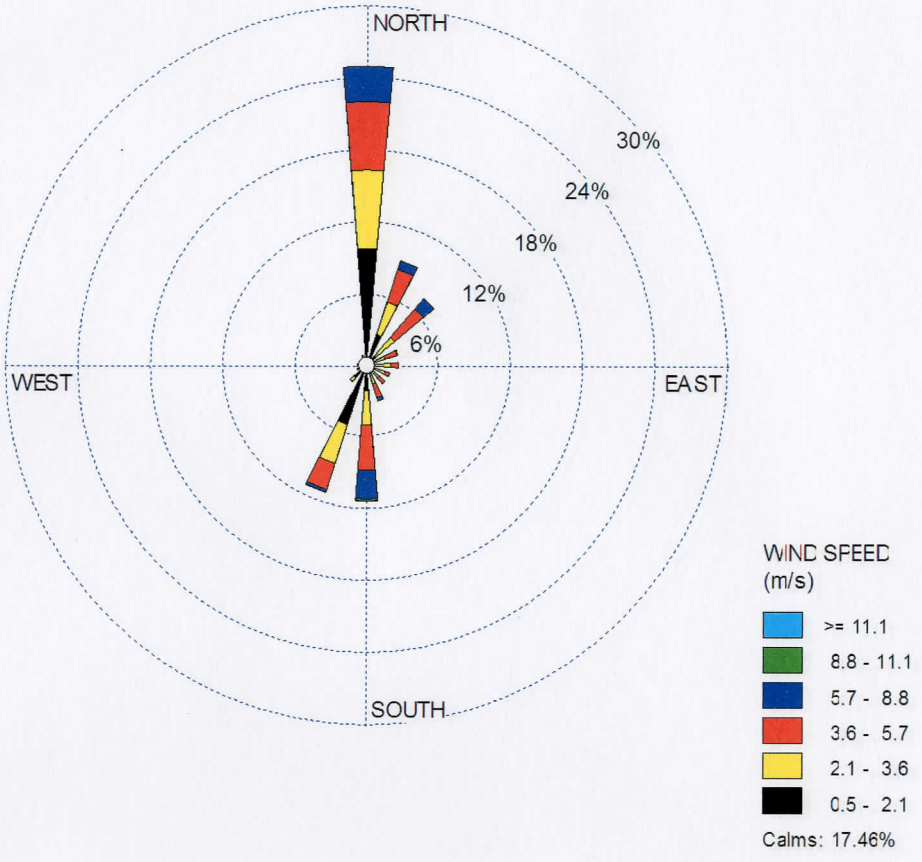

Figure 3.1: Wind rose plot for the entire study period: March 2001 - August 2003.

A strong northerly component, and a weaker southerly component, illustrated that the majority of winds originated from Mozambique (Fig. 1.2). Weaker alongshore winds were evident with the NNE and SSW components, with the coastline lying approximately 20° to the east of true north. Smaller onshore components were evident from the east (sea breezes), but no berg winds from the interior moving offshore were recorded (land breezes). The strongest wind speed category for most components was 5.7 - 8.8 m s^{-1} (blue). The southerly component showed a small section of the 8.8 - 11.1 m s^{-1} category (dark green), suggesting stronger winds occurred from the south.

The 30-month data set was divided into seasons to determine seasonal trends of wind direction forcing. The seasons were categorised as follows:

- Autumn - March, April and May
- Winter - June, July and August
- Spring - September, October and November
- Summer - December, January and February

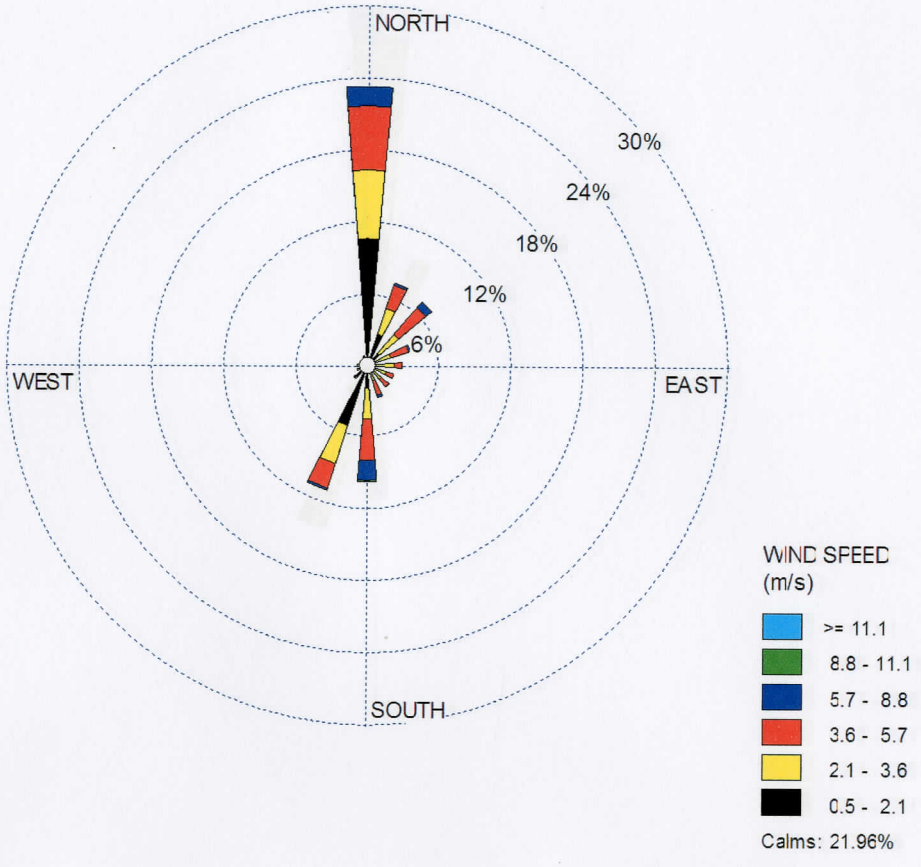

Figure 3.2: Autumn seasonal mean wind rose (March, April and May) for 2001, 2002 and 2003.

A seasonal mean wind rose is shown in Figure 3.2 for the three autumn seasons recorded for this study. The seasonal mean was calculated using 6556 hours of data. A strong northerly component was predominant. The alongshore component from the SSW was more prominent than the southerly component. Onshore and alongshore winds from the NNE and NE were also evident, although not as dominant. Calm periods were recorded for nearly a quarter of the study (21.96%) with an average wind speed of 2.73 m s^{-1} (SD: 1.87 m s^{-1}, variance: 3.52 m s^{-1}). The strongest wind speed category measured was 5.7 - 8.8 m s^{-1} (dark blue) on northerly, north-easterly and southerly components.

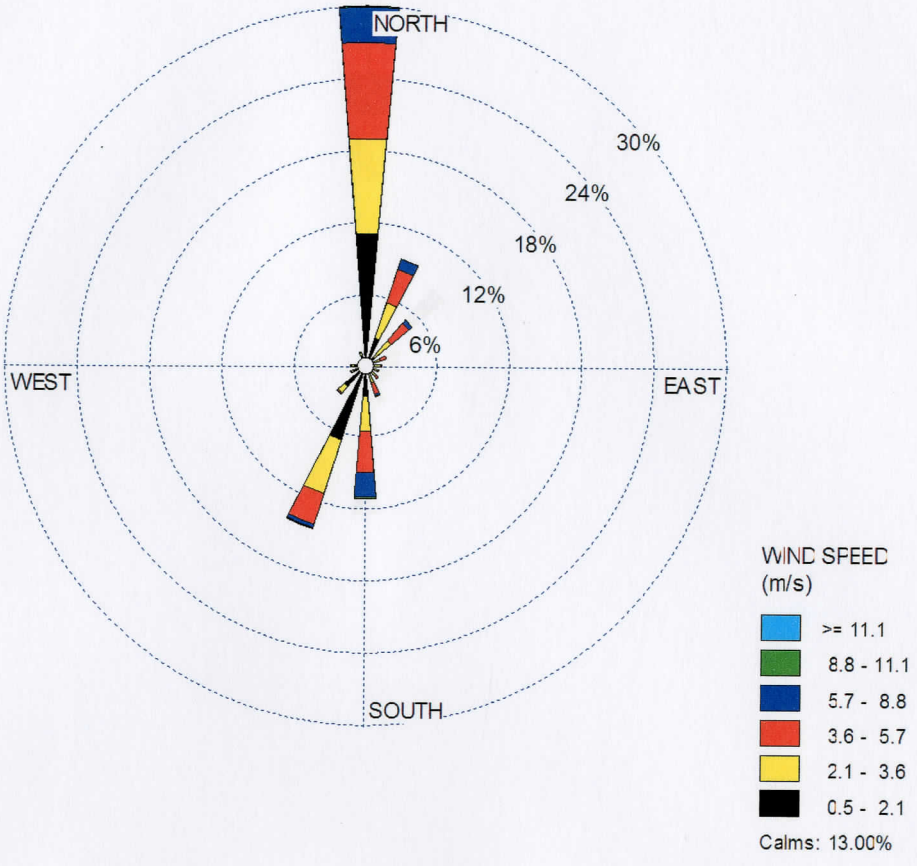

Figure 3.3: Winter seasonal mean wind rose (June, July and August) for 2001, 2002 and 2003.

Figure 3.3 shows the three winter seasons as one seasonal average, calculated from 6244 hours of data. A very strong northerly component dominated the wind rose, with alongshore components from the SSW and NNE and a southerly component being recorded as well. Small occurrences of offshore and onshore winds were noted. Only 13% of the winter periods were calms. As with autumn, the strongest wind speed categories evident were between 5.7 - 8.8 m s^{-1}, on the prominent components. The wind speed average was higher than autumn at 2.68 m s^{-1} (SD: 1.91 m s^{-1}, variance: 3.66 m s^{-1}).

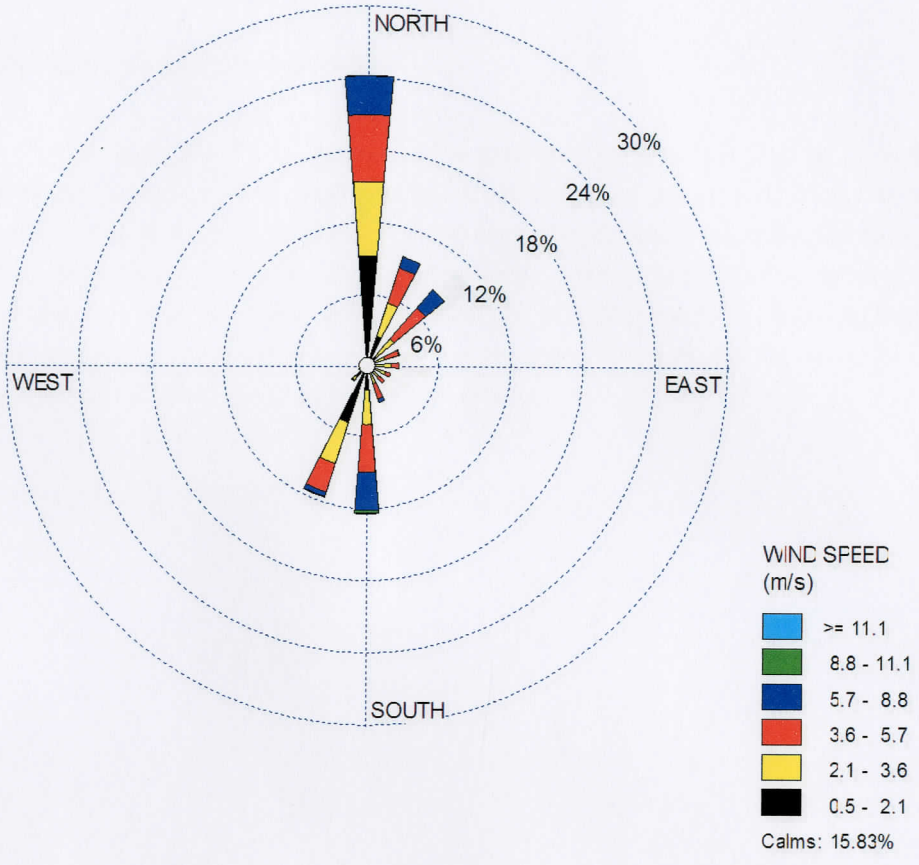

Figure 3.4: Spring seasonal mean wind rose (September, October and November) for 2001 and 2002.

The spring seasonal average in Figure 3.4 showed a much smaller northerly component than autumn and winter. The southerly component was also far larger with a stronger wind speed category of 8.8 - 11.1 m s^{-1} recorded. There also appears prominent alongshore components from the SW, NNE and NE, evidence of onshore winds from the east, but no offshore winds from the west. A low percentage of calms (11.29%), but strong average speeds, 3.42 m s^{-1}, were recorded (SD: 2.23 m s^{-1}, variance: 5.00 m s^{-1}). The number of hours used for calculation, 4368, was less than for Autumn and Winter means as only two spring seasons were recorded for the study period.

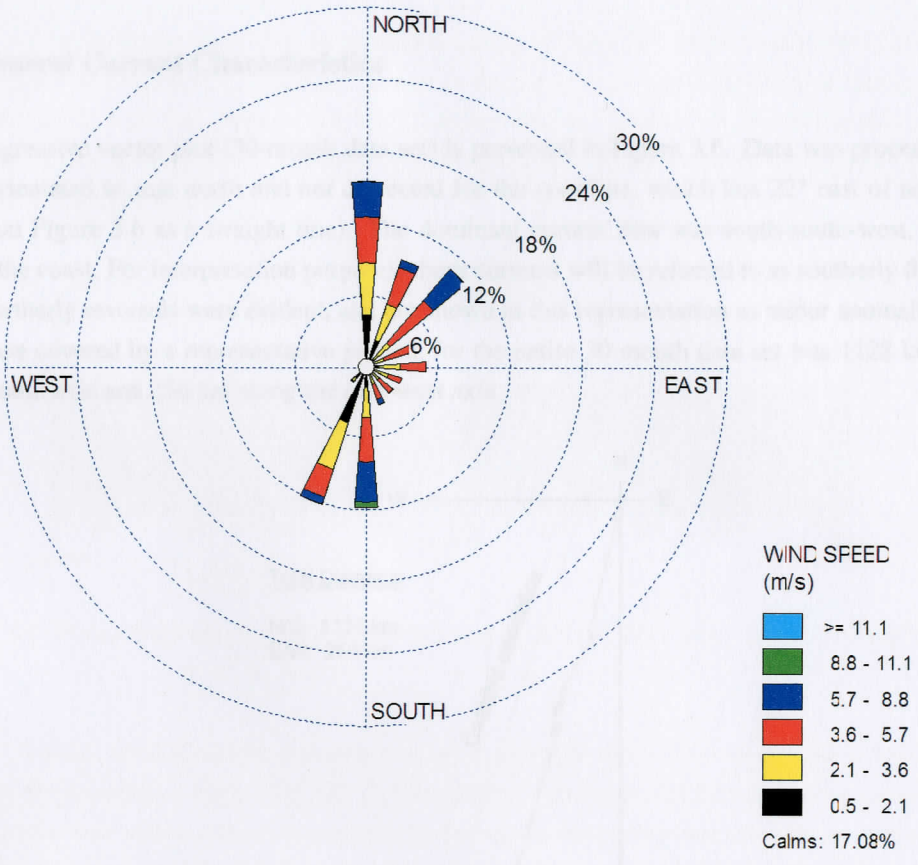

Figure 3.5: Summer seasonal mean wind rose (December, January and February) for 2001/2002 and 2002/2003.

In Figure 3.5 the alongshore components almost dominate the summer average wind rose, with smaller northerly and southerly components when compared to spring. The southerly component still recorded the strongest wind speed category of 8.8 - 11.1 m s^{-1}. A higher number of onshore winds are shown, with no offshore winds at all. A higher percentage of calms were recorded than for spring (17.08%) with a wind speed average of 3.05 m s^{-1} (SD: 2.19 m s^{-1}, variance: 4.79 m s^{-1}). Total number of hours used for calculation was 4320.

3.2 Acoustic Doppler Current Profiler (ADCP) Data

3.2.1 General Current Characteristics

A total progressive vector plot (30-month data set) is presented in Figure 3.6. Data was processed and analysed orientated to true north and not corrected for the coastline, which lies 22° east of north (represented on Figure 3.6 as a straight line). The dominant current flow was south-south-west, flowing parallel to the coast. For interpretation purposes, these currents will be referred to as southerly flow. Occasional northerly reversals were evident, and are shown in this representation as minor anomalies. The total distance covered by a representative particle for the entire 30-month data set was 1128 km along the north-south axis and 256 km along the east-west axis.

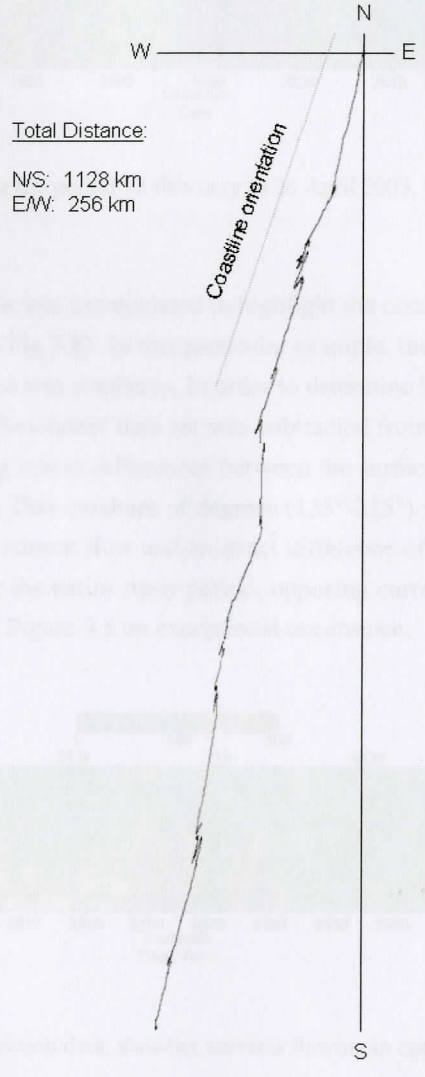

Figure 3.6: Total progressive vector plot for the entire data set (30 months).

Interpretation of the surface data (6 m) confirmed southerly currents were recorded 73% and northerly currents 27% of the time (where current strength was greater than 5 cm s^{-1}). Slack water (< 5 cm s^{-1})

was recorded for less than 5% of the total study period, and was thus excluded from directional analysis.

ADCP data (prior to data processing as per section 2.2.2 above) from the deployment period 12 February to 26 April 2003 is illustrated in a vertical section in Figure 3.7 and represents current flow direction. Bad surface data (0-5 m) was removed for ease of interpretation. Direction flow was interpreted as the same throughout the water column, as southerly flow (green-yellow) or northerly flow (purple-pink) for the majority of the study period.

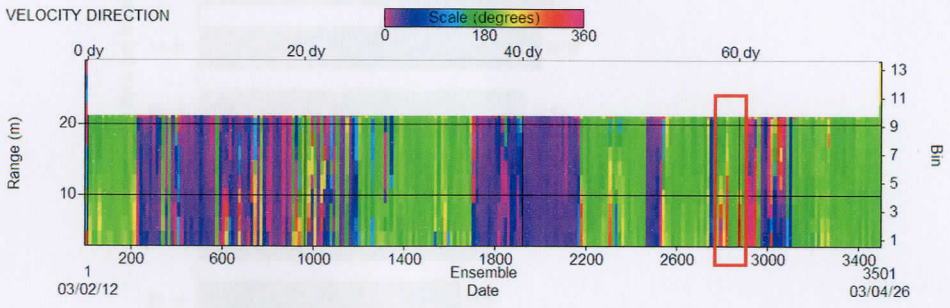

Figure 3.7: ADCP directional data for the period 12 February to 26 April 2003, with a sub-section highlighted in red.

A sub-section of the vertical section was extrapolated to highlight the occasional opposing currents between the sea-floor and the surface (Fig 3.8). In this particular example, the flow above the sea-floor was northerly and the flow on the surface was southerly. In order to determine how often this occurred throughout the study period, the 22 m directional data set was subtracted from the 6 m directional data set. Currents were considered opposing where differences between the surface and bottom directions were calculated between 135° and 225°. This quadrant of degrees (135°-225°) was considered representative due to the unpredictable nature of current flow and an exact difference of 180° to be a rare occurrence (only one result out of 42054). For the entire study period, opposing currents were only recorded 4.5% of the time, making the example in Figure 3.8 an exceptional occurrence.

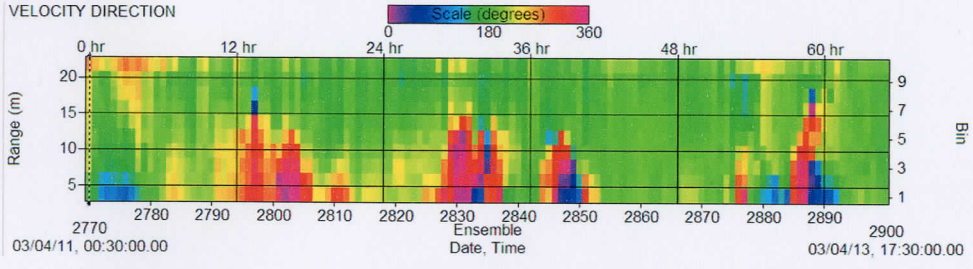

Figure 3.8: Sub-section of ADCP direction data, showing currents flowing in opposing direction on the sea-floor and surface.

Mean velocities in cm s^{-1} were calculated for each depth bin from 6 m to 22 m and is represented in Figure 3.9 as a histogram. A classic decrease in current strength was evident with increasing depth, with a more substantial decrease between the last three depth bins.

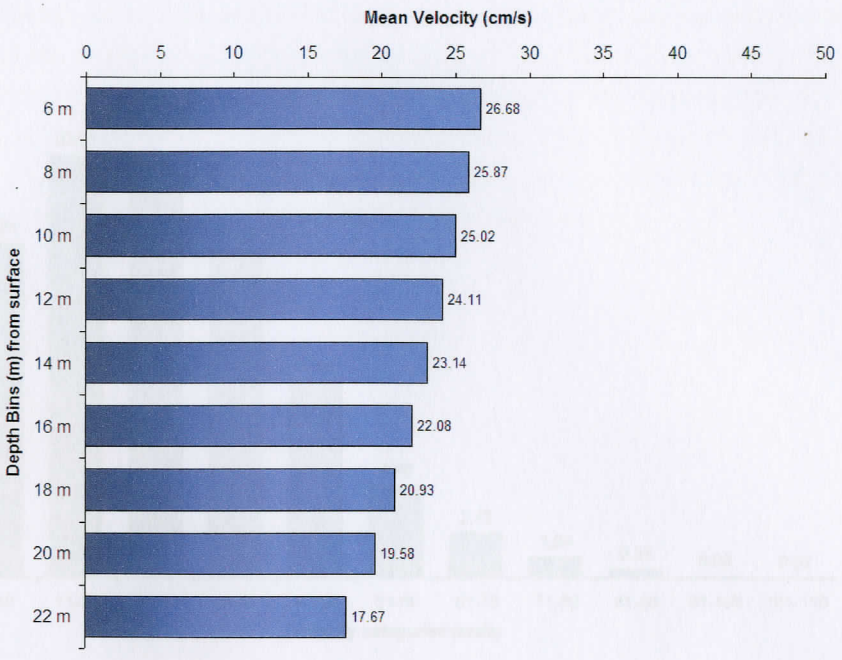

Figure 3.9: Histogram of mean velocities per depth bin.

The surface velocity data (6 m) was used to determine the frequency at which current strengths occurred during the study period regardless of current direction. These data were divided into 10 cm s^{-1} categories, with the first category (1-10 cm s^{-1}) including the slack water conditions discussed earlier. The majority of currents were recorded within the 11-20 cm s^{-1} current strength category (Figure 3.10) with a percentage of 23.01. A decreasing trend exists with subsequent current strength categories occurring gradually initially, but with a sharper decline with increased current strength. Less than 9% of currents had a velocity greater than 50 cm s^{-1} and only 0.02% above 100 cm s^{-1}. Maximum velocities of 108 cm s^{-1} (to the south) and 106 cm s^{-1} (to the north) were recorded for the study period.

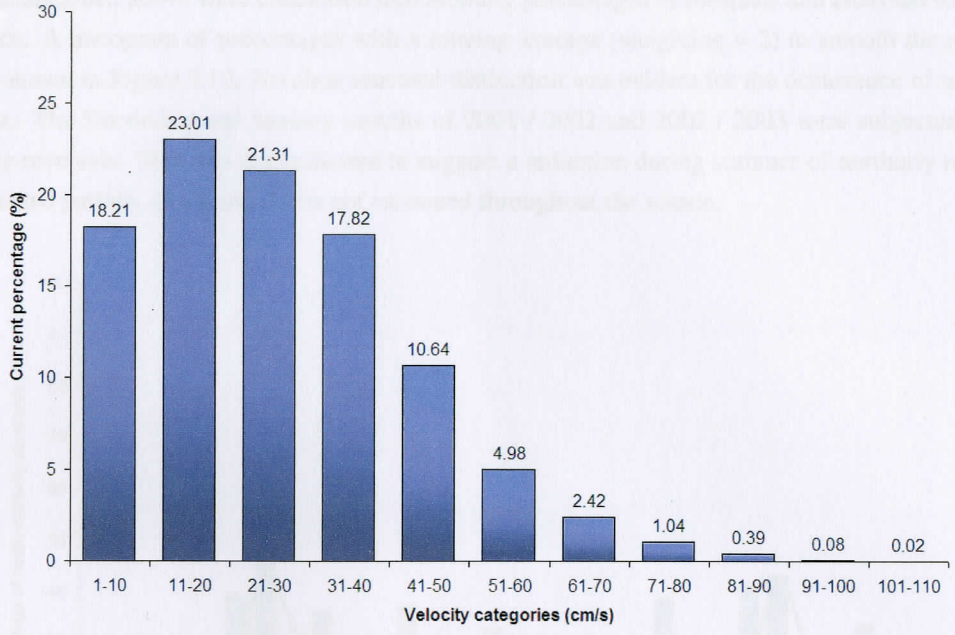

Figure 3.10: Frequency of velocity measurements as per current strength categories.

3.2.2 Northerly Reversals

The progressive vector described above showed northerly reversals in current direction to be an anomaly of the physical oceanography of Sodwana Bay. A total of 206 northerly current reversal events were recorded for the study period determined by analysis of stick vector plots of the surface measurements (6 m). Figure 3.11 shows an example of a northerly reversal event using stick vectors for the period 5 to 13 June 2002. Southerly currents dominated the first four days, with the reversal to the north occurring during the early hours of the ninth of June 2002. The reversal was evident for approximately 36 hours increasing in current strength gradually, before a sharp decline, and an eventual reversal of currents to the south.

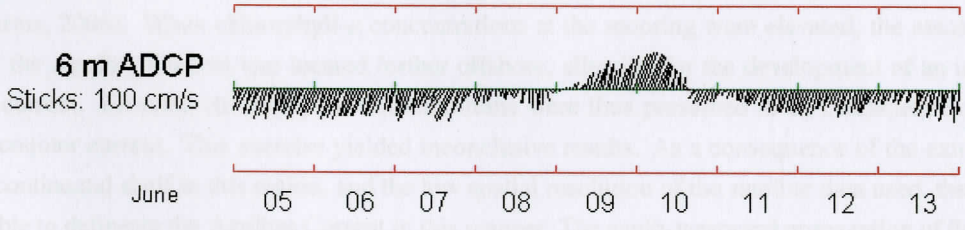

Figure 3.11: A northerly reversal event for the period 5-13 June 2002.

The 206 northerly reversal events were further analysed with regards duration. The shortest event lasted only half an hour and the longest event 138 hours. The average duration was calculated to be 23.15 hours.

The data described above were condensed into monthly percentages of reversals and analysed for seasonal trends. A histogram of percentages with a moving average (weighting = 2) to smooth the resultant trend is shown in Figure 3.12. No clear seasonal distinction was evident for the occurrence of northerly reversals. The December and January months of 2001 / 2002 and 2002 / 2003 were subjected to less northerly reversals. This was not sufficient to suggest a reduction during summer of northerly reversals as a seasonal pattern, as the trend was not sustained throughout the season.

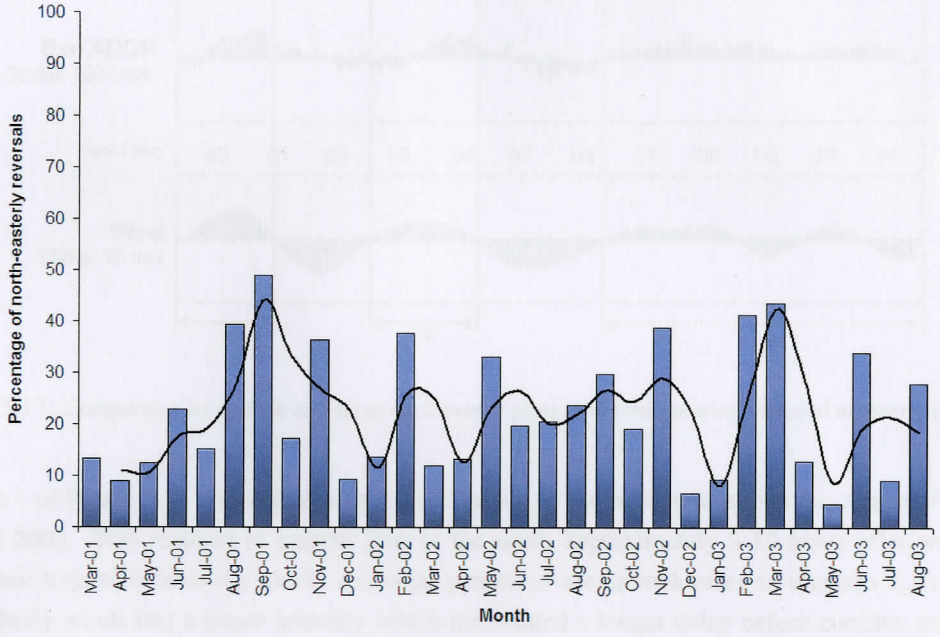

Figure 3.12: Percentage northerly reversals per month with a trendline (weighting=2) for seasonal determination.

3.2.3 Current Driving Forces

In an attempt to delineate the edge of the Agulhas Current, a time series of chlorophyll-*a* concentration just offshore of the ADCP was extracted from maps of SeaWiFS ocean colour imagery. It was thought that when the Agulhas Current was located further inshore, the chlorophyll-*a* concentration at the ADCP mooring would be lower as low chlorophyll-*a* concentrations are characteristic of Agulhas Current water (Lutjeharms, 2006). When chlorophyll-*a* concentrations at the mooring were elevated, the assumption was that the Agulhas Current was located further offshore, allowing for the development of an inshore counter current. Elevated chlorophyll-*a* concentrations were thus presumed to be characteristic of an inshore counter current. This exercise yielded inconclusive results. As a consequence of the extremely narrow continental shelf in this region, and the low spatial resolution of the satellite data used, the study was unable to delineate the Agulhas Current in this manner. The south-westward propagation of flow for this study was thus assumed to be due to the Agulhas Current, but the affect of meandering offshore and causing an inshore counter current remains a theory only.

3.2.3.1 Wind

Stick vector plots from the surface ADCP measurement (6 m) and wind data were compared in order to determine whether wind could be considered a driving force of currents in Sodwana Bay. A manual

identification analysis approach was taken, and northerly current reversals were identified first before establishing whether or not a southerly wind was forcing the reversal to eliminate bias. Figure 3.13 shows a stick vector comparison described above for the period 30 April to 11 May 2002 and illustrates two examples of wind-induced northerly reversals (1 and 2) and an example of northerly current intensification due to the southerly winds (3).

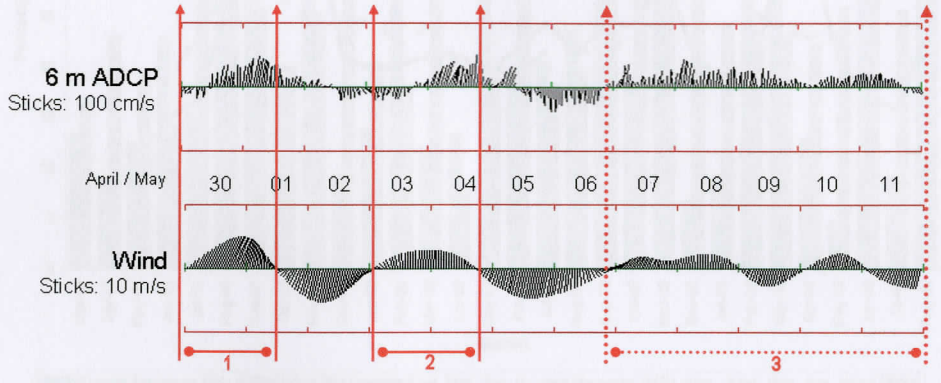

Figure 3.13: Comparison of surface and wind stick vector plots to determine wind-induced northerly reversals.

Scenario 1 of Figure 3.13 above shows an intensification of southerly winds over the course of the 30th of April 2002. This resulted in current flow to the north approximately 9-10 hours after winds first began their trajectory from the south. A similar pattern of events took place in scenario 2, except that the southerly winds had a lesser intensity which manifested a longer delay before currents reversed to the north. The third scenario was not of a wind induced current reversal but rather an intensification of northerly currents during periods of southerly winds. On the 9th of May, the wind reverted to a north-easter which had a diminishing affect on the current strength. Current flow was seen to strength again with a change in wind direction on the 10th of May.

In section 3.2.2 above, 206 northerly current reversal events were identified by stick vector analysis. On further analysis, in conjunction with the wind stick vectors, it was found that 62% of the northerly reversal events were caused by wind forcing from the south, as shown in Figure 3.13.

The data was condensed into monthly percentages of northerly current reversals and southerly winds to determine whether a relationship existed between the two parameters. These monthly percentages were calculated by dividing the number of hours currents were recorded flowing northwards (315° to 45°) by the total number of hours per month. Southerly winds (135° to 225°) were calculated by the same method. These data were plotted as histograms of percentages in Figure 3.14 with moving average trend lines (weighting = 2) being used to illustrate a smoothing trend for the two parameters. A scatterplot of the two sets of percentages were plotted in Figure 3.15 to show the relationship between the current reversals and wind as a driving force ($R^2 = 0.0326$).

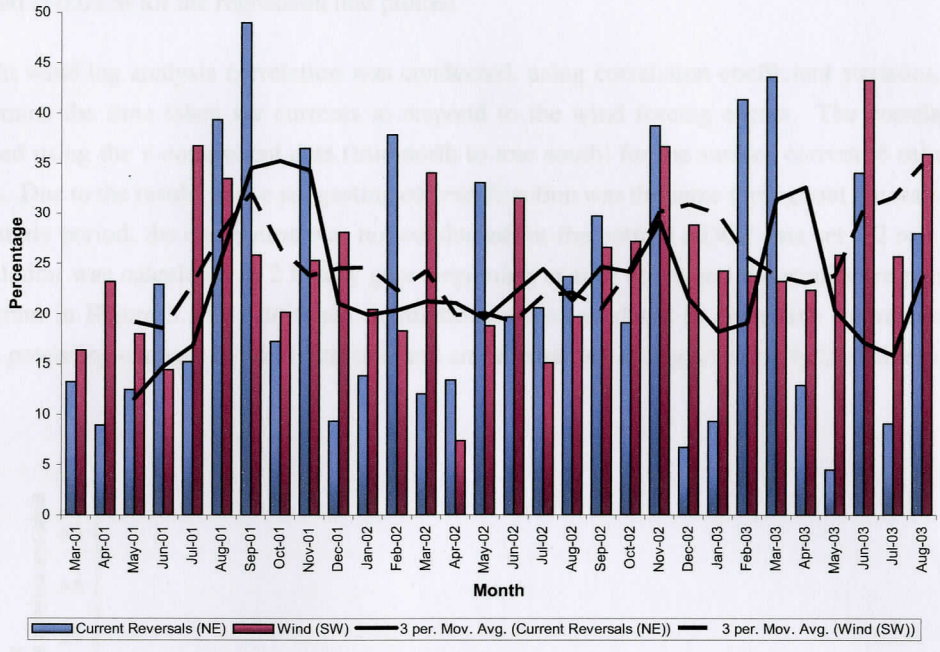

Figure 3.14: Histogram of monthly percentages of northerly reversals and south-westerly winds with moving average trend lines (weighting = 3 months).

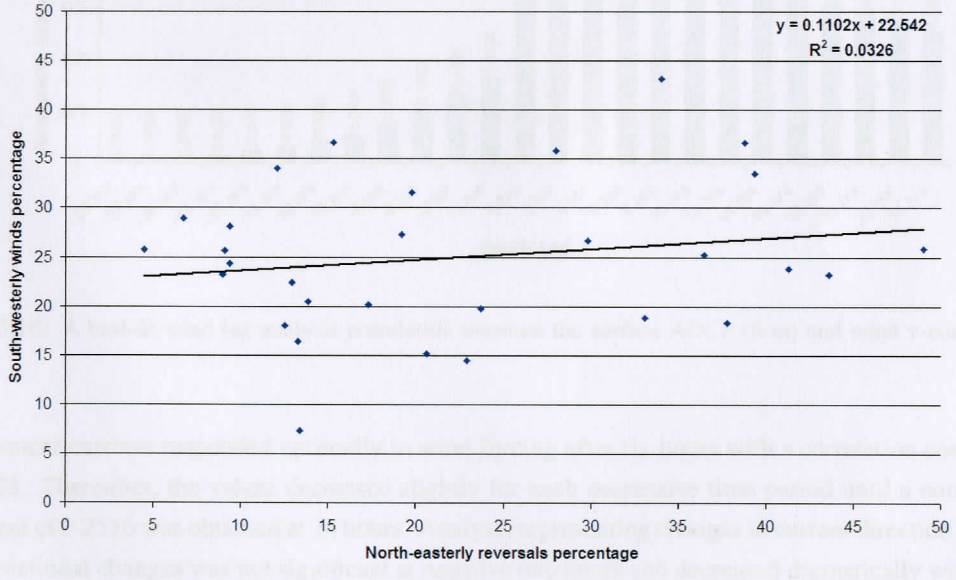

Figure 3.15: Scatterplot showing the linear relationship between monthly percentages of northerly current reversals and southerly winds.

Of the thirty month data set, seventeen months show a greater percentage of southerly winds to northerly reversals and thirteen months show the reverse (Figure 3.14). This suggests that northerly reversals were not caused solely by southerly winds. The histograms showed a relationship between the two parameters as verified by the relationship of the moving average trend lines, but was not always synchronous. The relationship was further illustrated in Figure 3.15, where the coefficient of determination (R^2) was

calculated at 0.0326 for the regression line plotted.

A best fit wind lag analysis correlation was conducted, using correlation coefficient statistics, in order to determine the time taken for currents to respond to the wind forcing events. The correlation was conducted using the v-component data (true north to true south) for the surface current (6 m) and wind data sets. Due to the results above suggesting current direction was the same throughout the water column for the study period, the correlation was not conducted for the bottom ADCP data set (22 m). The best fit correlation was calculated in 2 hourly gaps beginning at zero hours and the results are presented in a histogram in Figure 3.16. Additional correlations were calculated to determine the relationship of currents preceding changes in wind direction and are represented as negative hourly lag values on Figure 3.16.

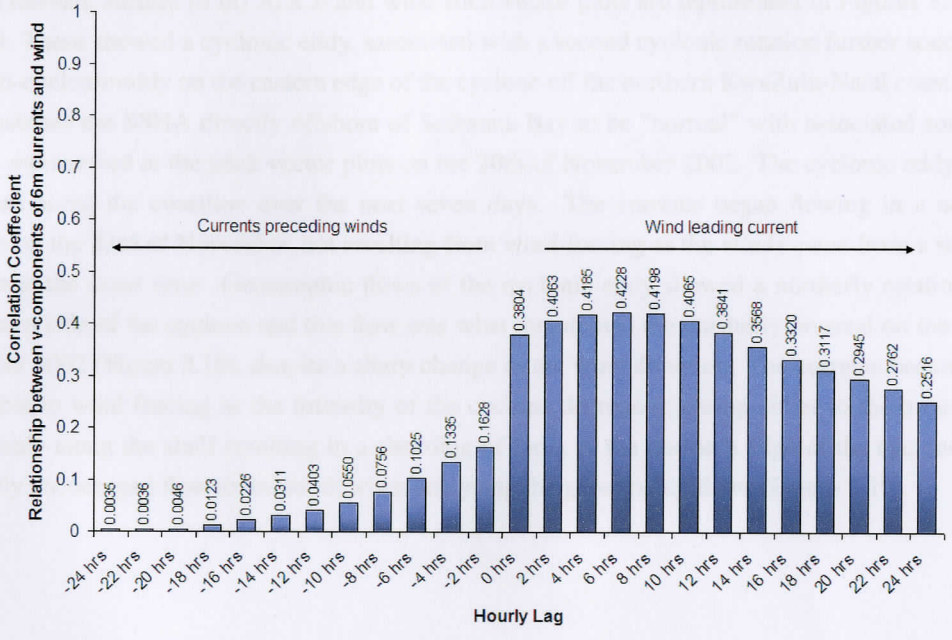

Figure 3.16: A best-fit wind lag analysis correlation between the surface ADCP (6 m) and wind v-component data.

V-component currents responded optimally to wind forcing after six hours with a correlation coefficient of 0.4228. Thereafter, the values decreased slightly for each successive time period until a correlation coefficient of 0.2516 was obtained at 24 hours. Analysis representing changes in current direction leading wind directional changes was not significant at negative two hours and decreased dramatically with time. This correlation was calculated for the entire v-component data set for surface currents and wind, and thus includes wind forcing of current to the south by northerly winds.

3.2.3.2 Cyclonic / Anti-cyclonic Eddies

Two case studies were used to illustrate the affect mesoscale eddies had on the current data at Sodwana Bay for the study period. Case study 1 shows the resultant effect of a cyclonic eddy on the shelf region and case study 2 illustrates positive SSHA satellite data linked to an anti-cyclonic eddy. A cautionary note of SSHA satellite data should be made due to the proximity of the events to the coastline. These SSHA data were fairly course and the affects on the shelf regions are not very well understood yet, thus a best attempt at resolving potentially links to mesoscale activities was taken here.

Case study 1: Cyclonic eddy (27 November 2002)

A series of three SSHA satellite images overlaid with satellite derived geostrophic flows and associated with the relevant surface (6 m) ADCP and wind stick vector plots are represented in Figures 3.17, 3.18 and 3.19. These showed a cyclonic eddy, associated with a second cyclonic rotation further south, and a large anti-cyclonic eddy on the eastern edge of the cyclone off the northern KwaZulu-Natal coast. Figure 3.17 illustrates the SSHA directly offshore of Sodwana Bay to be "normal" with associated southward currents represented in the stick vector plots on the 20th of November 2002. The cyclonic eddy moved southward along the coastline over the next seven days. The currents began flowing in a northerly direction on the 23rd of November, not resulting from wind-forcing as the winds came from a southerly direction at the same time. Geostrophic flows of the cyclonic eddy showed a northerly rotation along the western side of the cyclone and this flow was what maintained the northerly reversal on the 27th of November 2002 (Figure 3.18), despite a sharp change in the wind direction. The currents became more susceptible to wind forcing as the intensity of the cyclone decreased, owing either to the trajectory of the anomaly along the shelf resulting in a shedding of force or the northern edge of the cyclone which eventually encouraged flow to the south when analysing the geostrophic flows (Figure 3.19).

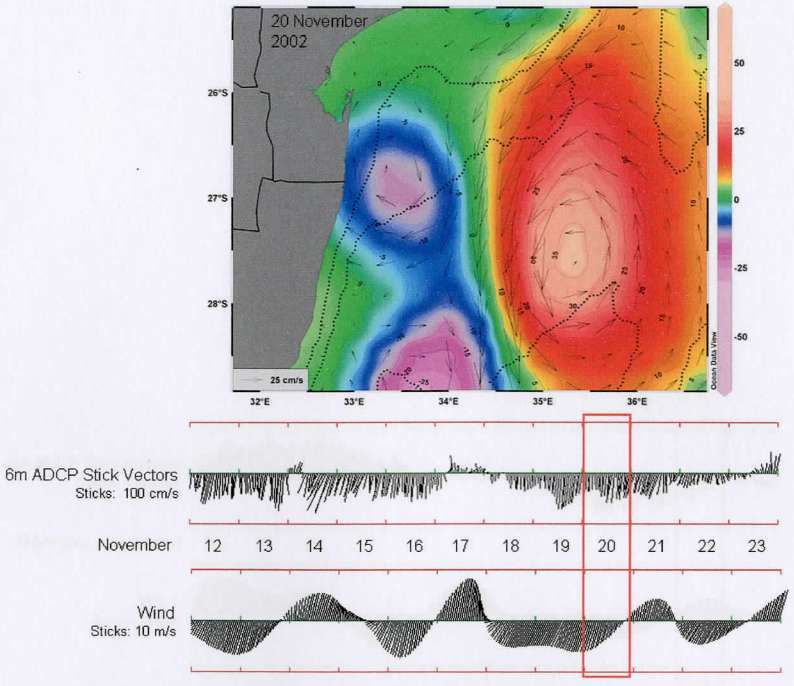

Figure 3.17: 20 November 2002 SSHA satellite image overlaid with satellite derived geostrophic flows, with associated surface ADCP and wind stick vector plots.

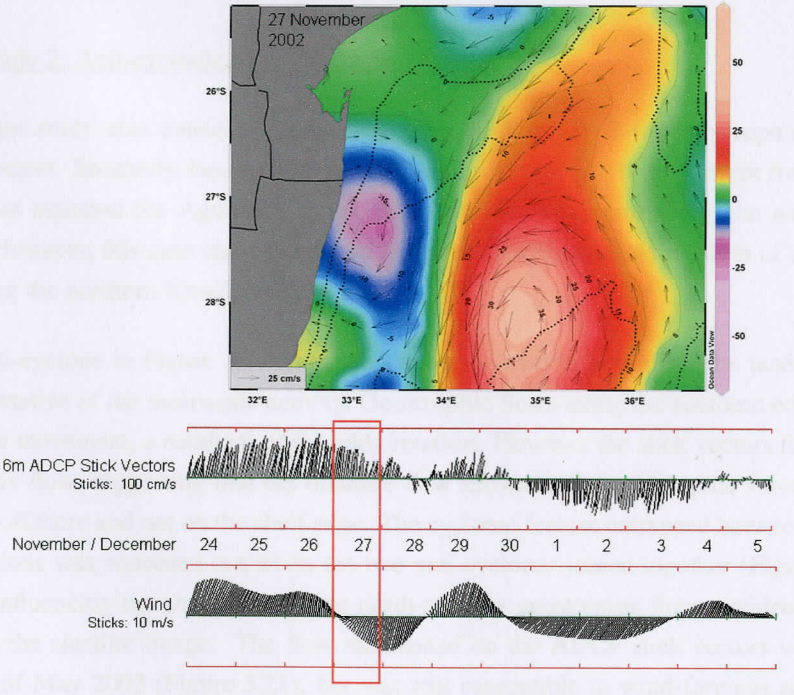

Figure 3.18: 27 November 2002 SSHA satellite image overlaid with satellite derived geostrophic flows, with associated surface ADCP and wind stick vector plots.

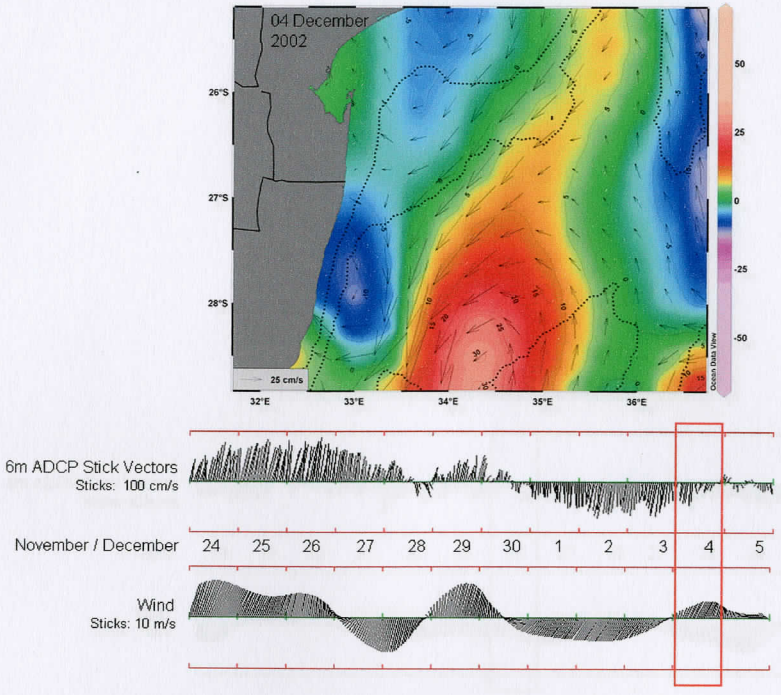

Figure 3.19: 04 December 2002 SSHA satellite image overlaid with satellite derived geostrophic flows, with associated surface ADCP and wind stick vector plots.

Case study 2: Anti-cyclonic eddy (24 April 2002)

This case study also consists of three figures consisting of SSHA, geostrophic flows and associated stick vectors. Southerly forcing was more difficult to prove as a forcing event from mesoscale activities as it was assumed the Agulhas Current played a role in currents along the northern KwaZulu-Natal coast. However, this case study illustrated current characteristics at the edges of the mesoscale events to influence the northern KwaZulu-Natal shelf.

The anti-cyclone in Figure 3.20 illustrated strong southerly flow along the landward side of the eddy, representative of the mesoscale activity. Geostrophic flows along the southern edge of the eddy showed offshore movement, a resultant of the eddy rotation. However the stick vectors from the ADCP showed southerly flow, suggesting that the offshore flow shown in the geostrophic velocities was taking place further offshore and not on the shelf edge. The cyclonic feature entrapped between the two anti-cyclonic circulations was squeezed out when the two anti-cyclones joined together (Figure 3.21). The cyclone began influencing the shelf with strong north-easterly geostrophic flows, evident offshore of Sodwana Bay on the satellite image. The flow manifested on the ADCP stick vectors with northerly flows on the 1st of May 2002 (Figure 3.21), but was still susceptible to wind-forcings as was evident over the following five days. The cyclone eventually moved onshore due to the forcing of the anti-cyclone on the eastern side of the cyclone and the northerly currents remained evident (Figure 3.22). Wind forcing from the north-east only minimised the affect of the northerly current flow, but did not reverse to a southerly flow again.

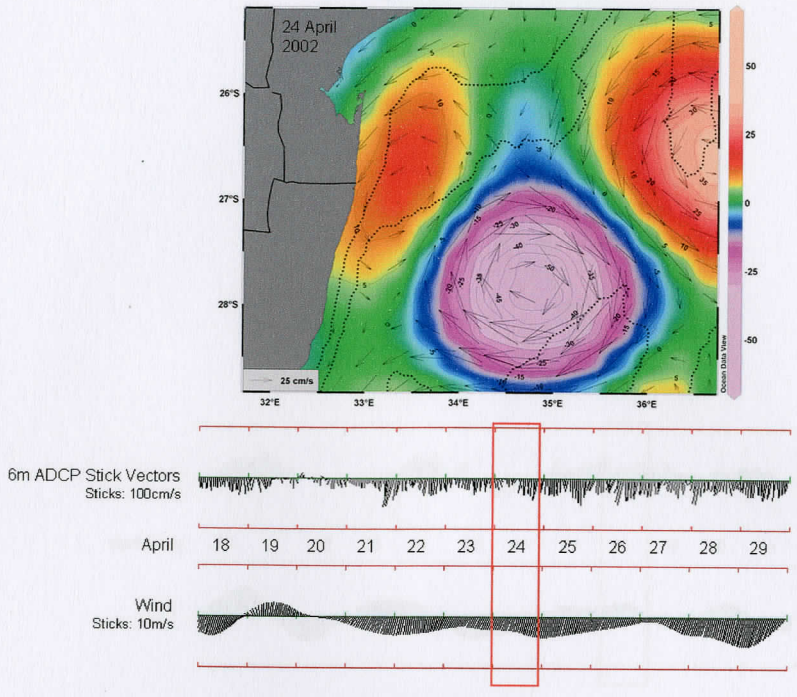

Figure 3.20: 24 April 2002 SSHA satellite image overlaid with satellite derived geostrophic flows, with associated surface ADCP and wind stick vector plots.

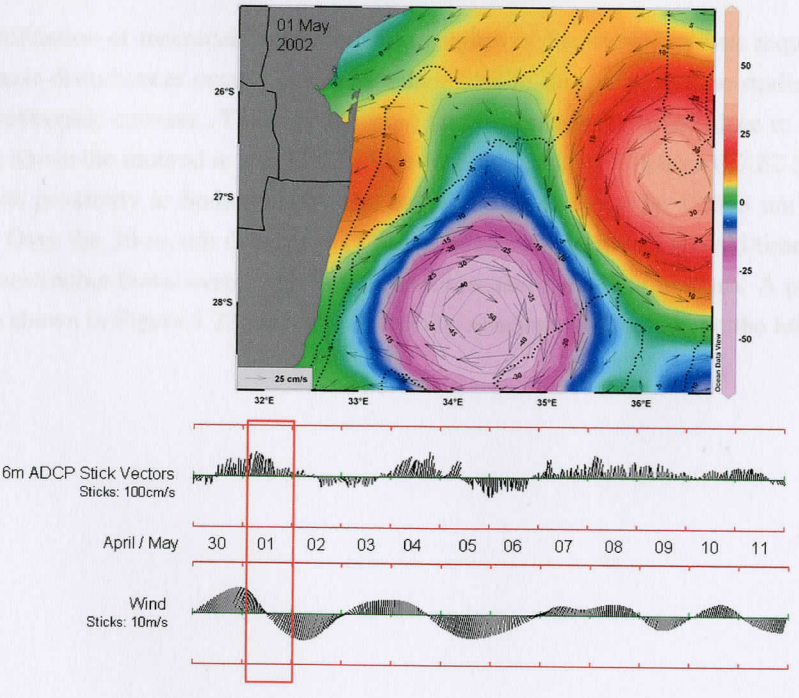

Figure 3.21: 01 May 2002 SSHA satellite image overlaid with satellite derived geostrophic flows, with associated surface ADCP and wind stick vector plots.

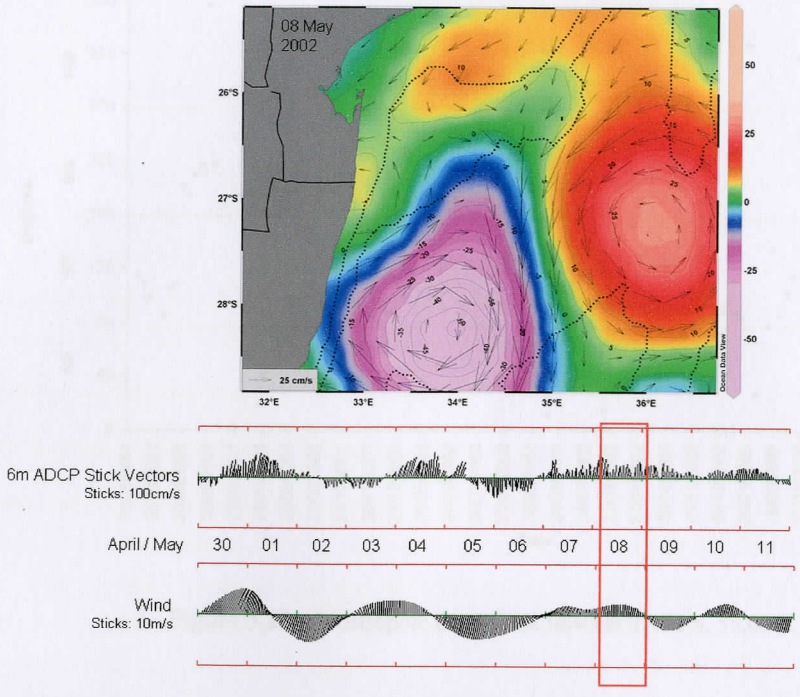

Figure 3.22: 08 May 2002 SSHA satellite image overlaid with satellite derived geostrophic flows, with associated surface ADCP and wind stick vector plots.

A quantification of mesoscale activities in the region of Sodwana Bay was required to determine how often these disturbances occur. The SSHA data used to illustrate the case studies above were overlaid with geostrophic currents. These geostrophic flows cannot be resolved close to the coastline, and thus directly above the moored *in situ* ADCP. A geostrophic position offshore (27.62 S, 33.00 E) was chosen due to its proximity to Sodwana Bay and has been calculated to be 19.513 nm (36.132 km) from the ADCP. Over the 30-month data set, 127 observations via satellite (delayed time data) were made and these geostrophic flows were resolved into direction and speed components. A plot of these directional flows is shown in Figure 3.23, with the directional quadrant highlighted on the left-hand side.

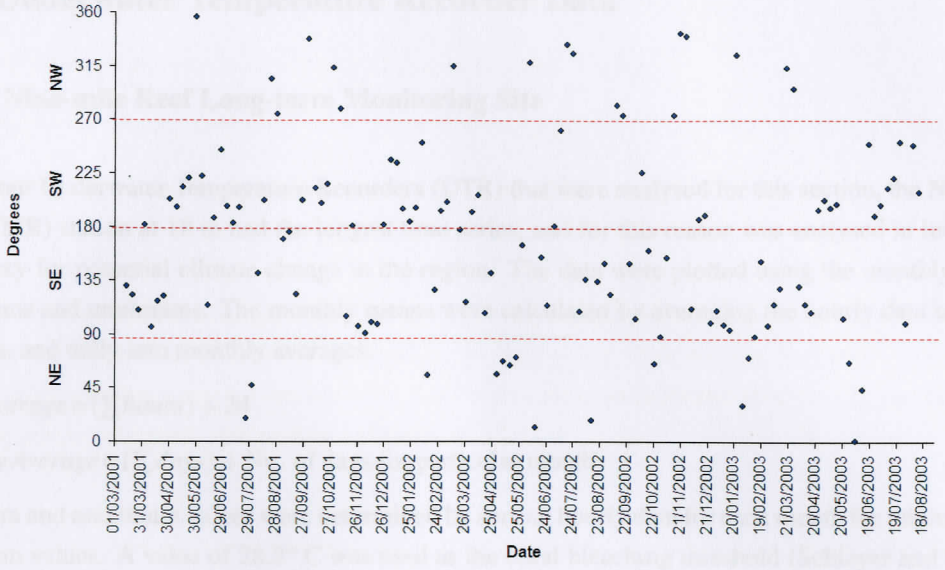

Figure 3.23: Geostrophic directional flows at 27.62 S, 33.00 E.

Of the 127 observations, 13.38% were north-easterly (0° - 90°), 37.00% south-easterly (90° - 180°), 35.45% south-westerly (180° - 270°) and 14.17% north-westerly (270° - 360°). If it is assumed that north-easterly and north-westerly flows are linked to the landward edge of cyclonic eddies and south-easterly and south-westerly flows the landward edge of anti-cyclonic eddies (due to the distance offshore of the extracted geostrophic flows), then only 27.55% of the mesoscale activities extracted above were cyclonic in nature. A far larger percentage (72.45%) were linked to anti-cyclonic perturbations or the flow of the Agulhas Current where it extends a considerable distance offshore. Direction data from the ADCP was extracted for the same days the satellite observations were made. The noon hour recorded ADCP data was used for this comparison. When comparing the results to the satellite geostrophic flows, it was established that only 11.81% of northerly ADCP flow (north-east and north-west quadrants) successfully coincided with the extracted satellite geostrophic flows (resulting in 42% of the 27.55% assumed cyclonic perturbations). With regards the southerly flow comparisons of data (south-east and south-west quadrants), 70.65% of the two data agree.

3.3 Underwater Temperature Recorder Data

3.3.1 Nine-mile Reef Long-term Monitoring Site

Of the four Underwater Temperature Recorders (UTR) that were analysed for this section, the Nine-mile Reef (NMR) station at 18 m had the longest time series, and for this reason was analysed in its entirety as a proxy for potential climate change in the region. The data were plotted using the monthly means, maximums and minimums. The monthly means were calculated by averaging the hourly data into daily averages, and daily into monthly averages:

$$Daily\,Average = (\sum hours) \div 24$$

$$Monthly\,Average = (\sum days) \div \text{No. of days for particular month}$$

Minimum and maximum values were determined by sorting hourly data for each month for minimum and maximum values. A value of 28.8° C was used as the coral bleaching threshold (Schleyer and Celliers, 2003b). The resultant linear graphs are not ideal as data are smoothed out and anomalies may have been overlooked. However seasonal trends can be identified, with warming during the summer months (October - March) and cooling during the winter months (April - September). Figure 3.24 is a plot of the first six years of data where two coral bleaching events (1998/1999 and 1999/2000) occurred. Figure 3.25 is of the entire data set as of February 2008.

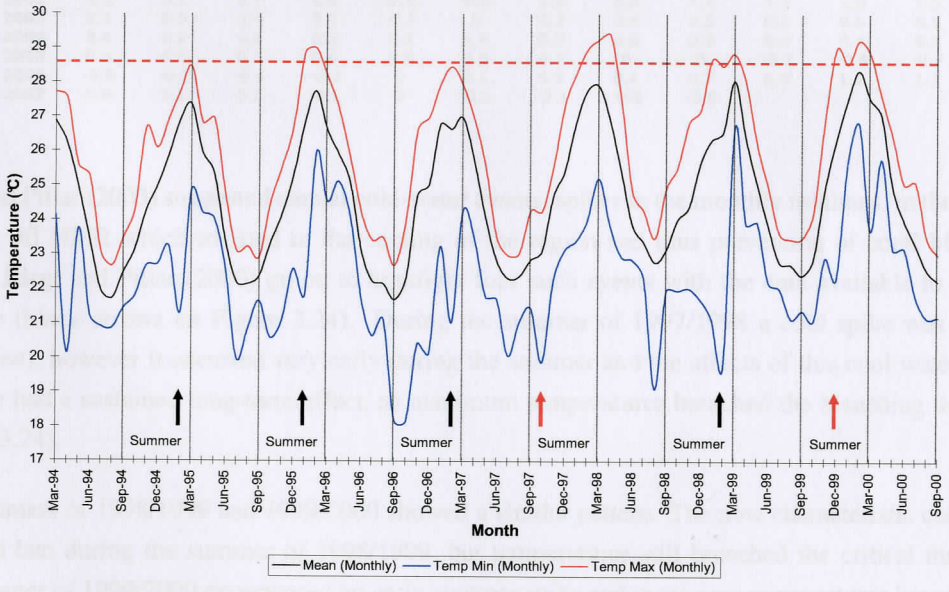

Figure 3.24: Monthly average, monthly maximum and monthly minimum: 1994 - 2000

Four summer periods occurred within this long term data-set where the monthly maximum exceeded the coral bleaching threshold: 95/96, 97/98, 98/99, 99/00. When compared to data extracted from the NOAA website for the El-Niño Southern Oscillation Index, in Table 3.1 the following associations were determined:

- 1995/1996 was a cooling period of seven months (ASO - FMA)
- 1997/1998 was a warming period of 12 months (AMJ - MAM)
- 1998/1999 was the beginning of a 24 month cooling period (JJA of 98 - MJJ of 00)
- 1999/2000 was the end of a 24 month cooling period (JJA of 98 - MJJ of 00)

NOAA uses three month averages when calculating warming and cooling events month per month, i.e. The value for September 2001 was calculated by averaging data from August, September and October 2001 (Table 3.1). This value is represented as ASO on the table and adopted for this analysis. Months of warming are shown in red, and cooling in blue (Table 3.1).

Table 3.1: ENSO years calculated as three month averages (i.e. January value taken as an average of December, January and February values).
http://www.cpc.ncep.noaa.gov/products/analysis_monitoring/ensostuff/ensoyears.shtml

	DJF	JFM	FMA	MAM	AMJ	MJJ	JJA	JAS	ASO	SON	OND	NDJ
1994	0.2	0.3	0.4	0.5	0.6	0.6	0.6	0.6	0.7	0.9	1.2	1.3
1995	1.2	0.9	0.7	0.4	0.2	0.1	0	-0.3	-0.5	-0.6	-0.7	-0.8
1996	-0.8	-0.7	-0.5	-0.3	-0.2	-0.2	-0.1	-0.2	-0.2	-0.2	-0.3	-0.4
1997	-0.4	-0.3	0	0.4	0.9	1.4	1.7	2	2.3	2.4	2.5	2.5
1998	2.4	2	1.4	1.1	0.4	-0.1	-0.8	-1	-1.1	-1.1	-1.3	-1.5
1999	-1.6	-1.2	-0.9	-0.7	-0.8	-0.8	-0.9	-0.9	-1	-1.2	-1.4	-1.6
2000	-1.6	-1.5	-1.1	-0.9	-0.7	-0.6	-0.4	-0.3	-0.4	-0.5	-0.7	-0.7
2001	-0.7	-0.5	-0.4	-0.2	-0.1	0.1	0.2	0.1	0	-0.1	-0.2	-0.2
2002	-0.1	0.1	0.3	0.4	0.7	0.8	0.9	0.9	1.1	1.3	1.5	1.3
2003	1.1	0.8	0.6	0.1	-0.1	0	0.3	0.4	0.5	0.5	0.6	0.5
2004	0.4	0.2	0.2	0.2	0.3	0.4	0.7	0.8	0.9	0.9	0.9	0.8
2005	0.6	0.5	0.3	0.4	0.5	0.3	0.2	0	0	-0.2	-0.4	-0.7
2006	-0.8	-0.7	-0.4	-0.2	0	0.1	0.3	0.4	0.7	0.9	1.1	1.1
2007	0.8	0.3	0.1	-0.1	0	-0.1	-0.2	-0.6	-0.8			

Riegl and Pillar (2003) suggested annual cold-water events, spikes in the monthly minimas, in the marine summer off NMR which assisted in the cooling of the region and thus prevention of coral bleaching events. Riegl and Pillar (2003) go on to highlight four such events with the data available to them at the time (black arrows on Figure 3.24). During the summer of 1997/1998 a cold spike was evident (red arrow), however it occurred very early during the summer and the affects of this cool water would not have had a sustained long-term affect, as maximum temperatures breached the bleaching threshold (Figure 3.24).

The summers of 1998/1999 and 1999/2000 showed a similar pattern. The now characteristic cold spike occurred late during the summer of 1998/1999, but temperatures still breached the critical threshold. The summer of 1999/2000 experienced an early summer spike and maximum temperatures breached the threshold again, resulting in a higher bleaching incidence as opposed to that of 1998 (Floros et al., 2004).

When analysing the entire data set (Figure 3.25), mid to late summer cold water spikes were seen throughout the time series except for the two scenarios highlighted above. The cold spikes in the summers of 2003/2004 and 2004/2005 were fairly substantial reaching minimum values of nearly 17° C.

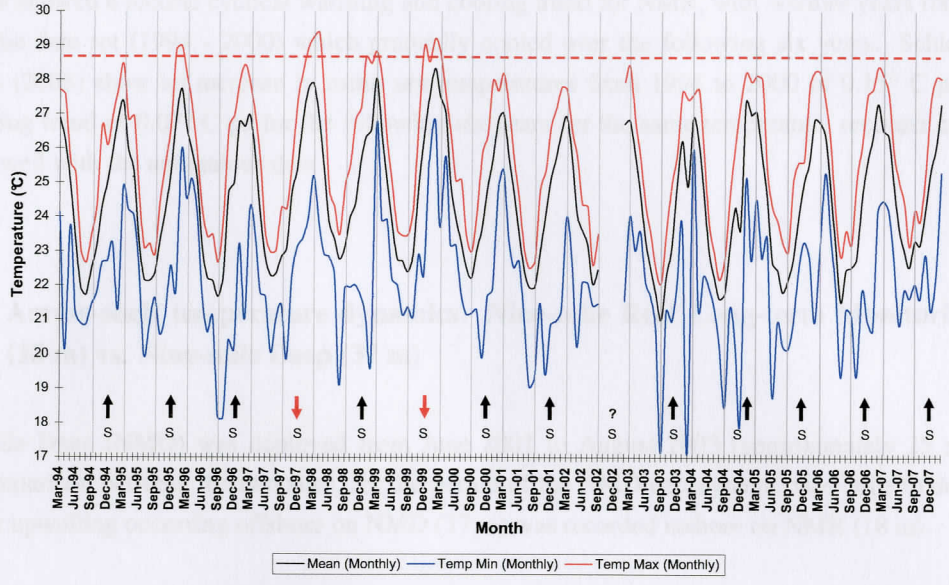

Figure 3.25: Monthly average, monthly maximum and monthly minimum: entire data set

A monthly mean was calculated for each month for the entire data set (i.e. all the January values used to calculate one mean for January), and was subtracted from each individual January monthly average in order to calculate the anomaly value for that particular month. This was further refined by subtracting from the monthly mean calculated, the ENSO months (both warming and cooling) to calculate the "normalised" monthly mean. The resultant anomaly plot in Figure 3.26 was plotted with a three month moving average (to mimic the smoothing tool used on the El-Niño Southern Oscillation Index table described above).

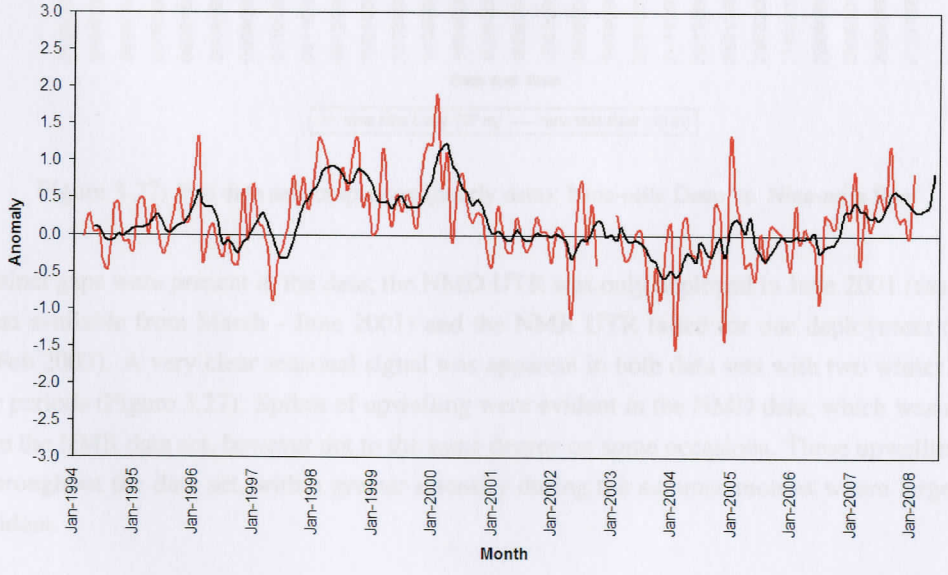

Figure 3.26: Monthly anomaly data plotted with a three month moving average.

The plot showed a natural cyclical warming and cooling trend for NMR, with warmer years for the first six of the data set (1994 - 2000) which gradually cooled over the following six years. Schleyer and Celliers (2008) show an increase in mean sea temperatures from 1994 to 2000 of 0.15° C pa, and a decreasing trend of 0.07° C pa for the following six years for the same temperature recorder and these data fit well with the anomalous data.

3.3.2 Across-shelf temperature dynamics: Nine-mile Reef Long-term Monitoring Site (18 m) vs. Nine-mile Deep (37 m)

Nine-mile Deep (NMD) was deployed from June 2001 to August 2003 (approximately 25 months). The comparison between the two sites, for the period of the NMD deployment, was done to determine whether upwelling occurring offshore on NMD (37 m) was recorded inshore on NMR (18 m).

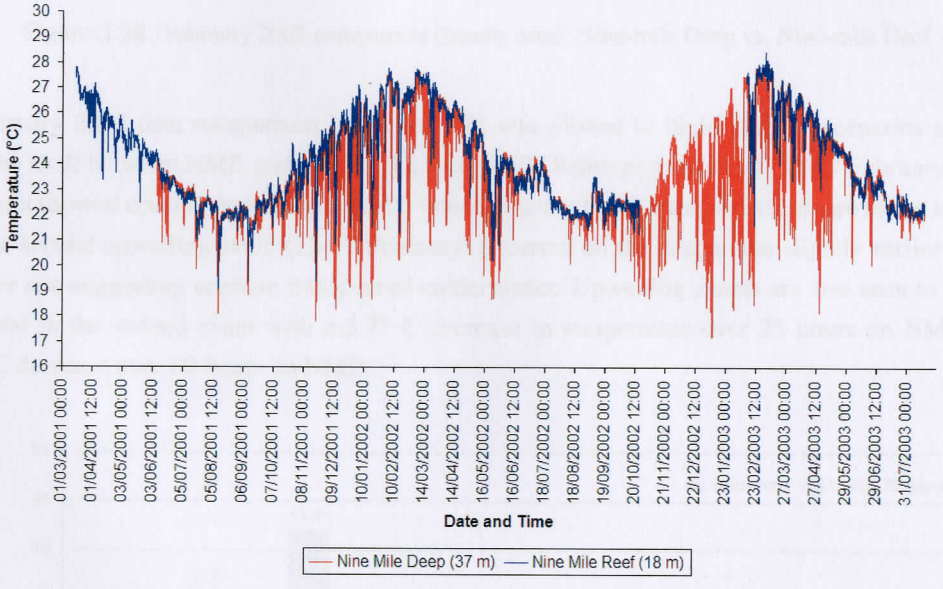

Figure 3.27: Full data set comparison (hourly data): Nine-mile Deep vs. Nine-mile Reef

Two distinct gaps were present in the data; the NMD UTR was only deployed in June 2001 (thus 9-Mile Reef data available from March - June 2001) and the NMR UTR failed for one deployment (October 2002 - Feb 2003). A very clear seasonal signal was apparent in both data sets with two winter and two summer periods (Figure 3.27). Spikes of upwelling were evident in the NMD data, which was mirrored in part in the NMR data set, however not to the same degree on some occasions. These upwelling spikes occur throughout the data set, with a greater intensity during the summer months where larger spikes were evident.

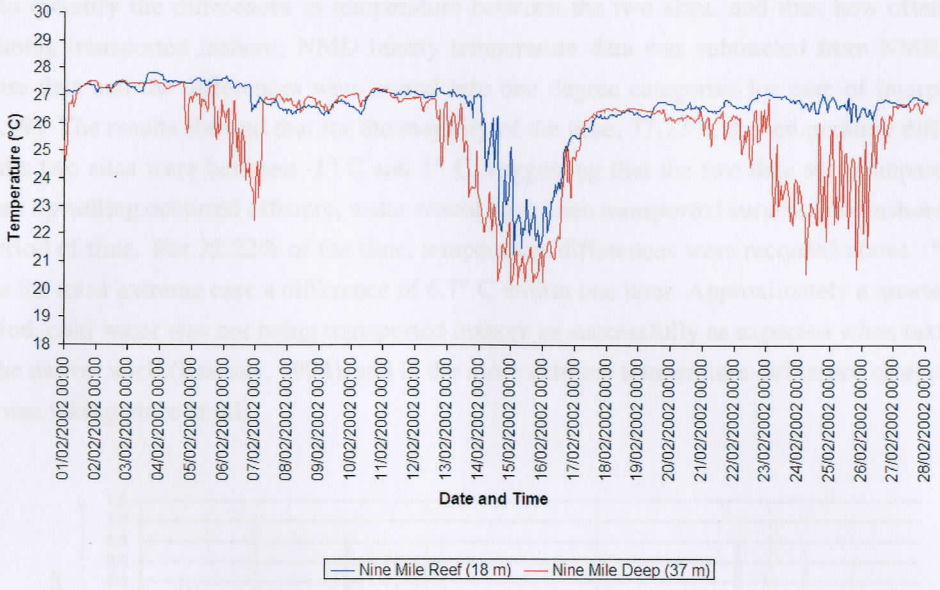

Figure 3.28: February 2002 comparison (hourly data): Nine-mile Deep vs. Nine-mile Reef

The February 2002 data comparison in Figure 3.28 was plotted to highlight two scenarios occurring across the shelf between NMR and NMD. The first (04-07 February) and third (22-27 February) upwelling events showed cooling occurring at NMD which was not being transported inshore to the shallower site. The second upwelling event (13-17 February) occurred on the deeper site slightly earlier than the shallower site suggesting onshore transport of colder water. Upwelling events are also seen to be fairly substantial in the second event with a 5.7° C decrease in temperature over 25 hours on NMR and a 6.275° C decrease over 29 hours on NMD.

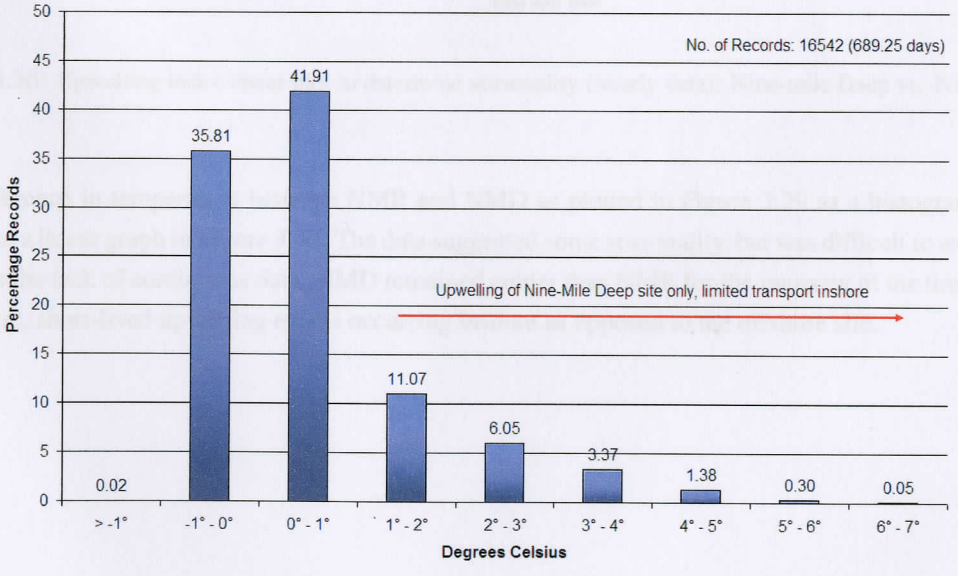

Figure 3.29: Upwelling index histogram plot (hourly data): Nine-mile Deep vs. Nine-mile Reef

In order to quantify the differences in temperature between the two sites, and thus how often cooler water is being transported inshore, NMD hourly temperature data was subtracted from NMR hourly temperature data and the differences were sorted into one degree categories for ease of interpretation (Figure 3.29). The results showed that for the majority of the time, 77.72%, the temperature differences between the two sites were between -1° C and 1° C, suggesting that the two data sets compared well. Thus where upwelling occurred offshore, water would have been transported successfully inshore within a short period of time. For 22.22% of the time, temperature differences were recorded above 1° C, and reached in the most extreme case a difference of 6.7° C within one hour. Approximately a quarter of the study period, cold water was not being transported inshore as successfully as expected when taking into account the narrow shelf (Ramsay, 1994), and in the more extreme temperature difference categories, no transport was taking place at all.

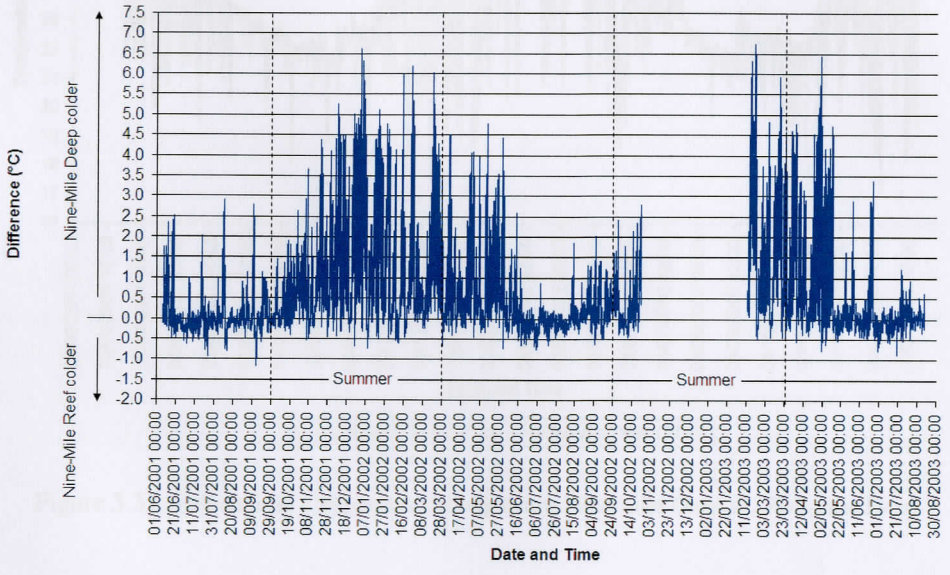

Figure 3.30: Upwelling index linear plot to determine seasonality (hourly data): Nine-mile Deep vs. Nine-mile Reef

The difference in temperature between NMR and NMD as plotted in Figure 3.29 as a histogram, was plotted as a linear graph in Figure 3.30. The data suggested some seasonality, but was difficult to ascertain owing to the lack of continuous data. NMD remained colder than NMR for the majority of the time, with infrequent, short-lived upwelling events occurring inshore as opposed to the offshore site.

3.3.3 Along-shelf temperature dynamics: Five-mile Deep (37 m) vs. Nine-mile Deep (37 m)

NMD was situated on the shelf, while Five-mile Deep (FMD) was deployed on Wright Canyon head. The comparison was thus made to determine whether canyon-induced upwelling occurred at Sodwana Bay and if so, to what extent.

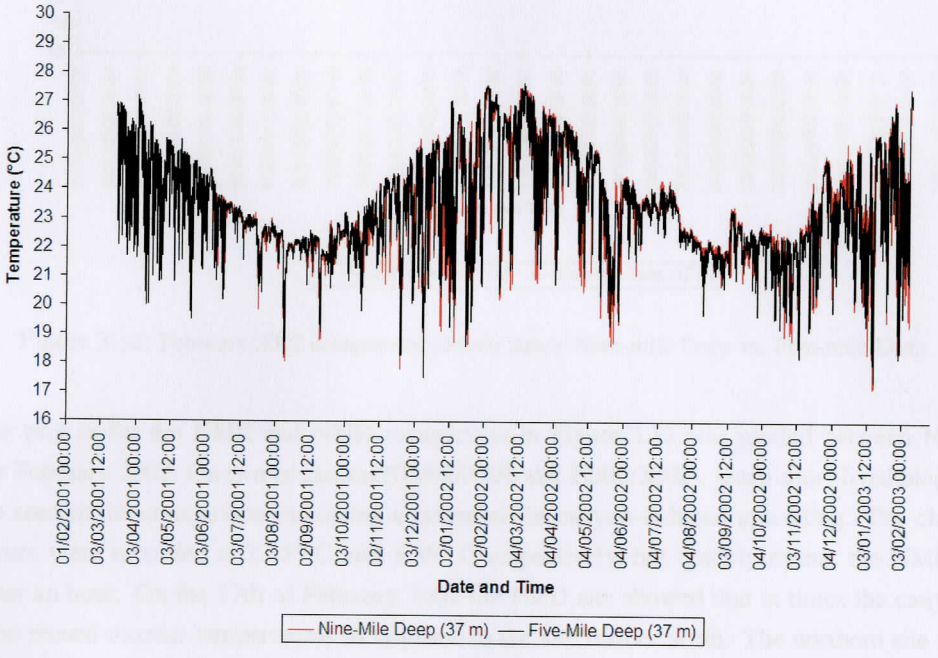

Figure 3.31: Full data set comparison (hourly data): Nine-mile Deep vs. Five-mile Deep

A clear seasonal signal was again apparent with the two data sets in close agreement (Figure 3.31). Upwelling spikes were fairly intense and occurred throughout the data sets, regardless of season. Both sites seemed to mimic the upwelling spikes fairly closely and on first interpretation, little to no difference was apparent between the two sites.

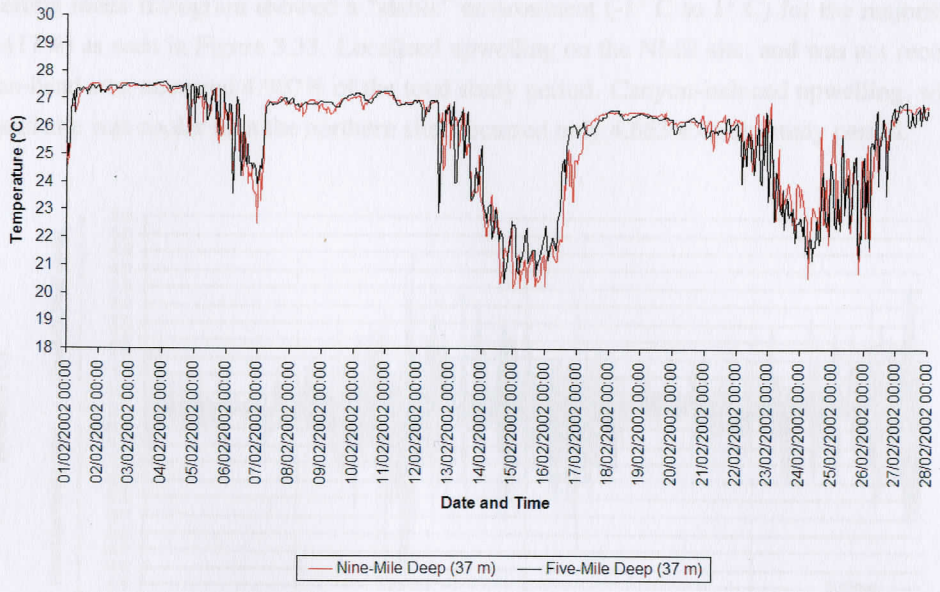

Figure 3.32: February 2002 comparison (hourly data): Nine-mile Deep vs. Five-mile Deep

A similar plot as for the NMR and NMD comparison in Figure 3.32 was plotted between NMD and FMD for February 2002. On two occasions (05/02/2002 and 12/02/2002), sharp short-lived black spikes could be seen in the comparison indicating a potential for canyon-induced upwelling. The changes in temperature were recorded at 1.45° C and 3.35° C respectively, but quickly mimic the NMD values again after an hour. On the 17th of February 2002 the FMD site showed that at times the canyon head could also record warmer temperatures as opposed to the site further north. The northern site recorded temperatures 2.75° C cooler than the canyon head, with the event lasting approximately 17 hours.

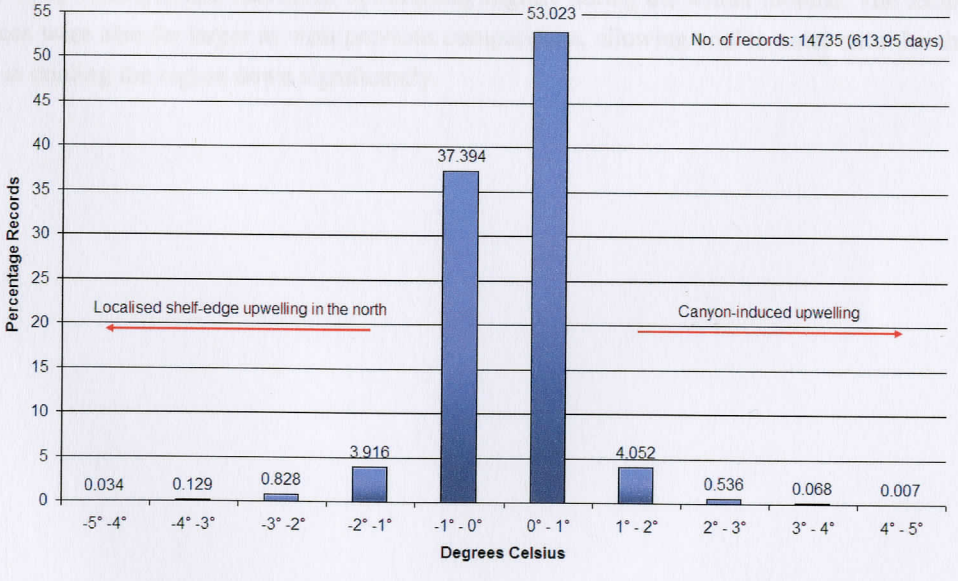

Figure 3.33: Upwelling index histogram plot (hourly data): Nine-mile Deep vs. Five-mile Deep

The upwelling index histogram showed a "stable" environment (-1° C to 1° C) for the majority of the time (90.417%) as seen in Figure 3.33. Localised upwelling on the NMR site, and was not recorded on the canyon-head site, occurred 4.907% of the total study period. Canyon-induced upwelling, where the canyon head site was cooler than the northern site, occurred only 4.663% of the study period.

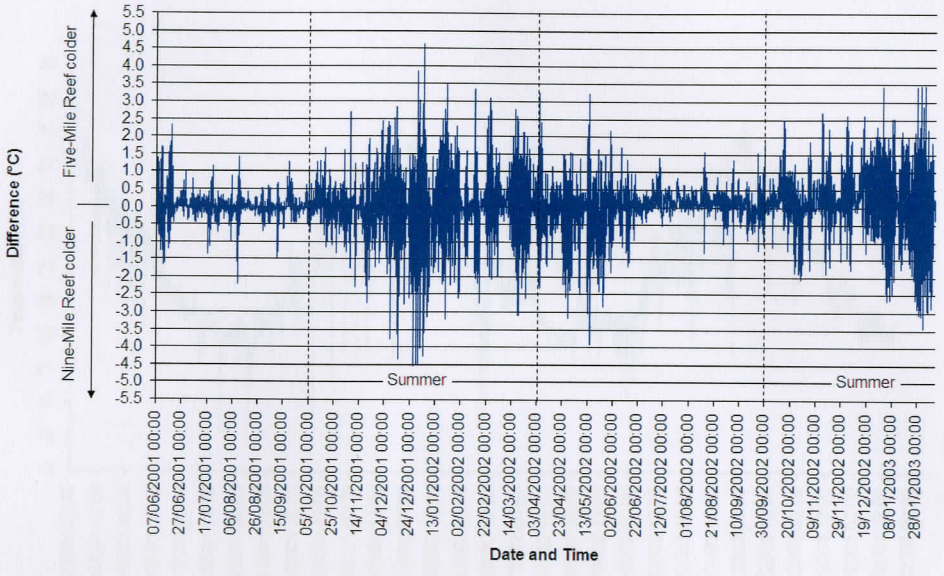

Figure 3.34: Upwelling index linear plot to determine seasonality (hourly data): Nine-mile Deep vs. Five-mile Deep

Differences in temperature between the two sites were plotted as a simple linear graph to show seasonality of upwelling events at the shelf edge in Sodwana Bay (Figure 3.34). During the summer, the intensity of upwelling events increases, diminishing slightly during the winter months. The temperature differences were also far larger as with previous comparisons, allowing cooler water onto the shelf and assisted in cooling the region down significantly.

3.3.4 Along-shelf temperature dynamics: Nine-mile Reef (18 m) vs. Two-mile Reef (12 m)

This final comparison was plotted to determine whether cooler water being upwelled or introduced in the north of Sodwana Bay on NMR was evident in the south of Sodwana Bay on Two-mile Reef (TMR).

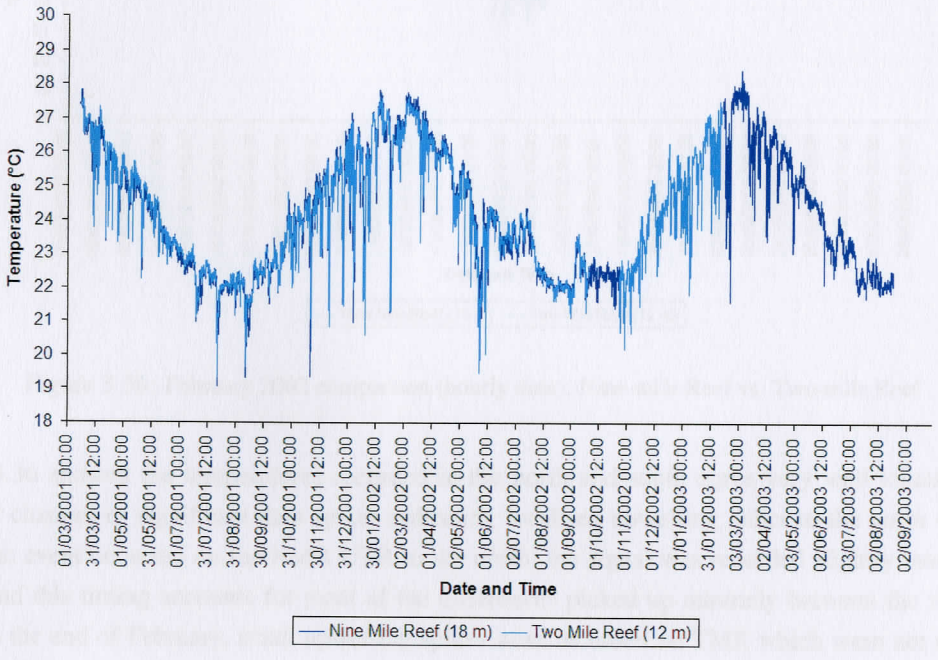

Figure 3.35: Full data set comparison (hourly data): Nine-mile Reef vs. Two-mile Reef

As with previous comparisons, upwelling spikes were more common in summer as opposed to winter, but not with the same intensity as sites on the shelf edge or at the canyon head (Figure 3.35). Only one summer and two winter comparisons were analysed as the two sensors lost data on adjacent deployments (Two-mile Reef loss Sept, Oct 2002 and Nine-mile Reef loss, October 2002 to February 2003). Thereafter, the Two-mile Reef sensor was removed.

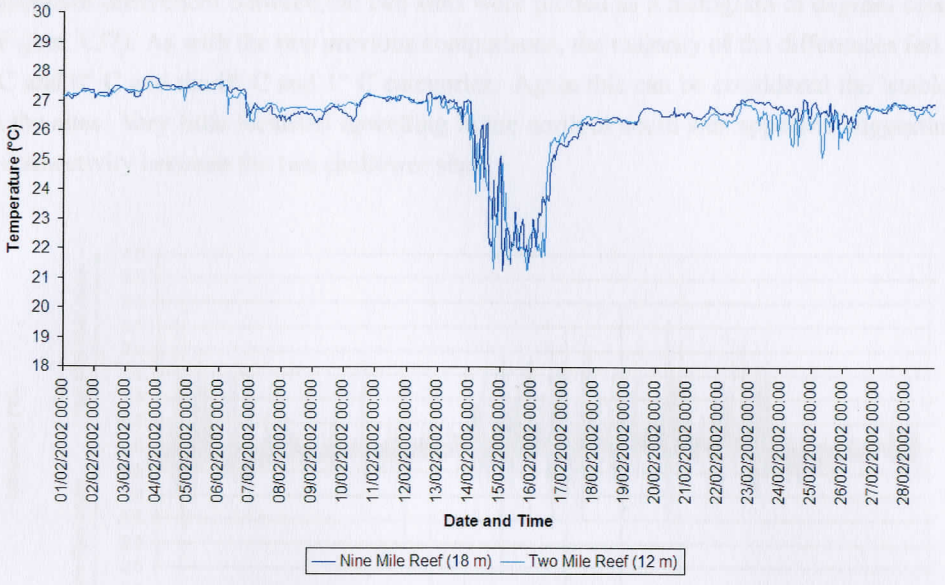

Figure 3.36: February 2002 comparison (hourly data): Nine-mile Reef vs. Two-mile Reef

Figure 3.36 showed the temperatures recorded in the north and south agree very well together, with minimal changes or significant data spikes indicating localised upwelling either to the north or south. Where an event occurred on the NMR UTR to the north, the signal was recorded slightly later further south, and this timing accounts for most of the differences picked up minutely between the two sites. Towards the end of February, small upwelling spikes were recorded on TMR which were not observed further north. At the most extreme the difference in temperature was 1.5° C.

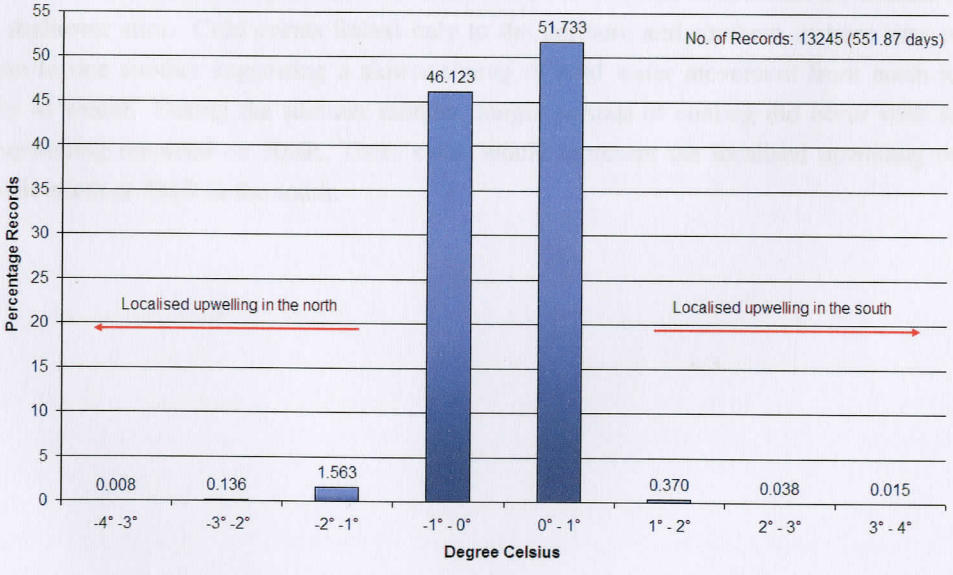

Figure 3.37: Upwelling index histogram plot (hourly data): Nine-mile Reef vs. Two-mile Reef

The temperature differences between the two sites were plotted as a histogram in degrees celsius categories (Figure 3.37). As with the two previous comparisons, the majority of the differences fell between the -1° C and 0° C and the 0° C and 1° C categories. Again this can be considered the 'stable' region between the sites. Very little localised upwelling in the north or south was apparent, suggesting a high level of connectivity between the two shallower sites.

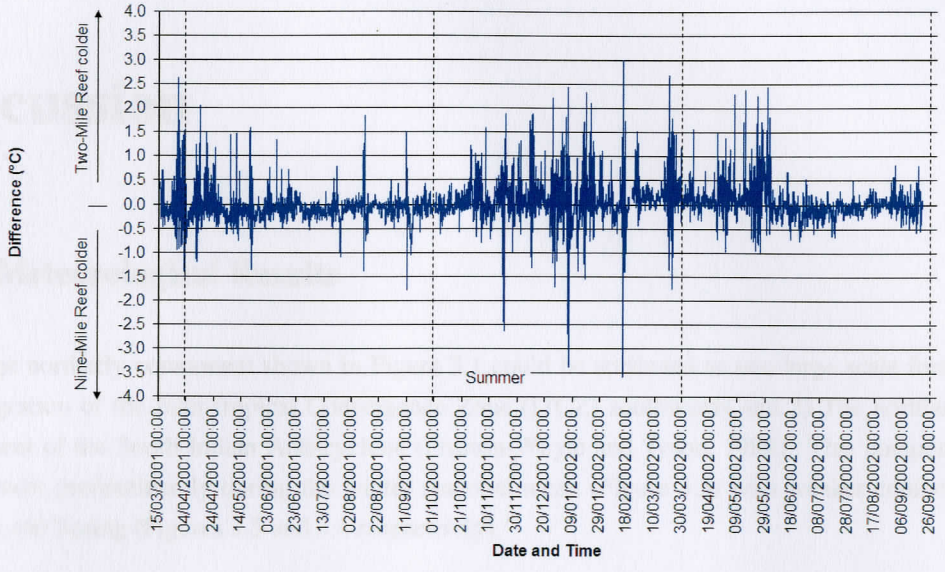

Figure 3.38: Upwelling index linear plot to determine seasonality (hourly data): Nine-mile Reef vs. Two-mile Reef

As with the NMD and FMD comparison, seasonality can be seen for the temperature differences between the two shallower sites. Cold events linked only to the northern and southern inshore sites occurred in relation to one another suggesting a slower timing of cold water movement from north to south, especially in winter. During the summer months, longer periods of cooling did occur with the more intense upwelling recorded on NMR. These cases would represent the localised upwelling on either NMR in the north or TMR in the south.

Chapter 4

Discussion

4.1 Meteorological Results

The large northerly component shown in Figure 3.1 could be attributed to two large scale forcings; 1) The migration of the Inter-tropical Convergence Zone (ITCZ) southwards and 2) The northerly wind component of the South Indian Anti-cyclone (Preston-Whyte and Tyson, 1988). This component was shown most predominantly during the winter seasonal mean (Figure 3.3) with weaker components in Autumn and Spring (Figures 3.5 and 3.4 respectively).

Winds originating from the south-west were forced by frontal systems travelling along the coast from the southern Cape coast (Preston-Whyte and Tyson, 1988; Hunter, 1988). Baroclinic wave disturbances (waves in the westerlies) will travel from Cape Town to Durban in 2.1 days and to Maputo in 2.8 days (Preston-Whyte and Tyson, 1988). South-westerly originating winds were evident throughout the study period with greater components in winter.

North-easterly component winds could be attributed to the north-easterly monsoon winds travelling southward (Preston-Whyte and Tyson, 1988). The presence of the ITCZ in the south over the summer months was shown with larger north-easterly components during the spring and summer seasons (Figures 3.4 and 3.5). The summer months also exhibited strong westerlies (onshore component) originating from the Indian Ocean, which could also be associated with the migration of the ITCZ (Preston-Whyte and Tyson, 1988).

A low frequency of berg winds (offshore components) from the west were observed for the study period. Coastal lows, as described by Schumann (1981), Hunter (1988) and Shillington (1992), are caused as air descends from the escarpment to the coast generating sudden cyclonic vorticities. These are common along the south and east coasts of South Africa, but evidently are not a feature of the coastline further north of Durban (Hunter, 1988).

Wind components from the south were seen to be greater in spring as opposed to other seasons. Of all the components, they also exhibited the strongest winds. This may be attributed to frontal systems travelling northward from the Indian Ocean as opposed to coastal fronts (Preston-Whyte and Tyson, 1988).

The strongest winds were recorded in spring (6.65 knots) with a corresponding lowest percentage of calms (11.29%). Coupled with strong north-easterly components and substantial northerly and south-westerly components, these strong winds could be attributed to the actual southward migration of the

ITCZ (Preston-Whyte and Tyson, 1988) and the last remnants of coastal troughs travelling north-eastward along the coast as winter cold fronts (Hunter, 1988). The weakest winds were recorded in Autumn (4.60 knots) with corresponding highest percentage calms (21.96%). Thus proving to be the mildest season in the northern KwaZulu-Natal region.

4.2 Acoustic Doppler Current Profiler (ADCP) Results

4.2.1 General Current Characteristics and North-Easterly Current Reversals

The literature reviewed (Lutjeharms, 2006; Lutjeharms et al., 2001; Shouten, 2002; Schumann, 1988; Shillington, 1992) highlighted the distinct lack of physical oceanographic knowledge for the northern region of KwaZulu-Natal. The primary focus of historical studies were the areas around Durban and Richards Bay where the understanding of physics on commercial shipping, factory outfall pipes and associated environmental impact studies took preference (Gründlingh, 1980). South Africa's major fisheries are also concentrated on the west and south coasts, leaving the east coast to be studied by line fish and coral reef experts due to its abundant biodiversity (Schleyer, 1999). Due to this lack of knowledge, many fundamental physical oceanography questions remain unanswered: Where does the Agulhas Current begin? What impact (if any) does it have on the relatively exposed northern KwaZulu-Natal shelf? And what are the implications to the sensitive high-latitude coral reefs, unique to this region? This 30-month ADCP data set provides some clarification to these queries.

South-westerly currents dominated the shelf for 73% of the total study period, and was assumed to be the Agulhas Current. Both Schumann (1983) and Lutjeharms (2006) were unable to determine exactly where the Agulhas Current begins. They place the origins north of 30° S (approximately Durban) and south of 25° S (approximately Maputo). However, Lutjeharms (2006) defined the generic boundaries of the northern Agulhas Current based on kinematics of the current to be 27° S in the north and 34° S in the south, which includes Sodwana Bay. The occurrence of northerly reversals suggested that on occasion either the Agulhas Current was not fully constituted, or had moved far enough offshore to allow a small cyclonic rotation within the embayment. Current direction was considered stable throughout the water column with bottom flow mimicking the surface flow the majority of the study. A small percentage of the study period showed opposing currents.

The current velocities recorded for the study period were not very strong. A very small percentage of records exceeded the 100 cm s^{-1} threshold (0.02%) and only 9% of the study exceeded 50 cm s^{-1}. The majority flow was recorded between 11 and 20 cm s^{-1}. The velocity data also showed stable currents with a very slight decrease of mean velocities between the surface and bottom data bins. It would be expected that southerly currents would record maximum velocities, which was the case at 108 cm s^{-1}. However, a northerly reversal was recorded at 106 cm s^{-1}, suggesting these northerly reversals were not inconsequential.

Of the entire 30-month data set, 206 northerly reversal events were recorded, with the shortest being a meagre event of half an hour, and the longest a substantial 38 hours. On average, a northerly reversal lasted 23 hours, which may have been sufficient to have an impact on the dynamics of the shelf. When plotted as monthly northerly reversal percentages, no clear seasonal trend could be distinguished. The months with the highest percentage of northerly reversals were September 2001, March 2003, February 2003 and August 2001 (in order). Both December and January months of 2001 and 2002 showed low

percentages of reversal events, but this was not sustained throughout the summer and cannot be considered a seasonal attribute. Lutjeharms (2006) after Gründlingh (1980) shows no seasonality in the volume transport of the northern Agulhas Current. Lutjeharms (2006) did however suggest that seasonal wind patterns over the Mozambique Channel may affect the volume flow of surface waters based on modelled data. Available current meter did not however support this seasonal variability (Lutjeharms, 2006).

Green (2009) has shown bedload parting of sediment along the northern KwaZulu-Natal shelf. These bedload parting zones are an indication of sediment transport direction, and by association, the current regime causing this movement (Green, 2009). Thus, along the northern KwaZulu-Natal shelf, sediment shifted northwards when situated north of a bedload parting, and southwards when south of a parting. Bedload partings were evident adjacent to canyon heads that encroach onto the shelf, especially further north off the Mabibi area shown in Figure 4.1 (after Green, 2009) and White Sands canyon which is situated just north of the Wright Canyon within the Sodwana Bay study area (Figure 2.2). Green (2009) also noted bedform parting off Nine-Mile Reef, particularly inshore, while offshore southerly transport of sediment dominated. The critical bed shear velocity needed to move medium sand (grain size = 0.255 mm), which Green (2009) found to be the dominant sand type for the northern KwaZulu-Natal shelf, is 17 cm s^{-1} based on work done by Harris et al. (1992). This velocity falls well within the range recorded for the *in situ* ADCP results presented within this study. Bedform partings became more frequent further north along the northern KwaZulu-Natal shelf, suggesting a greater frequency of northerly reversals to the north. This result, coupled with evidence of northerly reversals recorded *in situ* at NMR, concurs with Harris (1978) when he speculated a northerly counter-current, increasing with strength with the proximity to the border, occurring along the northern KwaZulu-Natal shelf.

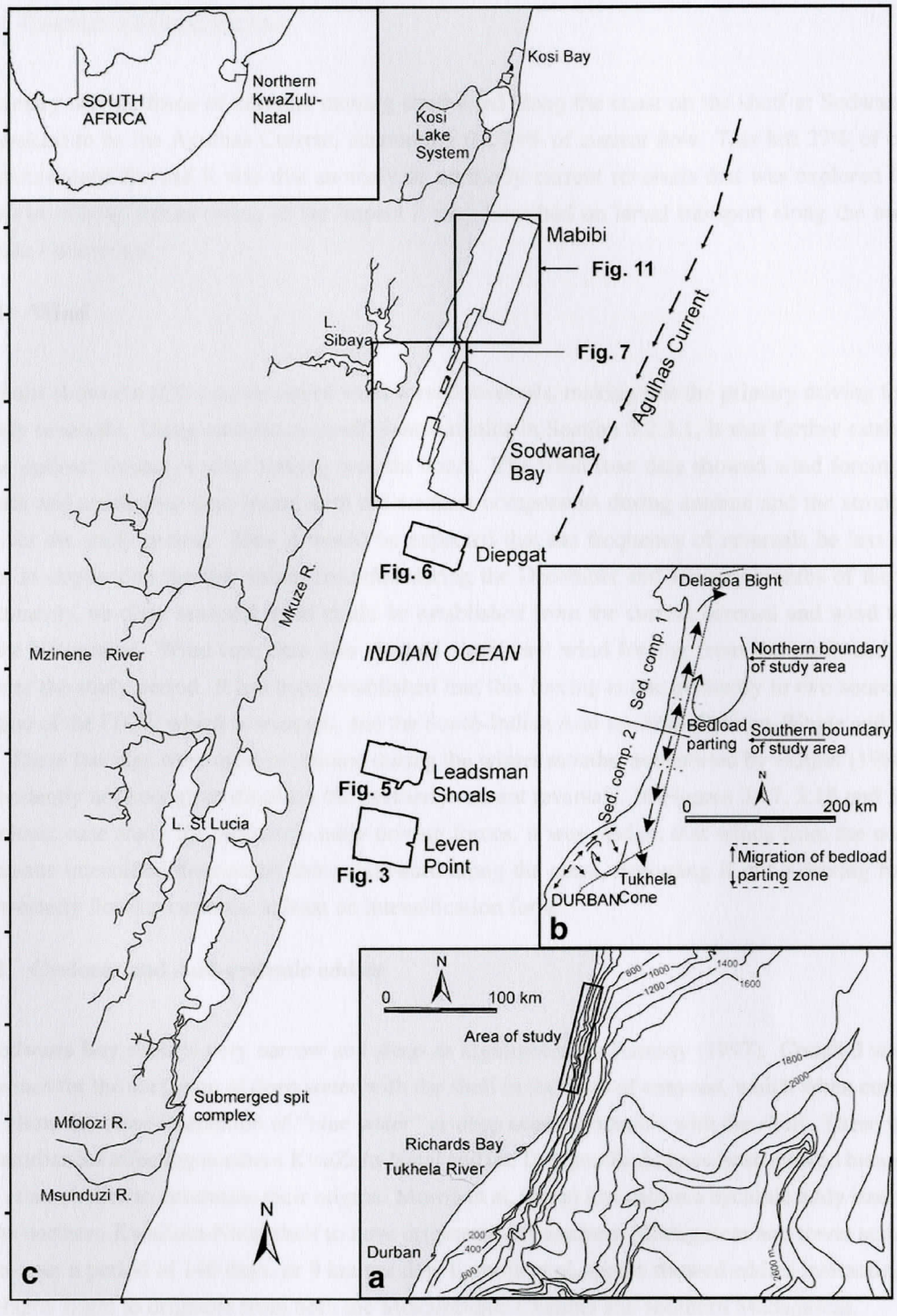

Figure 4.1: Locality map with recognised bedload parting zones (after Flemming and Hay, 1988) and the areas investigated by side-scan sonar where canyons are found (Green, 2009).

4.2.2 Current Driving Forces

The primary driving force of currents moving southward along the coast on the shelf at Sodwana Bay was assumed to be the Agulhas Current, accounting for 73% of current flow. This left 27% of current flow unaccounted for and it was this anomaly of northerly current reversals that was explored further in terms of driving forces owing to the impact it may have had on larval transport along the northern KwaZulu-Natal coast.

4.2.2.1 Wind

The results showed a 62% occurrence of wind-forced reversals, making this the primary driving force of northerly reversals. Using correlation coefficient statistics in Section 3.2.3.1, it was further established that the optimal timing of wind forcing was six hours. The wind rose data showed wind forcing from the south and south-west year round with the weakest components during autumn and the strongest in spring for the study period. Thus it would be expected that the frequency of reversals be less during autumn as opposed to the low values recorded during the December and January months of the study. Unfortunately, no clear seasonal trend could be established from the current reversal and wind forcing monthly histograms. Wind rose data also showed significant wind forcing from the north and north-west over the study period. It has been established that this forcing is due primarily to two sources; the migration of the ITCZ, which is seasonal, and the South-Indian Anti-cyclone (Preston-Whyte and Tyson, 1988). These forcings were most prominent during the winter months, as reported by Hunter (1988), but were evidently not enough to diminish the northerly current reversals. In Figures 3.17, 3.18 and 3.19 of the cyclonic case study for mesoscale eddy driving forces, it was evident that winds from the northern components intensified the current flow southward along the coast, becoming if not a driving force of south-westerly flowing currents, at least an intensification force.

4.2.2.2 Cyclonic and Anti-cyclonic eddies

The Sodwana Bay shelf is very narrow and steep as highlighted by Ramsay (1997). Coupled with this are avenues for the exchange of deep water with the shelf in the form of canyons, which when combined would allow the close interaction of "blue water" or deep ocean dynamics with the shelf. These mesoscale disturbances affecting northern KwaZulu-Natal and the Delagoa Bight have been tracked historically in two other studies to determine their origins. Morris et al. (prep) has shown a cyclonic eddy interacting with the northern KwaZulu-Natal shelf to have originated off southern Madagascar and travel across the channel over a period of 140 days, or 9 km per day. Lamont et al. (prep) showed eddies interacting with the Delagoa Bight to originate from both the Mozambique Channel and southern Madagascar.

Two case studies were presented to illustrate the usefulness of mesoscale eddies on the shelf region of Sodwana Bay. The first of these investigated the interaction of a cyclonic rotation with the shelf. It was shown that northerly flow was initiated simultaneous to wind forcing from the south west thus resulting in a reversal that was not wind induced. The current flow was maintained despite wind forcing from the north, however currents were diminished somewhat. The second case study was presented to show the affect of an anti-cyclone on the shelf. Theoretically, due to the anti-clockwise rotation of the anti-cyclone, flow should have intensified to the south which was difficult to determine given the forcing of winds from the north simultaneously. The interaction of the mesoscale eddies offshore and their eventual affect on

the shelf currents as seen in the resultant variability in Figures 3.21 and 3.22, highlights the dynamic and unpredictable nature of mesoscale rotations (Shouten et al., 2003) and thus a lesser importance in terms of driving forces. This conclusion can be augmented further with the comparison of directional flows between the satellite geostrophic flows offshore of the *in situ* ADCP measurements and the ADCP itself. The results showed that only 42% of assumed cyclonic perturbations were recorded on the ADCP for the time period. The southerly flow comparison indicated a significant relationship (70.65%), but it cannot be determined from the data which measurements related to anti-cyclonic landward edge southerly flow patterns and which measurements were related to the Agulhas Current. This method of using delayed time extracted surface geostrophic flows from SSHA images and comparing the results to the *in situ* ADCP may not be very reliable as SSHA data along the coastline can be coarse and incorrectly resolved (T. Lamont pers. comm.). Delayed time images were only available every seven days resulting in a smaller data set with which to work and thus a smaller chance of successful comparison.

4.3 Underwater Temperature Recorder (UTR) Results

4.3.1 Nine-mile Reef Long-term Monitoring Site

The fourteen year long term monitoring record showed the breach of temperatures across the coral bleaching threshold during four summers, including that of the 1998 global coral bleaching phenomenon and 2000, another devastating summer world-wide. When comparing the data to that of the ENSO years as calculated by NOAA (National Oceanic and Atmospheric Agency), these two summers of bleaching fell within a period of global temperature cooling or "La Niña". According to Le Treut et al. (2007), the coupled ocean-atmosphere phenomenon known as the El-Niño Southern Oscillation (ENSO) has its origins in the Pacific Ocean but affects climate globally through 'teleconnections'. An El-Niño will begin when warmer water occurs off the coast of Peru. This warmer water extends across the width of the Pacific Ocean as a plume and interacts with the atmosphere directly above it. These changes result in a seesaw of the surface pressure gradients impacting sea surface temperatures, altering ocean currents and weakening trade winds, and eventually having a global impact (Le Treut et al., 2007). The authors could not however give the time it takes for the affects of these teleconnections to be felt across the globe (Le Treut et al., 2007), hence the potential mis-match of "La Niña" cooling in ENSO years to the coral bleaching occurrences in Sodwana Bay. Goreau et al. (2000) showed that the Indian Ocean was affected by more than just the El Niño phenomenon, which would have worsened the 'teleconnections' already in place and caused the severe bleaching throughout the rest of East Africa. They describe two oscillations. The first is an internally generated climatic oscillation occurring every 11-12 years, but is not always in phase with El Niño. In 1998, they happened to coincide (Goreau et al., 2000). Coral cores taken from Indian Ocean corals show these cycles to occur irregularly over time, with the 1998 event being the strongest since 1888. The second oscillation is the Pacific Decadal Oscillation which has a period of several decades (Goreau et al., 2000). This particular oscillation boosts SST's in the Pacific and Indian Oceans north of the equator and was thought to be at its peak during 1998. However, if these oscillations were in place in 1998, causing severe devastation throughout the Indian Ocean and barely 1% of coral bleaching in Sodwana Bay, what caused the 2000 event which affected Sodwana Bay so much more? Further investigation on the time duration of particular decadal and ENSO oscillations would need to be made and the possibility of how long these responses affect the region. Coral bleaching events have the potential of being more enhanced when these climatic oscillations described above and ENSO oscillations are temporarily in phase.

Riegl and Pillar (2003) showed the value of cold water spikes during the marine summer of NMR. These data were extended to illustrate that throughout the fourteen year data set, cold spikes were present in all except two seasons. The summers of 1998 and 2000 experienced cold spikes early during the summer which did not sustain the cooler temperatures, resulting in a warmer than usual maximum temperatures later on in the summer. This coincided very well with the occurrence of bleaching on coral reefs in 1998 and 2000. These cold water spikes appear to be a common trend throughout the data set as seen in Figure 3.25. Furthermore, no significant coral bleaching has been observed on Sodwana Bay's reefs since the summer of 2000 (Schleyer et al., 2008). The anomalous data showed a natural cyclical phenomenon of warming and cooling over the data set, and concurs well with local influences of a macro-cyclical nature described by Schleyer et al. (2008). These data were representative of the actual trends which occurred

at Sodwana Bay as ENSO warming and cooling months were excluded from the calculations. The trend also showed the region entering a new phase of warming with the potential for new occurrences of coral bleaching.

When taking into consideration the entire time series and the resultant products, it can be assumed that the effects of global warming as a phenomenon has not yet taken place at Sodwana Bay. The trends appear to be natural in occurrence and this may be a function of cold water intrusions occurring during the summer months which evidently cool the region down substantially. Should the frequency of these cold water spikes begin to decrease, the resultant affect on coral reefs may be damaging.

4.3.2 Across-shelf and along-shelf temperature dynamics

Three comparisons of the shorter deployed temperature recorders and the long-term monitoring site were made to determine whether upwelling was taking place at Sodwana Bay, what types of upwelling were interacting with the region and if there were any seasonal trends. The first comparison was an across-shelf analogy of the NMR recorder at 18 m and the NMD recorder at 37 m. This comparison highlighted very well the upwelling of cold water occurring on the deep site was not always transported inshore to the shallow site. This was true for about a quarter of the data comparison. Upwelling events could be quite substantial with decreases in temperature of up to 6 or 7° C. Upwelling appeared to be more frequent during the summer months, but occurred year round. Infrequent and small upwelling spikes were evident inshore but may be linked to the timing of transported water ashore. Due to the proximity of NMD to the shelf edge, and there being no canyons evident in the bathymetry offshore of this northern reef community (Ramsay and Miller, 2006), it can thus be assumed that this upwelling was caused by the forcing of the Agulhas Current along the shelf edge. The cold water spikes described by Riegl and Pillar (2003) could thus be attributed to this shelf edge upwelling. Inshore reefs may not be as well protected, as transport of cooler water inshore was inconsistent, leaving shallower reefs susceptible to changes and potentially bleaching.

To determine whether the region was affected by canyon-induced upwelling, a comparison of the two deeper sites was made to determine differences occurring in upwelling timing and intensity. As previously highlighted, the Sodwana Bay shelf is breached by three canyons; White Sands, Wright and Jesser Canyons (Ramsay, 1997). The FMD UTR was deployed at Wright Canyon, south of the main canyon head (Figure 2.2). Upwelling occurred throughout the year with greater intensity during the summer months. The two sites mimicked one another very well in terms of events with less than 5% each way for localised shelf edge upwelling to the north and canyon-induced upwelling south. The canyon-induced upwelling may not be substantial as the canyon may not be wide enough or long enough to form a decent avenue for cold water to breach the shelf. Allen et al. (2001) showed that the Barkley Canyon off Canada to be affected by canyon-induced upwelling, and the vorticity stretching over the canyon can form a closed off cyclonic rotation entrapping biological material travelling up from depth. The Barkley Canyon is 13 km wide and 6 km long. Wright Canyon is less than 1 km wide at its head and only slightly wider than 1 km deeper down. Furthermore Wright Canyon is only 2 to 3 km long when analysing Figure 2.2.

The final comparison was made to determine the connectivity of the northern and southern reaches of the Sodwana embayment. These two recorders at NMR (18 m) and TMR (12 m) were also the shallowest of those deployed. The comparison showed strong connectivity between the sites, with upwelling spikes

occurring throughout the year with a greater intensity in summer. On occasion, localised upwelling to the north or south was recorded, but the occurrence was very low. The probable cause of this apparent localised upwelling may be the timing of water flowing from the north to the south. The localised upwelling not associated to transport timing may be attributed to reversals in current entrapping cold water in the north and transporting it northwards.

In order to resolve these apparent localised upwelling events on the various temperature recorders, a definitive study of the circulation of the entire embayment would need to be made. This would resolve whether northerly reversals in the north are extending southwards affecting the cooler water intrusions onto the shelf.

Chapter 5

Implications and Conclusions

5.1 Coral Larval Transport

The physical dynamics and associated driving forces of the Sodwana embayment have significant affects on planktonic coral larvae spawned in the water column by the coral reef communities that inhabit the northern KwaZulu-Natal shelf. Fertilisation can take place internally and larvae are released into the water column (brooder corals) or fertilisation is external in broadcast spawning corals (Richmond, 1997). The planktonic larvae float in the water column, developing into planulae that then find suitable substratum on which to settle (Richmond, 1997). The time before settlement varies and will depend on the environmental conditions and the species of coral (Richmond, 1997).

The results showed that a predominantly southerly flow was recorded for the study period. This flow is not as strong as flow found further south (Schumann, 1988; Lutjeharms, 2006), with an average speed at the surface of 27 cm s^{-1}. Northerly reversals were recorded 27% of the time with velocities reaching similar speeds as the dominant southerly flow. Larvae spawned at Sodwana Bay would theoretically travel south along the coast before finding suitable substratum on which to settle. If an average speed of 27 cm s^{-1} is assumed from the data and the approximate distance from NMR to the Jesser Point in the south is 15 km, assuming no additional external forcing, the time taken to traverse the embayment would be approximately 15 hours. This time would decrease rapidly with increasing velocity, a particle entrapped in a 100 cm s^{-1} velocity flow would need only four hours to travel to the southern reaches of the embayment. Miller and Mundy (2003) showed the settlement time of two faviid species to be between 2.5 and 2.75 days. These results were considered shorter in comparison to the more accepted settlement time of between 14 and 36 days as shown by Williams et al. (1984) for acroporiid and faviid species. Even if the settlement times of Miller and Mundy (2003) are accepted and the average current velocity travelling south taken into account, spawned coral larvae would be lost from the Sodwana Bay area on a regular basis. Byers and Pringle (2006) described how adult populations would have died off in an area with the consistent downstream export of spawned material, but a 'drift paradox' (the persistence of sedentary adult populations against mean currents) exists where coral reefs have survived, regardless of this. Sammarco and Andrews (1989) conducted, on the Helix Reef within the Great Barrier Reef, an experiment using two current meter moorings and 24 settlement plate moorings, deployed along four arms of a spiral (270° counter-clockwise), to determine how far coral larvae travel before settling, and whether reefs were self-seeding. They assumed a larval settlement time of 24-72 hours for external

fertilisation (broadcast spawners) and four hours for brooders. Species that rely on broadcast spawning will have a longer dispersal capacity than brooding species. The majority of coral spat settled within 300 m of the reef perimeter, decreasing dramatically with distance offshore (Sammarco and Andrews, 1989). However Sammarco and Andrews (1989) were confident that sufficient genetic exchange existed to prevent allopatric speciation. Peaks in *Acropora* plate settlement correlated with areas of highest water residence time (areas of low currents and / or trapped lee eddies) and where flushing rates were low (Sammarco and Andrews, 1989). Conclusively, the Helix Reef could be considered self-seeding and the understanding of current dynamics extremely important in determining recruitment patterns of coral larvae (Sammarco and Andrews, 1989).

Two mechanisms may play a role in retaining larvae in Sodwana Bay: 1) Larval positioning in the water column and 2) Northerly reversals in the current flow. Using a 3D model, made up of a number of 2D models, Black et al. (1991) showed the positioning of larvae within the water column to be a deciding factor in larval retention. Effectively, larvae at the sea-floor have a 95% chance of retention on natal reefs as opposed to those on the surface affected by wind-driven currents. Results from Sodwana Bay showed the current direction to be the same throughout the water column for the majority of the study. More importantly, the current velocities were shown to decrease between the surface and the bottom of the water column (27 cm s^{-1} to 18 cm s^{-1}). Thus, larvae that remain close to the bottom after spawning have a better chance of being retained on the natal reefs. The ADCP used in this study was deployed on a sand mooring, slightly offshore of the reef complex. The flow around the reef complex itself would be weaker than that directly above the ADCP due to the topography of the reef, creating areas of higher water residence time linked to higher spat settlement as described by Sammarco and Andrews (1989).

On the fringing reef of Coconut Island, Hawaii, a plankton net tow study was undertaken to capture coral planulae and determine coral larval distribution and potential export (Hodgson, 1985). What limited data was available showed coral planulae of some coral species to undertake diurnal migration, moving to the surface at night and sinking downwards again during the day (Hodgson, 1985). Furthermore, the results showed the planulae to exhibit a highly patchy horizontal distribution similar to phytoplankton blooms. Both of these mechanisms may be related to coral spawning and planulating at night in synchronised spawning groups, or coral larvae may to a certain degree have limited control over their swimming capabilities. Should the latter be the case this may assist in larval retention in Sodwana Bay on or close to their natal reefs. Hodgson (1985) concluded that a large number of planulae were exported from Coconut Island, although how it affected the potential recruitment of surrounding areas was not clear.

Northerly reversals in current flow were shown to occur periodically throughout the data set regardless of season. These reversals lasted on average 23 hours and were thought to be primarily driven by southerly winds, approximately six hours after their commencement. These reversals, when occurring intermittently with southerly currents, would provide the ideal mechanism for self-seeding of natal reefs. Larvae would be carried backwards and forwards with the variable current flows described above over potential coral communities until they are developed enough to settle. With the reversal events not being linked as a seasonal anomaly, larvae spawning throughout the year (depending on species) would be able to take advantage of the current flow changes to ensure self-seeding of natal reefs or at least settlement on suitable substrata, potentially even further upstream. Schleyer et al. (1997) showed how coral species in Sodwana Bay may use lunar cycles as cues to time spawning events. Three species were studied in detail, one hard coral and two soft corals, and cues were linked to either the new moon or full moon events, predominantly from January to March, although extending to June for *Anthelia glauca*. From these results,

a table was constructed which shows these spawning preferences in relation to the current velocity and direction data collected from March 2001 to August 2003 (Table 5.1). The majority of spawning, fertilisation and planulation would have occurred during southward flow, with only four in thirty-one events occurring during northerly flow. Data from the particular days in question were extracted at 19h00, which may or may not be the optimal time for spawning, and the results are used for illustrative purposes only. However, coral species that make use of multiple spawning sessions have a greater chance of being caught up in a northerly flow and retention on natal reefs is enhanced. This theory of retention on reefs was proposed by Black et al. (1991) as one of their results of their numerical model of Davies reef within the Great Barrier Reef. Zaslow et al. (1999) show a higher fecundity during summer months and almost zero deformation of planulae for the species *Heteroxenia fuscescens* in the Gulf of Eilat, northern Red Sea.

Table 5.1: Potential dates within the lunar cycle for coral spawning at Sodwana Bay (Schleyer et al., 1997) linked to ADCP data for the study period.

New Moon	Speed (cm/s)	Direction		Activity	Full Moon	Speed (cm/s)	Direction		Activity
24 Jan 01	No data	No data	No data	PV / AG-p	09 Jan 01	No data	No data	No data	AG-f
23 Feb 01	No data	No data	No data	AG-p	08 Feb 01	No data	No data	No data	AG-f
25 Mar 01	50	185°	SSW	AG-p	09 Mar 01	No data	No data	No data	SG / AG-f
23 Apr 01	53	192°	SSW	AG-p	08 Apr 01	20	169°	SSE	AG-f
23 May 01	31	192°	SSW	AG-p	07 May 01	57	194°	SSW	AG-f
21 Jun 01	28	201°	SSW	AG-p	06 Jun 01	No data	No data	No data	AG-f
13 Jan 02	8	87°	ENE	PV / AG-p	28 Jan 02	67	195°	SSW	AG-f
12 Feb 02	18	189°	SSW	AG-p	27 Feb 02	22	160°	SSE	AG-f
14 Mar 02	21	177°	SSE	AG-p	28 Mar 02	10	358°	NNW	SG / AG-f
12 Apr 02	34	169°	SSE	AG-p	27 Apr 02	31	178°	SSE	AG-f
12 May 02	34	179°	SSE	AG-p	26 May 02	64	195°	SSW	AG-f
10 Jun 02	19	200°	SSW	AG-p	24 Jun 02	23	29°	NNE	AG-f
2 Jan 03	55	193°	SSW	PV / AG-p	18 Jan 03	51	183°	SSW	AG-f
1 Feb 03	21	149°	SSE	AG-p	16 Feb 03	24	180°	S	AG-f
3 Mar 03	13	157°	SSE	AG-p	18 Mar 03	53	181°	SSW	SG / AG-f
1 Apr 03	38	191°	SSW	AG-p	16 Apr 03	17	4°	NNE	AG-f
1 and 31 May 03	51 / 36	194° / 204°	SSW	AG-p	16 May 03	51	194°	SSW	AG-f
29 Jun 03	39	204°	SSW	AG-p	14 Jun 03	9	211°	SSW	AG-f

Key:

PV: *Pocillopora verrucosa* spawning

SG: *Sarcophyta glaucum* spawning

AG-f: *Anthelia glauca* fertilization

AG-p: *Anthelia glauca* planulation

Cyclonic eddies travelling south or westwards from the Indian Ocean were also shown to be responsible for northerly reversals in currents at Sodwana Bay. Although not as prominent a driving force as wind-induced reversals, cyclonic eddies could cause currents to reverse or intensify reversals already taking place. Cyclonic eddies and conversely anti-cyclonic eddies, are large mesoscale features that have the ability of drawing biological material offshore from the shelf (Gaughan, 2007; Roberts et al., 2006). Moore et al. (2007) show, using satellite and in situ measurements of surface chlorophyll values, that there is a higher planktonic biomass in anti-cyclonic eddies as opposed to cyclonic eddies. They also

found two types of phytoplankton communities in conjunction with anti-cyclonic eddies, shelf communities within the eddy and offshore subtropical communities within the deep chlorophyll maximum on the anti-cyclone edge (Moore et al., 2007). Gaughan (2007) was however not confident that the warm-core (anti-cyclonic) eddy described in his work, once it had entrained material offshore, could sustain larvae until suitable substrata are once again attained due to the deep-ocean characteristics of mesoscale eddies. Sabates et al. (2007) showed how anti-cyclonic eddies in the North West Mediterranean were instrumental in transporting anchovy larvae from the spawning grounds to the nursery areas further south, while sustaining them long enough in order to reach their final destination. Off Hawaii, a similar conclusion was reached for reef fish larvae, only this time the mechanism was a cold-core eddy which entrained the larvae offshore, with passive drift the most likely mechanism responsible for ensuring the return of larvae to the shelf (Lobel and Robinson, 1988). Coral planulae have the ability, based on metabolic calculations, to forgo settlement for periods, known as competency periods, of 49 days (Zaslow and Benayahu, 1996) to 100 days (Richmond, 1987). However the viability of planulae to settle was querstioned by Nishikawa and Sakai (2005) who showed between 18% and 25% of planulae were able to settle for two *Acropora* species. Until further studies can be carried out on the potential transport mechanism of eddies to coral gene flow, it needs to be assumed that mesoscale eddies have the ability to entrain coral larvae offshore of Sodwana Bay and be lost, especially when taking into consideration the narrow shelf of the region.

5.2 Coral Bleaching

One of the most prominent and newsworthy consequences of global climate change has been the occurrence of coral bleaching, especially after the globally devastating 1998 event (Sheppard, 2003). The causes of coral bleaching include freshwater flooding, pollution, sedimentation, disease and importantly elevated temperatures and solar radiation (Grimsditch and Salm, 2006). Prominent in the literature have been studies focusing on determining the affect of bleaching on coral reef communities and the potential loss of biodiversity (Wilkinson et al., 1999; Obura et al., 2000; Schleyer et al., 2008). Coral bleaching occurs when the zooxanthella resident in the coral tissue is lost or their photosynthetic pigment is reduced (Celliers and Schleyer, 2002). This causes a whitening of coral tissue. The questions raised within this study, are how the coral communities resident at Sodwana Bay have fared with gradual warming, and what factors would have protected the reefs from severe bleaching? As highlighted in the discussion, coral bleaching occurred at Sodwana Bay in 1998 (< 1%) and 2000 (< 12% coral cover affected). The cause for this bleaching was attributed to elevated temperatures and high insolation, and in 2000 coral disease also played a role. The coincidental coupling of decadal climate oscillations and ENSO events are thought to be the primary factor for the elevated temperatures (Goreau et al., 2000).

Grimsditch and Salm (2006) and West and Salm (2003) have shown a number of resistance and resilience factors that would protect corals from bleaching events. Resilience factors relate mainly to ecological and conservation factors, and explain how corals are able to recover from disturbance or change. Resistance factors (the ability to withstand disturbances), were grouped into two categories, that of 1) tolerance (coral acclimatisation, adaptive bleaching hypothesis, zooxanthellae clades and coral morphology) and 2) avoidance (local upwelling and currents) which is of primary interest here (Grimsditch and Salm, 2006). Currents are beneficial on coral reefs as they flush harmful toxins and oxygen radicals away from coral species emitting them and also improve coral reef resilience by preventing ecological phase shifts (i.e. corals to macro-algae), (Grimsditch and Salm, 2006). West and Salm (2003) discussed two examples where corals remained unscathed during the 1998 coral bleaching event: The branching and fire corals within the channel leading to the Alphonse Atoll, Seychelles, remained healthy while the rest of the Seychelles experienced intense bleaching and the southern reaches of the Komodo National Park, Indonesia, are subjected to strong currents and were spared bleaching while the northern regions were affected, where currents are sluggish. Currents at Sodwana Bay, although appear sluggish in this study compared to the downstream measurements of the Agulhas Current (27 cm s^{-1} vs. 60-120 cm s^{-1} off Richards Bay), are still considered substantial enough to provide resistance to bleaching in Sodwana Bay.

Localised upwelling was also shown to play a role in bleaching resistance in corals and has perhaps been better studied (West and Salm, 2003). It is thought that large-scale upwelling could inhibit development of coral communities, but smaller localised events were considered beneficial in some regions (West and Salm, 2003). In north Binh Thuan, Vietnam, reefs were shown to recover very quickly from bleaching in 1998 due to localised upwelling, and certain reefs affected by upwelling were largely spared during the 1998 bleaching event in Central Indonesia, Maldives and Zanzibar (West and Salm, 2003). More reliable means of cooling reef communities were considered by West and Salm (2003) to be mixing, due mainly to tidal or wind regimes, and proximity to the cooler shelf edge as opposed to upwelling of cold water from the deep. Upwelling can be caused by sheer-edge forcing of currents along the

shelf edge which forces cool water up onto the shelf, or by means of mesoscale eddies travelling from deep water towards the coast (Lutjeharms, 2006). During El Niño or other climatic perturbations, these mechanisms may become disrupted and not operate effectively (Grimsditch and Salm, 2006). Cold water may not always be available during times of elevated temperatures as was the case in Panama in 1983 (Grimsditch and Salm, 2006). Upwelling protected corals initially but, due to the persistence of the 1983 ENSO, corals bleached after the three month upwelling period had run its course (Grimsditch and Salm, 2006). Furthermore, West and Salm (2003) show that in some cases, corals become more sensitive when they are constantly exposed to these cooler upwelled waters and, when a sudden shut-down takes place, bleaching mortality may occur quite rapidly.

The results of this study showed that Sodwana Bay was affected by localised upwelling. It was proven that shelf edge upwelling was the predominant type of upwelling, but the effects of mesoscale features on the shelf and the canyon-heads forming an avenue onto the shelf cannot be discounted. It was shown that the entire shelf was protected by these cooler waters, more prominently at the deeper sites, but cold water was transported inshore on occasion.

Celliers and Schleyer (2008) created an index of the Sodwana Bay reefs for management purposes, with regards to their structure and risks to which they are exposed. The fore-reefs (18-20 m) of Seven-mile Reef and NMR represent mixed hard-coral and soft-coral communities, and the pinnacles (11-14 m) and reef flats (15-17 m) of TMR consisting of *Montipora* and *Pocillopora* and were considered to have the highest susceptibility to coral bleaching. Coincidentally, bleaching took place on TMR and NMR in 2000 on these reefs (Celliers and Schleyer, 2002), and also represent, to a certain extent, the "inshore" study sites used for this study. We can thus assume that, when conditions are conducive for bleaching, and cool upwelled water is not being transported inshore (which occurs approximately 25% of the time), these inshore reefs will be most affected. Even though physical bleaching has not been noted over the last eight years, other consequences of the earlier events have been documented. Schleyer and Celliers (2005) showed a shift in coral community structure from soft to hard corals which resulted in a 5.5% decrease in coral cover. Coral recruitment decreased until 2004, before it appeared to recover and improve again (Schleyer et al., 2008). The effects were termed "silent effects" of these temperature increases by Schleyer et al. (2008).

5.3 Conclusions

This physical oceanographic study was the first to be undertaken at Sodwana Bay. The aim of the study was to understand the embayment oceanographically and apply this knowledge to coral communities resident here. The main conclusions of this study in relation to key questions posed were as follows:

1. What are the current characteristics of Nine-mile Reef, and by assumption, Sodwana Bay?

- Current flow is predominately southward (73%), and assumed to be the Agulhas Current.
- Mean surface velocities recorded were 27 cm s^{-1}, with maximum velocities of 108 cm s^{-1} to the south. Less than 9% of the total currents exceeded 50 cm s^{-1}.
- Direction flow was consistent throughout the water column, with opposing surface and bottom flow recorded less than 5% of the study period.

2. Do northerly reversals in current flow occur at Sodwana Bay?

- Yes. Northerly flow was recorded 27% of the study period.
- Maximum velocities for northerly flow were recorded at 106 cm s^{-1}.
- The maximum duration of northerly reversals was 138 hours with an average duration of 23 hours.

3. What are the driving forces of the current characteristics described above?

- Three driving forces were identified for current flow in Sodwana Bay: The Agulhas Current, wind and mesoscale eddies.
- The Agulhas Current was assumed to drive flow along the shelf southwards. Unfortunately, with a single point ADCP measurement and satellite imagery too course to resolve close to the coastline due to the narrow shelf edge, this was inconclusively shown. Please refer to recommendations for project expansion possibilities to address this issue.
- Furthermore, due to this assumed forcing of southerly currents by the Agulhas Current, the resolution of driving forces on current flow in Sodwana Bay was concentrated on northerly reversals.
- Wind dynamics were proven to be the primary driving force for currents to the north.
- Mesoscale eddy dynamics were shown to influence current flow to the north with cyclonic eddies, and by assumption to the south with anti-cyclonic eddies.

4. Does upwelling occur at Sodwana Bay? If so, what types of upwelling occur?

- Shelf edge upwelling was proven to be the primary type of upwelling affecting the Sodwana Bay shelf.
- Canyon-induced upwelling was proven to exist, but its affects are short-lived and minor.

- A third type of upwelling may exist at Sodwana Bay, that of cyclonic eddy upwelling, or dynamic uplift of the thermocline onto the shelf by a cyclonic eddy. Further investigation is needed to understand this form of upwelling.

5. What are the implications of the physical oceanographic parameters described by the above objectives on:

a) Coral larval transport?

- Southerly flow has the potential of losing spawned material from the shelf, while northerly currents would assist in retaining larvae to the region.
- Coral species making use of multiple spawning periods to capture differing current flows, and remaining close to the sea-floor after fertilisation, will have be more successful in terms of retention to Sodwana Bay.
- The Agulhas Current could transport spawned material from reefs north of Sodwana Bay southwards.
- Mesoscale eddies were shown to potential entrap spawned material within their cores and transport either southwards (anti-cyclones) or northwards (cyclones). Competency periods of larvae could theoretically withstand this transport, but larvae may return to the shelf in a weakened condition.

b) Coral bleaching in the context of global climate change?

- Upwelling was proven to exist at Sodwana Bay which protects the shelf region from warming events and acts as a mechanism of resistance to coral bleaching.
- Offshore, deeper reefs are better protected as cooler water is not always transported inshore.
- Connectivity, with regards temperature dynamics, exists at Sodwana Bay both along-shelf and cross-shelf.
- The long-term temperature record at Nine-mile Reef does not show increased climatic change, but rather natural cyclical perturbations. Warming in 1998 and 2000 was linked to the coupling of natural climatic oscillations and the simultaneous occurrence of a La Niña event.

5.4 Recommendations

This study was undertaken to determine the physical parameters defining the oceanography of Sodwana Bay and the affects on larval transport and coral bleaching. A number of new questions have been suggested from the data analysed for this study: Are the northerly reversals constrained to the northern reaches of Sodwana Bay or do they extend across the entire embayment? Are the reversals linked to the Delagoa Bight eddy phenomenon? How far do the coral larvae disperse from their natal reefs and could these events be tracked using ADCP backscatter technology and zooplankton nets? To assist with some of these questions and address other general questions about the area, a number of ideas are presented below for future studies:

1. A weather station, preferably maintained by a reliable source, should be installed at Jesser Point. The SAWB weather station at Mbzwana Airfield is situated 14 kilometers inshore and 80 m above sea-level, and does not record the subtle air and sea breezes occurring at sea level which may or may not have an affect on the oceanography.

2. A water level recorder could be installed at Jesser Point on a long-term basis to monitor the gradual changes in sea level over time. With the onset of global climate change and the predicted melting of various ice-caps, sea level changes are expected to have an impact across the globe. Coral reefs at Sodwana Bay are deeper than traditional reefs and should not be affected by this.

3. A long-term UTR to be deployed at TMR, preferably the same depth as the NMR long-term monitoring site of 18 m. This would provide an ongoing comparison of the northern and southern extremities of the embayment and provide hind-sight of the potential affects of global climate change.

4. Only one ADCP was used in this study on the northern coral community of the embayment. In order to characterise the circulation of the embayment absolutely, the following ADCP deployment configuration could be considered:

   (a) The return of the NMR ADCP to a depth of 26 m.

   (b) A new deployment offshore of the NMR site within the Agulhas Current proper, at approximately 100 - 150 m. This deployment may pose problems owing to the sharp slope of the continental shelf. However, should the deployment be possible, the data would show when a strong south-westward forcing of the Agulhas Current occurs and how this forcing affects the shelf area. For instance, do strong southerly flows force currents on the shelf in a south-westerly or does it force a cyclonic rotation on the shelf?

   (c) A third shelf ADCP should be deployed to the south of the embayment just offshore of TMR at the same depth as the NMR deployment (26 m). This would show whether the flow recorded in the north is recorded further south, and the timing of events (i.e. linked to wind forcing or separate events such as mesoscale eddies).

5. Coral larval dispersal and natal reef retention will be fairly difficult to quantify. Storlazzi et al. (2006) have developed a mechanism using a moored, upward-looking ADCP, self-logging optical backscatter, tide and wave gauge with a conductivity and temperature sensor units, set at a very high resolution of data collection (every four minutes and 1 m depth bins for the ADCP). These instruments were able to record the backscatter in the water column caused by a coral spawning event and track the extent to which the larvae would travel in time. The data was complemented with successive plankton tows to "catch" larvae at varying distances from the reef under study and determine at what stage they entered their planktonic life-cycle. Such an experiment could be undertaken at NMR (the reef with the least interference from human activities) to determine how larvae at Sodwana Bay are affected by current dynamics. The research team at ORI are currently undertaking genetic research on corals to study larval distribution on natal reefs.

References

Allen, S. E., Vindeirinho, C., Thomson, R. E., Foreman, M. G. G., and Mackas, D. L. (2001). Physical and biological processes over a submarine canyon during an upwelling event. *Canadian Journal of Fisheries and Aquatic Sciences*, 58:671–684.

Bang, N. D. (1968). Submarine canyons off the Natal coast. *South African Geographical Journal*, 50:45–54.

Black, K. P., Moran, P. J., and Hammond, L. S. (1991). Numerical models show coral reefs can be self-seeding. *Marine Ecology Progress Series*, 74:1–11.

Byers, J. E. and Pringle, J. M. (2006). Going against the flow: Retention, range limits and invasions in advective environments. *Marine Ecology Progress Series*, 313:27–41.

Celliers, L. and Schleyer, M. H. (2002). Coral bleaching on high-latitude marginal reefs at Sodwana Bay, South Africa. *Marine Pollution Bulletin*, 44:1380–1387.

Celliers, L. and Schleyer, M. H. (2008). Coral community structure and risk assessment of high-latitude reefs at Sodwana Bay, South Africa. *Biodiversity and Conservation*, 17:3097–3117.

Conand, C., Chabanet, P., Quod, J. P., and Bigot, L. (1999). Coral reef monitoring in the South-West region of the Indian Ocean. Report, Regional Environment Programme.

Cooper, J. A. G. (1991). Beachrock formation in low latitudes: Implications for coastal evolutionary models. *Marine Geology*, 98:145–154.

Duchon, C. E. (1979). Lanczos filtering in one and two dimensions. *Journal of Applied Meteorology*, 18:1016–1022.

Farre, J. A., McGregor, B. A., Ryan, B. F., and Robb, J. M. (1983). Breaching the shelf break: Passage for youthful to mature-phase in submarine canyon evolution. *The Shelfbreak: Critical interface on continental margins.*, SEPM Special Publication(33):25–39.

Flemming, B. and Hay, R. (1988). Sediment distribution and dynamics on the Natal continental shelf. *Lecture notes on coastal and estuarine studies. Coastal ocean studies off Natal, South Africa*, 26:47–80.

Floros, C. D., Samways, M. J., and Armstrong, B. (2004). Taxonomic patterns of bleaching within a South African coral assemblage. *Biodiversity and Conservation*, 13:1175–1194.

Gaughan, D. J. (2007). Potential mechanisms of influence of the Leeuwin Current eddy system on teleost recruitment to the Western Australian continental system. *Deep-Sea Research Part II*, 54:1129–1140.

Glassom, D., Celliers, L., and Schleyer, M. H. (2006). Coral recruitment patterns at Sodwana Bay, South Africa. *Coral Reefs*, 25:485–492.

Goreau, T., McClanahan, T., Hayes, R., and Strong, A. (2000). Conservation of coral reefs after the 1998 Global Bleaching Event. *Conservation Biology*, 14(1):5–15.

Green, A. (2009). Sediment dynamics on the narrow, canyon-incised and current swept shelf of the northern KwaZulu-Natal continental shelf, South Africa. *Geo-Marine Letters*, 29(4):201–219.

Grimsditch, G. D. and Salm, R. V. (2006). *Coral Reef Resilience and Resistance to bleaching. IUCN, Gland, Switzerland*, pages 1–52.

Gründlingh, M. L. (1980). On the volume transport of the Agulhas Current. *Deep-Sea Research*, 27(A):557–563.

Gründlingh, M. L. (1984). An eddy over the northern Mozambique Ridge. *South African Journal of Science*, 80(7):324–329.

Gründlingh, M. L. and Pearce, A. F. (1984). Large vortices in the northern Agulhas Current. *Deep-Sea Research*, 31(9):1149–1156.

Harris, P. T., Pattiaratchi, C. B., Cole, A. R., and Keene, J. B. (1992). Evolution of subtidal sandbanks in Moreton Bay, Eastern Australia. *Marine Geology*, 103:225–247.

Harris, T. F. W. (1978). Review of coastal currents in Southern African waters. Report 30, South African National Scientific Programmes.

Hodgson, G. (1985). Abundance and distribution of planktonic coral larvae in Kaneohe Bay, Oahu, Hawaii. *Marine Ecology Progress Series*, 26:61–71.

Hunter, I. T. (1984). Coastal lows from a synoptic point of view. Coastal Low Workshop, Simonstown.

Hunter, I. T. (1988). Climate and weather off Natal. *Lecture Notes on Coastal and Estuarine Studies. Coastal Ocean Studies off Natal, South Africa*, 26:81–100.

Jordan, I. E. and Samways, M. J. (2001). Recent changes in coral assemblages of a South African coral reef, with recommendations for long-term monitoring. *Biodiversity and Conservation*, 10:1027–1037.

Lamont, T., Morris, T., van den Berg, M. A., Roberts, M. J., and Barlow, R. G. (in prep.). Hydrographic and satellite observations of the physical characteristics of the Delagoa Bight.

Largier, J. L. (2003). Considerations in estimating larval dispersal distances from oceanographic data. *Ecological Applications*, 13(1):Supplement S71–S89.

Le Treut, H., Somerville, R., Cubasch, U., Ding, Y., Mauritzen, C., Mokssit, A., Peterson, T., and Prather, M. (2007). Historical overview of climate change science. *Climate Change 2007: The Physical Basis. Contribution of Working Group I to the Fourth Assessment Report of the Intergovernmental Panel on Climate Change*, pages 93–127.

Lobel, P. S. and Robinson, A. R. (1988). Larval fishes and zooplankton in a cyclonic eddy in Hawaiian waters. *Journal of Plankton Research*, 10(6):1209–1223.

Lutjeharms, J. R. E. (2004). *The coastal oceans of south-eastern Africa.*, volume 14 B. Harvard University Press.

Lutjeharms, J. R. E. (2006). *The Agulhas Current.* Springer.

Lutjeharms, J. R. E. and Da Silva, A. J. (1988). The Delagoa Bight Eddy. *Deep-Sea Research*, 35(4):619–634.

Lutjeharms, J. R. E., Monterio, P. M. S., Tyson, P. D., and Obura, D. (2001). The oceans around southern Africa and regional effects on global change. *South African Journal of Science*, 97(119-130).

Martin, A. K. (1978). Physical oceanography in the northernmost Natal Valley. Progress Reports for the year 1978. Technical report No. 11, Marine Geoscience Unit - University of Cape Town.

Maud, R. R. (1980). *Studies on the ecology of Maputaland.* Rhodes Univeristy and the Natal branch of The Wildlife Society of Southern Africa.

Miller, K. and Mundy, C. (2003). Rapid settlement in broadcast spawning corals: Implications for larval dispersal. *Coral Reefs*, 22:99–106.

Miller, W. R. and Ramsay, P. J. (2002). South African Coelacanth Conservation and Genome Resource Programme - Multibeam geophysical mapping of coelacanth habitats. Report no. 2002-003, Marine Geosolutions.

Moore, T. S., Matear, R. J., Marra, J., and Clementson, L. (2007). Phytoplankton variability off the Western Australian Coast: Mesoscale eddies and their role in cross-shelf exchange. *Deep-Sea Research Part II*, 54:943–960.

Morris, T., Roberts, M. J., Lamont, T., Hancke, L., and van den Berg, M. A. (in prep.). Effects of a cyclonic eddy on the Northern KwaZulu Natal shelf.

Muthiga, N., Costa, A., Motta, H., Muhando, C., Mwaipopo, R., and Schleyer, M. (2008). Status of coral reefs in East Africa: Kenya, Tanzania, Mozambique and South Africa. *Status of the coral reefs of the World: 2008.*

Newell, R. E., Kidson, J. W., Vincent, D. G., and Boer, G. J. (1972). *The general circulation of the tropical atmosphere and interactions with extratropical latitudes, Vol. I.* MIT Press, Cambridge.

Nishikawa, A. and Sakai, K. (2005). Settlement competency period of planulae and genetic differentiation of the Scleractinian coral (*Acropora digitifera*). *Zoological Science*, 22(4):391–399.

Obura, D., Celliers, L., Machano, H., Mangubhai, S., Mohammed, M. S., Motta, H., Muhando, C., Muthinga, N., Pereira, M., and Schleyer, M. H. (2000). *Status of coral reefs in eastern Africa: Kenya, Tanzania, Mozambique and South Africa.*

Pearce, A. F. and Gründlingh, M. L. (1982). Is there a seasonal variation in the Agulhas Current? *Journal of Marine Research*, 40:177–184.

Preston-Whyte, R. A. and Tyson, P. (1988). *The atmosphere and weather of Southern Africa.* Oxford University Press.

Ramsay, P. J. (1994). Marine geology of the Sodwana Bay shelf, southeast Africa. *Marine Geology*, 120:225–247.

Ramsay, P. J. (1997). Quaternary marine geology and sea-level changes: Sodwana Bay shelf. *Maputaland Workshop Field Guide and Abstracts, 19-26 April, 1997*.

Ramsay, P. J. and Miller, W. R. (2006). Marine geophysical technology used to define coelacanth habitats on the KwaZulu-Natal shelf, South Africa. *South African Journal of Science*, 102:427–434.

Ramsay, P. J., Smith, A. M., and Mason, T. R. (1996). Geostrophic sand ridges, dune fields and associated bedforms from the Northern KwaZulu Natal shelf, south-east Africa. *Sedimentology*, 43:407–419.

Richmond, R. H. (1987). Energetics, competency, and long-distance dispersal of planulae larvae of the coral (*Pocillopora damicornis*). *Marine Biology*, 93(4):527–533.

Richmond, R. H. (1997). *Life and death of corals*. Springer.

Riegl, B. (2003). Climate change and coral reefs: Different effects in two high-latitude areas (Arabian Gulf, South Africa). *Coral Reefs*, 22:433–446.

Riegl, B. and Pillar, W. E. (2003). Possible refugia for reefs in times of environmental stress. *International Journal of Earth Science*, 92:520–531.

Riegl, B., Schleyer, M. H., Cook, P. J., and Branch, G. M. (1995). Structure of Africa's southernmost coral communities. *Bulletin of Marine Science*, 56(2):676–691.

Roberts, M. J., Ribbink, A. J., Morris, T., van den Berg, M. A., Engelbrecht, D. C., and Harding, R. T. (2006). Oceanographic environment of the Sodwana Bay coelacanths (*Latimeria chalumnae*), South Africa. *South African Journal of Science*, 102:435–443.

Sabates, A., Salat, J., Palomera, I., Emelianov, M., Fernandez De Puelles, M. L., and Olivar, M. P. (2007). Advection of anchovy (*Engraulis encrasicolus*) larvae along the Catalan continental slope (NW Mediterranean). *Fisheries Oceanography*, 16(2):130–141.

Sammarco, P. W. and Andrews, J. C. (1989). The Helix Experiment: Differential localized dispersal and recruitment patterns in Great Barrier Reef corals. *Limnology and Oceanography*, 34(5):896–912.

Schleyer, M. H. (1999). *A synthesis of KwaZulu-Natal coral research*, volume Special Publication No. 5. The Oceanographic Research Institute.

Schleyer, M. H. (2000). *Coral reefs of the Indian Ocean. Their ecology and conservation*. Oxford University Press, New York, USA.

Schleyer, M. H. and Celliers, L. (2003a). Biodiversity on the marginal coral reefs of South Africa: What does the future hold? *Zool. Verhand. Leiden.*, 345:387–400.

Schleyer, M. H. and Celliers, L. (2003b). Coral dominance at the reef-sediment interface in marginal coral communities at Sodwana Bay, South Africa. *Marine and Freshwater Research*, 54:967–972.

Schleyer, M. H. and Celliers, L. (2005). Modelling reef zonation in the Greater St. Lucia Wetland Park, South Africa. *Estuarine, Coastal and Shelf Science*, 63:373–384.

Schleyer, M. H., Kruger, A., and Benayahu, Y. (1997). Reproductive strategies of South African corals. In *Proceedings of the 6th International Conference on Coelentrate Biology, 1995*, pages 429–435.

Schleyer, M. H., Kruger, A., and Celliers, L. (2008). Long-term community changes on a high-latitude coral reef in the Greater St. Lucia Wetland Park, South Africa. *Marine Pollution Bulletin*, 56:493–502.

Schlitzer, R. (2007). *Ocean Data View, http://www-awi-bremerhaven.de/GEO/ODV, 2005*.

Schumann, E. H. (1981). Low frequency fluctutations off the Natal coast. *Journal of Geophysical Research*, 86(C7):6499–6508.

Schumann, E. H. (1983). Long-period coastal trapped waves off the southeast coast of Southern Africa. *Continental Shelf Research*, 2(2/3):97–107.

Schumann, E. H. (1988). Physical Oceanography off Natal. *Lecture notes on coastal and estuarine studies. Coastal ocean studies off Natal, South Africa*, 26:47–80.

Sebastian, C. R. and Sink, K. J. (2005). Extensive coral bleaching in southern Mozambique after the 2005 warm water season. Grande Baie, Mauritius. WIOMSA Conference, 2005.

Sheppard, C. R. C. (2003). Predicted recurrences of mass coral mortality in the Indian Ocean. *Nature*, 425:294–297.

Shillington, E. H. (1992). East Coast Oceanography. In *Proceedings of the 2nd Linefish Symposium (Fish, Fishers and Fisheries)*, volume Special Publication No. 2. The Oceanographic Research Institute.

Shouten, M. W. (2002). *Indian Ocean inter-ocean exchange: Variability and controls*. PhD thesis, Universiteit Utrecht.

Shouten, M. W., de Ruitjer, W. P. M., van Leeuwen, P. J., and Ridderinkhof, H. (2003). Eddies and variability in the Mozambique Channel. *Deep-Sea Research II*, 50:1987–2003.

SSALTO/DUACS User Handbook (2004). *(M)SLA and (M)ADT Near-Real Time and Delayed Time Products*, Version 1 rev 3 edition.

Storlazzi, C. D., Brown, E. K., and Field, M. E. (2006). The application of acoustic Doppler current profilers to measure the timing and patterns of coral larval dispersal. *Coral Reefs*, 25:369–381.

Stramma, L. and Lutjeharms, J. R. E. (1997). The flow field of the subtropical gyre of the South Indian Ocean. *Journal of Geophysical Research*, 102(C3):5513–5530.

West, J. M. and Salm, R. V. (2003). Resistance and resilience to coral bleaching: Implications for coral reef conservation and management. *Conservation Biology*, 17(4):956–967.

Wilkinson, C., Linden, O., Cesar, H., Hodgson, G., Rubens, J., and Strong, A. E. (1999). Ecological and socioeconomic impacts of 1998 coral mortality in the Indian Ocean: An ENSO impact and a warning of future change? *Ambio*, 28(2).

Williams, D., Wolanski, E., and Andrews, J. C. (1984). Transport mechanisms and the potential movement of planktonic larvae in the central region of the Great Barrier Reef. *Coral Reefs*, 3:229–236.

Zaslow, R. B. D. and Benayahu, Y. (1996). Longevity, competence and energetic content in planulae of the soft coral (*Heteroxenia fuscescens*). *Journal of Experimental Marine Biology and Ecology*, 206:55–68.

Zaslow, R. B. D., Henning, G., Hofmann, D. K., and Benayahu, Y. (1999). Reproduction in the Red Sea soft coral (*Heteroxenia fuscescens*): Seasonality and long-term record (1991-1997). *Marine Biology*, 133:553–559.